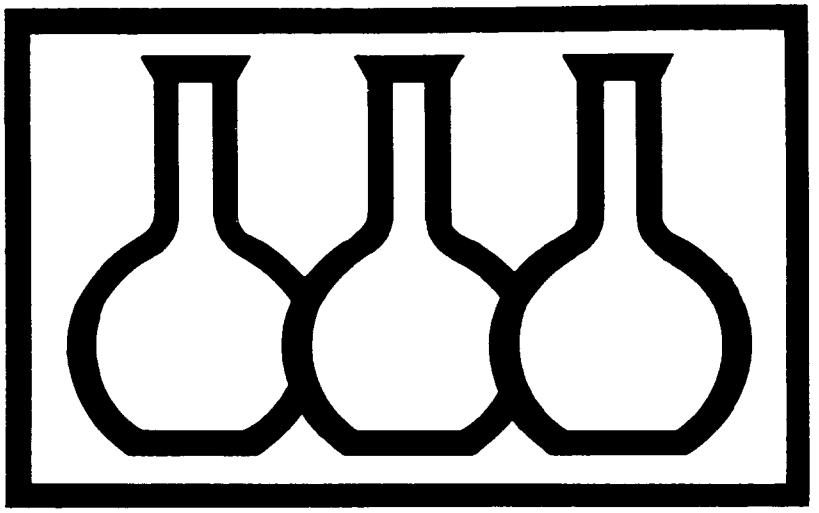

NIOSH RESEARCH REPORT

Engineering Control of Welding Fumes

U.S. DEPARTMENT OF HEALTH, EDUCATION, AND WELFARE
PUBLIC HEALTH SERVICE / CENTER FOR DISEASE CONTROL
NATIONAL INSTITUTE FOR OCCUPATIONAL SAFETY AND HEALTH

50272-101

REPORT DOCUMENTATION PAGE	1. REPORT NO.	2.	3. Recipient's Accession No. PB88-205 935
4. Title and Subtitle: NIOSH Research Report - Engineering Control of Welding Fumes.			5. Report Date: September 1974 6.
7. Author(s)			8. Performing Organization Rept. No. 75-115
9. Performing Organization Name and Address: NIOSH 4676 Columbia Parkway Cincinnati, Ohio 45226			10. Project/Task/Work Unit No. 11. Contract(C) or Grant(G) No. (C) 099-72-0076 (G)
12. Sponsoring Organization Name and Address: NIOSH 4676 Columbia Parkway Cincinnati, Ohio 45226			13. Type of Report & Period Covered 14.

15. Supplementary Notes

16. Abstract (Limit: 200 words)

An experimental investigation was conducted to define satisfactory criteria for the control of welding and cutting fumes using local exhaust ventilation methods. Based on the tests with breathing level fume samples, shielded manual metal arc welding on carbon steel and stainless steel, and gas shielded arc welding on carbon steel were judged to constitute the greatest potential health hazards. Analysis of breathing zone fume samples indicated that the prevailing standard of capture velocity, i.e. 100 feet per minute, is extremely effective on controlling fume concentrations. Ventilation system requirements were derived on the basis of a given set of ground rules which included environmental conditions and base materials. Recommendations are made for development of criteria for welding in confined spaces, welding with mixed facilities, and welding on paint-primed and zinc coated base metals.

17. Document Analysis a. Descriptors

b. Identifiers/Open-Ended Terms

WELDING WELDING-FUMES NIOSH-PUBLICATION INDUSTRIAL-HYGIENE ENVIRONMENTAL-ENGINEERING AIR-CONTAMINATION SAFETY-ENGINEERING VENTILATION-SYSTEMS EXPOSURE-LIMITS EXHAUST-SYSTEMS AIR-QUALITY-CONTROL

c. COSATI Field/Group

18. Availability Statement: AVAILABLE TO THE PUBLIC	19. Security Class (This Report) Unclassified	21. No. of Pages 124
	20. Security Class (This Page) Unclassified	22. Price

(See ANSI-Z39.18) See Instructions on Reverse OPTIONAL FORM 272 (4-77) (Formerly NTIS-35) Department of Commerce

ENGINEERING CONTROL OF WELDING FUMES

William Astleford
Southwest Research Institute
San Antonio, Texas

Contract No. HSM 99-72-76

U. S. DEPARTMENT OF HEALTH, EDUCATION, AND WELFARE
Public Health Service
Center for Disease Control
National Institute for Occupational Safety and Health
Division of Laboratories and Criteria Development
Cincinnati, Ohic
September 1974

This study was conducted by the Southwest Research Institute under Contract No. HSM 99-72-76 for the Division of Laboratories and Criteria Development, National Institute for Occupational Safety and Health. Technical monitoring was provided by C.M. Anglin and R.T. Hughes, Engineering Branch.

DHEW Publication No. (NIOSH) 75–115

ACKNOWLEDGEMENTS

We wish to express our gratitude to the following persons for their major contributions to this research program: Mr. Paul D. Watson for his guidance on process and electrode selection; Mr. John B. Tillery for performing the atomic absorption analyses; Mr. G. Andrew Lasater who performed the welding and cutting operations; Mr. James E. Johnson who designed and constructed the hot wire instrumentation; Mr. Victor J. Hernandez for drafting numerous figures; and Mrs. Sue Hyden for typing this manuscript as well as the interim report.

TABLE OF CONTENTS

		Page
LIST OF FIGURES		vii
LIST OF TABLES		x
I.	INTRODUCTION	1
II.	WELDING AND CUTTING TEST MATRICES AND TEST CONDITIONS	4
III.	BASELINE FUME SAMPLING AND ANALYSIS	10
III. 1	Fume Sampling System and Procedures	10
III. 2	Analysis Procedures	14
III. 3	Sampling System Performance	18
III. 4	Baseline Breathing Level Fume Composition	25
IV.	VENTILATION SYSTEM DESIGN	32
IV. 1	Crossdraft Table for Gas Shielded Arc Welding	32
IV. 2	Free-Standing Hood for Shielded Manual Metal Arc Welding	41
V.	CROSSDRAFT TABLE PERFORMANCE	48
V. 1	System Installation	48
V. 2	System Calibration	50
V. 3	Test Protocol and Experimental Results	56
VI.	FREE-STANDING RECTANGULAR HOOD	63
VI. 1	System Installation	63
VI. 2	Hood Performance for E-7018 Electrodes	63
VI. 3	Hood Performance for E-308-15 Electrodes	68
VII.	LOW VOLUME, HIGH VELOCITY FUME EXTRACTING WELDING GUN	72
VIII.	FLUORIDE ANALYSIS	76

TABLE OF CONTENTS (CONCLUDED)

		Page
IX.	CONCLUSIONS AND RECOMMENDATIONS	80
REFERENCES		83
APPENDIX A	BASELINE FUME CONCENTRATION DATA	A-1
APPENDIX B	HOT WIRE ANEMOMETER SYSTEM	B-1
APPENDIX C	BREATHING ZONE FUME CONCENTRATIONS FOR THE CROSSDRAFT TABLE	C-1
APPENDIX D	BREATHING ZONE FUME CONCENTRATIONS FOR THE RECTANGULAR HOOD	D-1

LIST OF FIGURES

Figure No.	Title	Page
1.	Schematic of Fume Collection System	11
2.	Operational Collection System	12
3.	Welding Helmet with Fume Sampling Ports	12
4.	Helmet Configuration for Breathing Zone Sampling	15
5.	Series Impinger Efficiency Equations	19
6.	Series Filter-Impinger Efficiency Equations	21
7.	Additive Effects at the Breathing Level for Fumes Generated by Shielded Manual Metal Arc Welding on Cold-Rolled Carbon Steel	28
8.	Additive Effects at the Breathing Level for Fumes Generated by Gas Shielded Arc Welding on Cold-Rolled Carbon Steel	29
9.	Additive Effects at the Breathing Level for Fumes Generated by Shielded Manual Metal Arc Welding on Stainless Steel	30
10.	Crossdraft Table Nomenclature	34
11.	Predicted Crossdraft Table Performance (K = 1.6)	36
12.	Predicted Crossdraft Table Performance (K = 2.8)	37
13.	Crossdraft Table Performance as a Function of Hood Transition Angle, Λ	38
14.	Slotted Hood for Crossdraft Table	40

LIST OF FIGURES (CONTINUED)

Figure No.	Title	Page
15.	Predicted Performance of a Round, Flanged Local Hood	43
16.	Predicted Performance of a Round, Flanged Local Hood (Continued)	43
17.	Predicted Performance for a Rectangular, Flanged Local Hood	44
18.	Predicted Performance for a Rectangular, Flanged, Local Hood (Continued)	44
19.	Flanged Rectangular Hood	47
20.	Crossdraft Ventilation System Assembly	49
21.	Example Hot Wire Anemometer Calibration Curve	51
22.	Crossdraft Table with Grid for Hot Wire Traverse	52
23.	Hot Wire Slot Voltage Profile for the Crossdraft Table	53
24.	Breathing Zone Additive Effect as a Function of Crossdraft Ventilation Flow Rate	58
25.	Fume Cloud from Gas Shielded Arc Welding Process	61
26.	Fume Control with Local Crossdraft Ventilation	61
27.	Rectangular Ventilation Hood System Assembly	64
28.	Rectangular Hood Face with Grid for Hot Wire Traverse	64
29.	Hot Wire Face Voltage Profile for the Rectangular Hood	66

LIST OF FIGURES (CONCLUDED)

Figure No.	Title	Page
30.	Breathing Zone Additive Effect as a Function of Rectangular Hood Ventilation Rate for Arc Welding on Cold-Rolled Carbon Steel	67
31.	Breathing Zone Additive Effect as a Function of Rectangular Hood Ventilation Rate for Arc Welding on Stainless Steel	69
32.	Fume Cloud From Shielded Manual Metal Arc Welding Process-No Ventilation	71
33.	Fume Control with Local Rectangular Hood Ventilation	71
34.	Breathing Zone Additive Effect as a Function of Low Volume, High Velocity Extraction Flow Rate	75
35.	Total Fluoride Sampling Apparatus	77
36.	Recommended Crossdraft Table Performance for Gas Shielded Arc Welding	81
37.	Recommended Rectangular Hood Performance for Shielded Manual Metal Arc Welding	81

LIST OF TABLES

Table No.	Title	Page
I.	Process Variables for Welding and Cutting of Carbon Steel	5
II.	Process Variables for Welding and Cutting Stainless Steel	7
III.	Machine Settings for Welding and Cutting	8
IV.	Design Point Performance for Crossdraft Table	39
V.	Design Point Performance for Best Rectangular and Round Hoods	45
VI.	Branch Duct Flow Rate Calibration	55
VII.	Crossdraft Table Test Conditions	57
VIII.	Rectangular Hood Test Conditions	65
IX.	Pneumatic Performance of Low Volume-High Velocity Fume Extraction System	73
X.	Total Fluoride Ion Concentration - No Local Ventilation	79
XI.	Effect of Local Ventilation on Total Fluoride Ion Concentration for E-7018 Electrodes	79

I. INTRODUCTION

The broad objective of this research program was to develop design criteria for local ventilation systems to control welding fumes. The criterion for the effectiveness of a given system was the minimum system operating point that resulted in a reduction of the breathing zone fume concentration below the appropriate Threshold Limit Value (TLV) in the case of individual components or the Exposure Threshold in the case of additive effects. To achieve this objective, the research effort described in this final report was divided into two phases.

Phase I

Eight test matrices were defined which represented combinations of commonly used welding and cutting processes, base metals, electrode diameters and electrode classifications. It was intended that the experimental results obtained from testing these matrices would be applicable to a significant portion of the welding community. The selected processes included

(1) Shielded manual metal arc welding

(2) Gas shielded arc welding with flux-core and solid wire electrodes

(3) Submerged arc welding

(4) Air-carbon arc gouging

(5) Oxy-acetylene cutting.

Base metals included uncoated carbon and low-alloy steels and stainless steel. Environmental conditions were designed to be representative of in-door, small-scale, job-shop production operations in an unconfined space. All tests were conducted in the Southwest Research Institute welding shop by professional welding personnel.

The next task, under Phase I, consisted of obtaining breathing level fume samples for each combination of parameters in the various test matrices. Samples were collected using water impingement techniques and analyzed by atomic absorption spectrophotometry (AAS) for

the concentrations of the dominant metallic components in the fume clouds. The breathing level samples will be referred to henceforth as baseline samples. These baseline tests provided the information for singling out those process-process variable combinations that indicated a high probability that the breathing zone concentration for the mixture would exceed the mixture TLV in the absence of local ventilation. All manual welding operations incorporated bead-on-plate techniques in the standard downhand position. This report also summarizes the baseline test results, which are presented in Reference 1. A discussion of the sampling train, collection system efficiency and analysis procedures is also contained in this report. Based on these breathing level, baseline tests, the following three process-base plate combinations were selected for local exhaust ventilation control studies.

(1) Shielded manual metal arc welding on carbon steel

(2) Shielded manual metal arc welding on stainless steel

(3) Gas shielded arc welding on carbon steel

The criterion for assessing the hazard potential of the fumes was the margin by which the breathing level additive effect exceeded a value of unity, which represented the mixture TLV or Exposure Threshold. The customary definition of additive effect was adopted, i.e., the summation of the normalized elemental concentrations.

Phase II

Various methods of local exhaust ventilation were then screened to qualitatively assess their ability to provide effective and efficient fume control. The underlying philosophy during this screening process and the subsequent preliminary design analyses were that the ventilation system should take maximum advantage of the natural motion of the fume cloud, i.e., tailor the system to the process. It was argued that this approach would result in a more efficient system in terms of size and power requirements. To this end, a crossdraft table was judged to be the most appropriate for the gas shielded process, while a free-standing, flanged, rectangular hood was indicated for the covered electrode processes. These two concepts were then subjected to a preliminary design analysis to predict system performance. The design procedures outlined in the Industrial Ventilation Manual,[2]* USAS-Z9.2[3] and the Handbook of

* Superscript numbers in parenthesis refer to references listed at the end of this report.

Air-Conditioning, Heating and Ventilation[4] were utilized in the analysis. Both systems were sized for the recommended, 100-fpm capture velocity and a minimal duct air flow rate. In each of these systems, the source of contamination was effectively placed between the operator and the extraction device.

A facility was constructed and instrumented to test the effectiveness of each design. System calibration was accomplished using standardized testing procedures. Breathing zone air samples were obtained at various system operating points to define the minimum air flow rate or capture velocity that resulted in an additive effect whose magnitude was less than the mixture TLV.

A low volume-high velocity fume extraction system was also evaluated in conjunction with the gas shielded process.

Finally, breathing zone fluoride levels were evaluated for the covered electrode processes. Ventilation requirements for fluoride removal were also investigated.

II. WELDING AND CUTTING TEST MATRICES AND TEST CONDITIONS

Tables I and II indicate the welding and cutting processes and process variables that were studied during Phase I. The five processes that are shown were selected on the basis of their frequency of useage, which reflects the number of operators that are involved with a particular process and the annual tonnage of metal that is joined or cut by a given process. The most common base metals that are used in conjunction with these processes are uncoated carbon, low-alloy and stainless steels. The electrode classifications and diameters represent a cross section of the most frequently used electrodes. A review of these tables indicates that cellulose-sodium, rutile-potassium, low hydrogen-potassium, low hydrogen-iron powder, dc-lime and dc-titania coatings were selected for the SMAW process. The indicated solid and flux cored wires were considered to be representative of the electrodes that are used in gas shielded processes. The AAC process included the most common electrode diameter, 3/8 inch. The electrode diameter for the SAW process was selected on the basis of industry useage. The largest heat input, 100,000 joules/inch, applies to normal groove welding, while the 50,000 joules/inch heat input corresponds to the stringer bead technique.

With the exception of the SAW and OFCA processes, all testing was conducted in either the manual or semi-automatic mode. Automatic equipment was utilized only on the SAW and OFCA experiments. Six electrode manufacturers and four equipment manufacturers were represented in this study. All tests were conducted in a 17,500-cu ft room which houses the Institute's welding and cutting facilities.

Table III summarizes the machine settings for each test condition. In all cases, the machine settings were initially adjusted to coincide with the mean values specified by the manufacturer. Any further adjustments resulted in test conditions that fell within the recommended operating ranges.

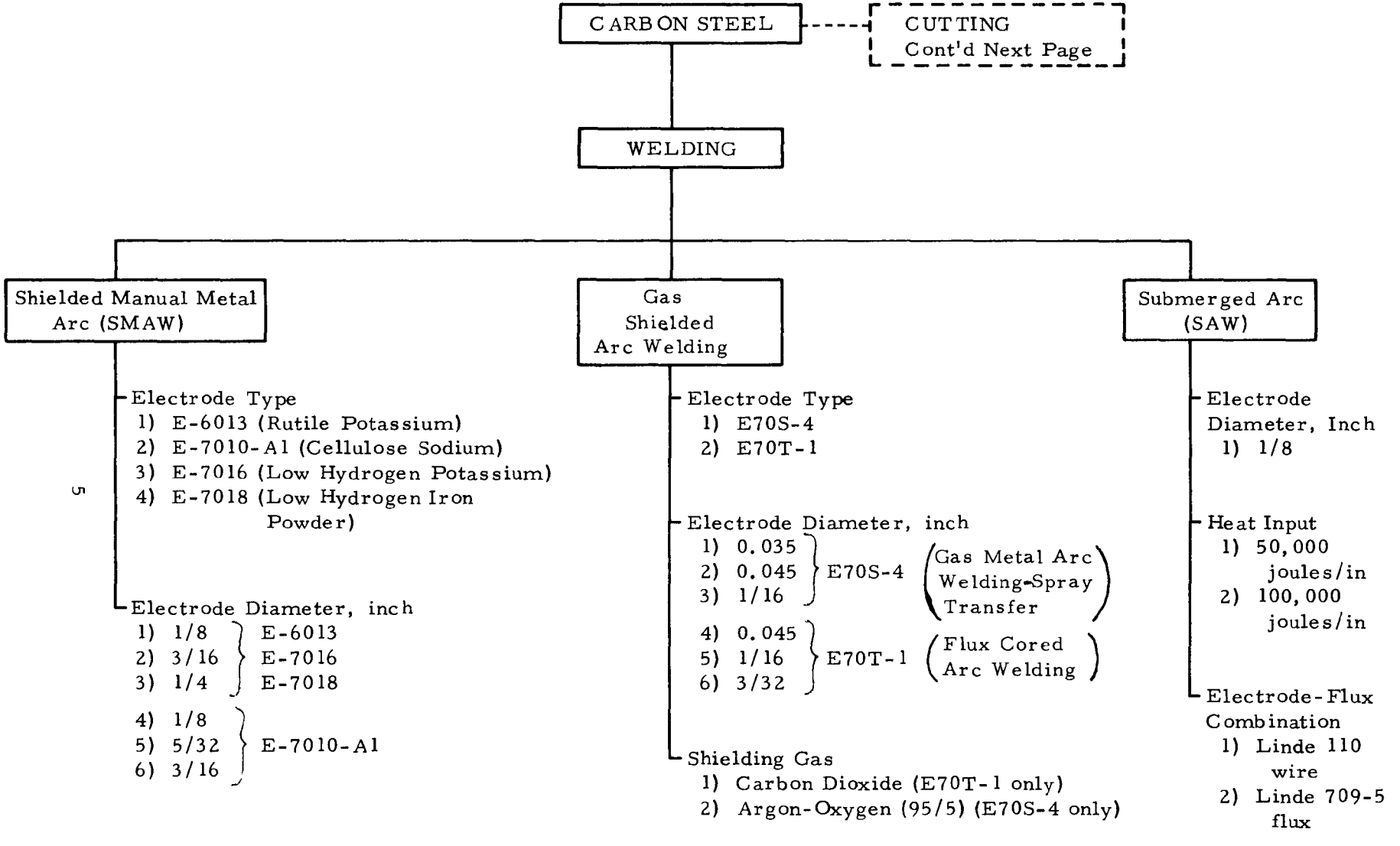

TABLE I. PROCESS VARIABLES FOR WELDING AND CUTTING OF CARBON STEEL

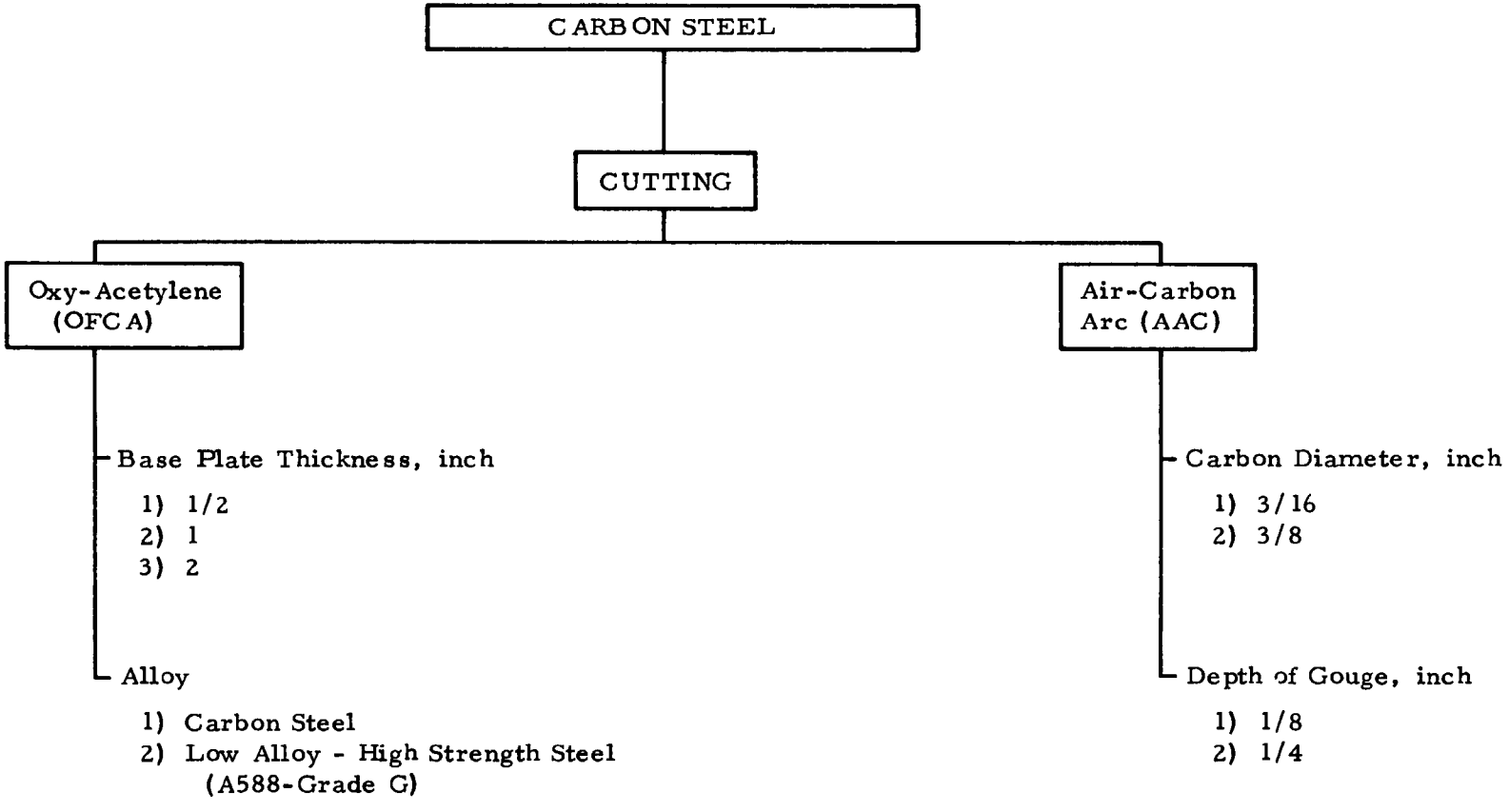

TABLE I. CARBON STEEL (CONTINUED)

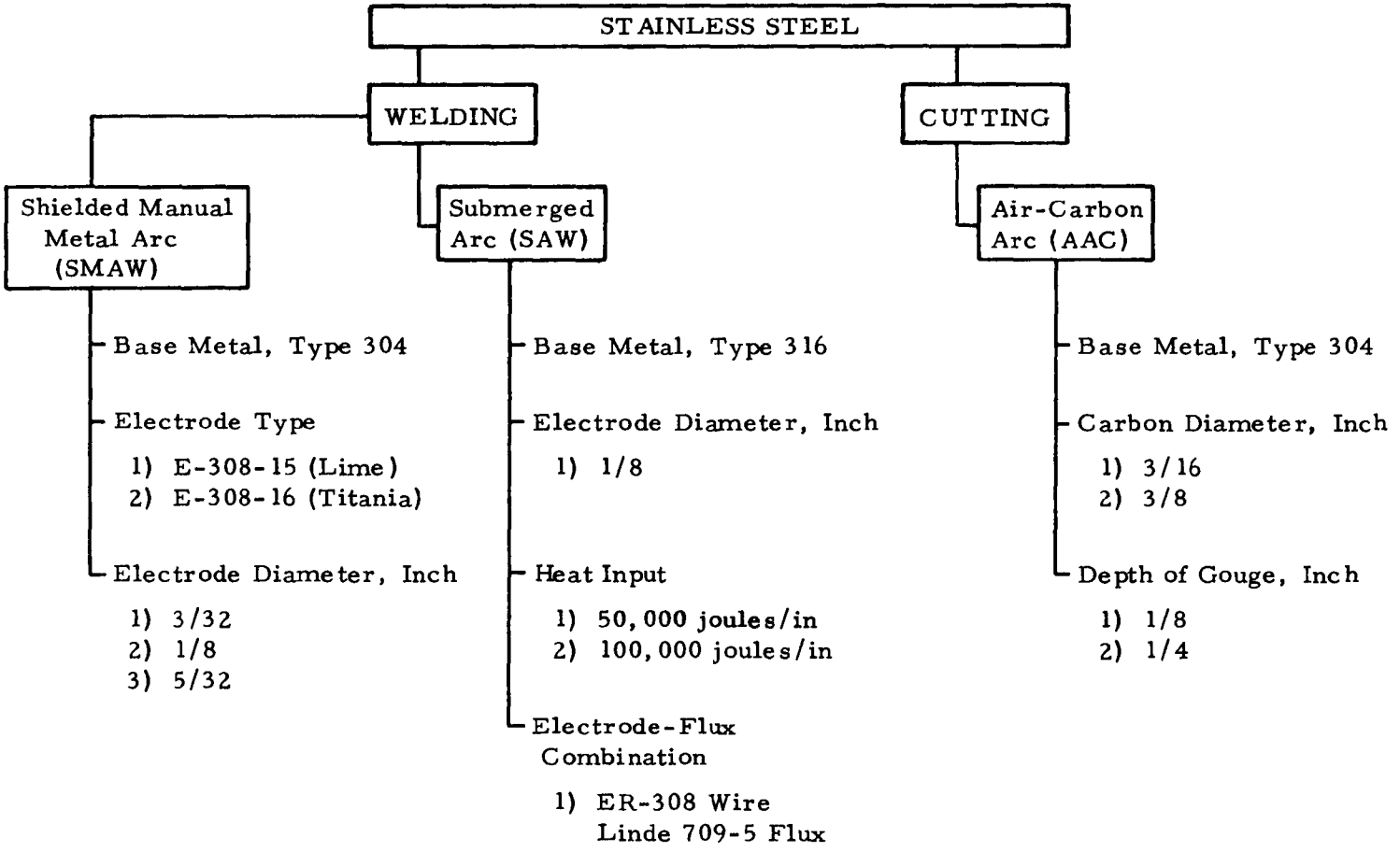

TABLE II. PROCESS VARIABLES FOR WELDING AND CUTTING STAINLESS STEEL

ELECTRODE TYPE	DIAMETER (INCHES)	AMPERAGE*
E-7010-A1	1/8	80-90
	5/32	100-105
	3/16	125-135
E-6013	1/8	120-130
	3/16	165-175
	1/4	235-245
E-7016	1/8	120-130
	3/16	195-205
	1/4	230-240
E-7018	1/8	140-150
	3/16	200-210
	1/4	235-245
E-308-16	1/8	120-130
	3/32	80-85
	5/32	135-140
E-308-15	1/8	120-130
	3/32	80-85
	5/32	135-140
Copper Coated Arc Gouging Electrodes	3/16	180
	3/8	375

* All covered electrode welding and arc gouging was conducted using d. c. reverse polarity.

TABLE III. MACHINE SETTINGS FOR WELDING AND CUTTING

ELECTRODE TYPE	DIAMETER (INCHES)	AMPERAGE	VOLTAGE	GAS FLOW RATE (CFH)	SLOPE	WIRE FEED SETTING
E-70T-1	0.045	235-245	26-28	(27)**	+2 1/2	70
	1/16	290-310	28-29	(25)	+4 1/2	50
	3/32	450-500	33-34	(28.5)	+4 1/2	49
E-70S-4	0.035	180-200	26.5-27.5	30-35	+2 1/2	65
	0.045	245-255	27-29	30	+2 1/2	55
	1/16	340-360	27-29	35	+2 1/2	36
ER-308	1/8	460	33	(TRAVEL SPEED = 8 inches/minute)		

** Numbers in parentheses are shielding gas pressures.

TABLE III. MACHINE SETTINGS FOR WELDING AND CUTTING (CONTINUED)

III. BASELINE FUME SAMPLING AND ANALYSIS

This section summarizes the structure and performance of the fume sampling system, the atomic absorption analysis procedures and the developments leading to the selection of the processes which were subjected to ventilation evaluations. For conciseness, both the breathing level and breathing zone sampling port configurations are presented in Section III. 1. The sample work-up procedures that are outlined in this section were applied to all determinations involving metallic fume components. The fluoride analysis procedures are discussed in Section VIII.

III. 1 Fume Sampling System and Procedures

Breathing level and breathing zone metallic fume samples were collected using the water impingement system that is shown in Figures 1 and 2. Figure 3 shows the breathing level configuration of the sampling ports on the helmet.

A standard curved chin, welding helmet was fitted, at the breathing level, with two 1/2-inch glass "Y-tubes" - one on each side of the exterior surface of the helmet. Each "Y-tube" has two sampling ports. The output of these helmet tubes is coupled via Tygon tubing (1/2-inch inside diameter) to a third glass "Y-tube". This tube ultimately bifurcates into Limb 1 and Limb 2, as shown in Figure 1. A Greenburg-Smith impinger, filled to the 100-ml level with de-ionized water, is located in Limb 2 near this branching point, i.e., point A. Downstream of the impinger is a normally closed solenoid valve; a similar valve is located in Limb 1. The output from each of these valves is fed into the appropriate port on a 3-way solenoid valve. Downstream of this 3-way valve is a calibrated and correlated rotameter flowmeter having a 3,000 to 77,000 ml/min (0.106 to 2.72 scfm) flow capacity. A bleed valve and a 1/12-hp, oil-less, rotary air pump in series with the rotameter complete the collection system. The pump, which exhausts to the atmosphere, has a maximum flow capacity of 1.5 scfm at zero pressure differential. The bleed valve serves two purposes: (1) to fine-tune the sampling flow rate through Limb 2 and (2) to prevent damage to the flowmeter when the pump is turned on and off. Tygon tubing (1/4-inch inside diameter) was used for all plumbing downstream of solenoid valves 1 and 3. The length of tubing between points A and C was 30 inches. The sampling rate through the impinger was nominally 1.0 cfm (28,320 ml/min), which coincides with impinger rating.

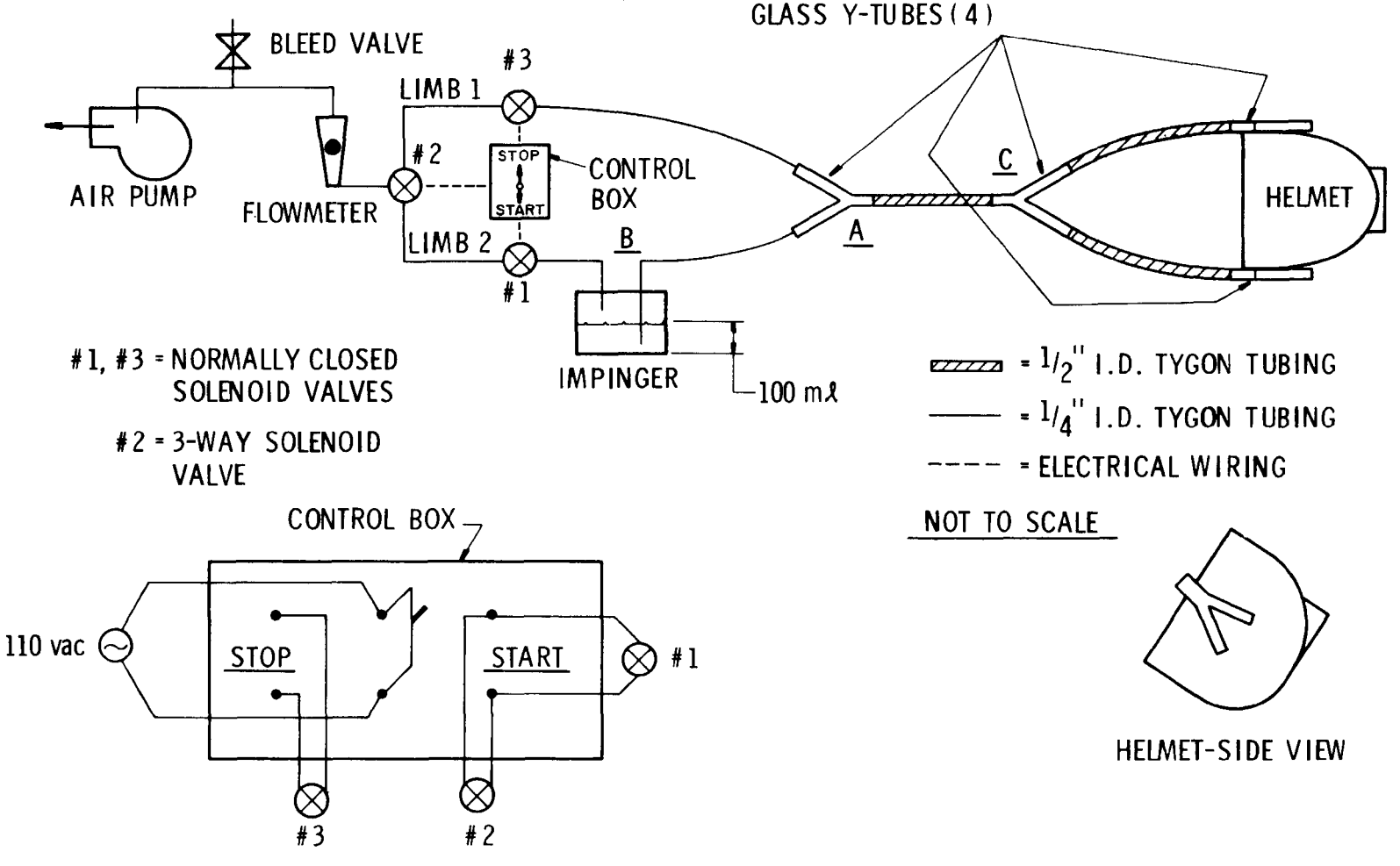

Figure 1. Schematic of Fume Collection System

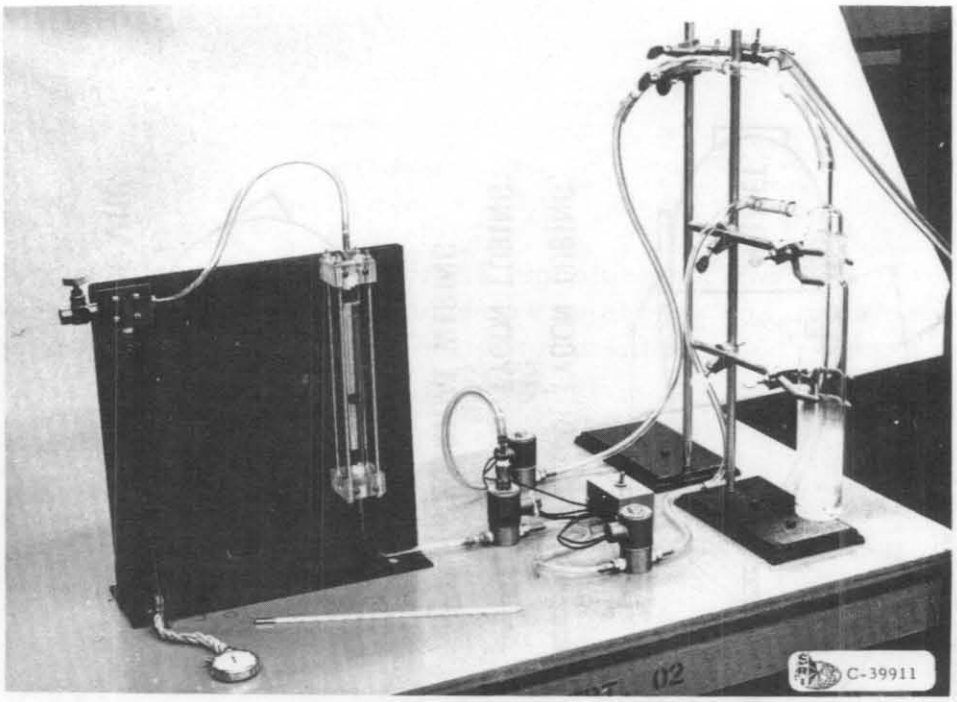

Figure 2. Operational Collection System

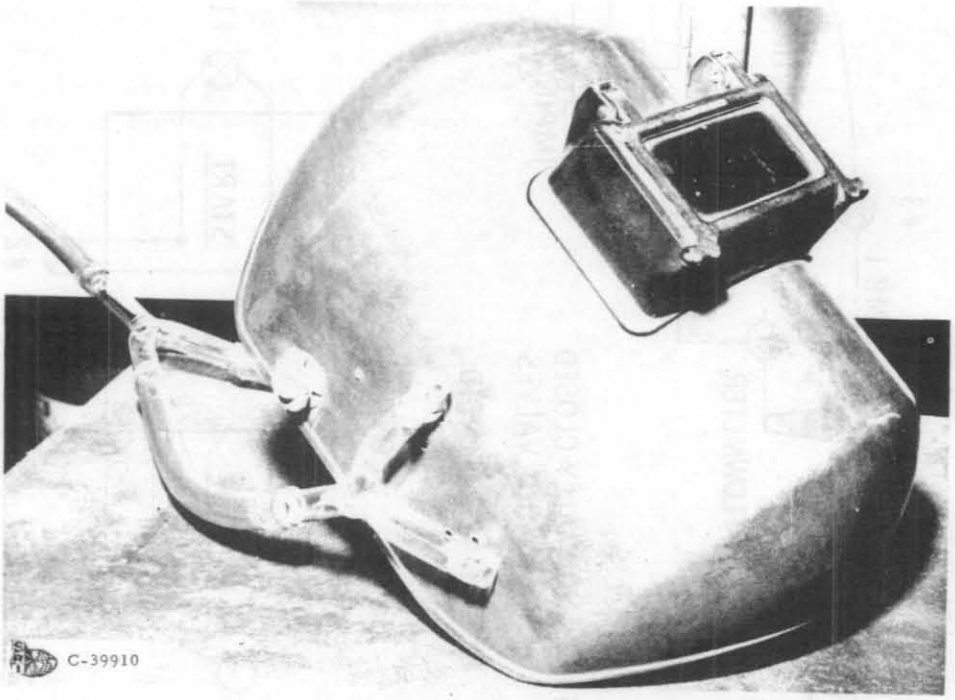

Figure 3. Welding Helmet with Fume Sampling Ports

All three solenoid valves, including an a-c power source, are hardwired into the control box which contains the double pole-double throw switch. In the STOP position, solenoids 2 and 3 are activated, and the fume flow is through Limb 1, thus isolating Limb 2 which contains the impinger. Switching to the START position deactivates solenoid 3, activates solenoid 1, and switches solenoid 2 into the Limb 2 position. Limb 1 is now isolated, and the fumes are bubbled through the impinger. The length of tubing between the bifurcation at point A and the impinger input port at point B is minimal. Consequently, the fumes are virtually at the impinger input port when the START switch is activated. This short-coupling minimizes the time lag or time constant of the system; fumes enter the impinger immediately upon activating the START switch. Fumes cannot be drawn into the impinger from Limb 1 because of the blocked line effect created in the line between point A and solenoid 3 as a result of closure of that valve.

A typical sampling procedure is as follows. With the control switch in the STOP position and the bleed valve partially open, the air pump is started. The bleed valve is then closed. The welder, wearing the instrumented helmet, strikes an arc and begins to lay bead-on-plate. The fumes are drawn into Limb 1 -- Limb 2 being isolated. Once fume flow has been established, the control switch is moved to the START position, thus isolating Limb 1, and fumes are drawn through the impinger. During collection, the scale reading at the center of the rotameter float is recorded. Room temperature and local station pressure are also noted for possible correction of the flow rate during data reduction. At the end of the test (collection), the switch is returned to the STOP position. A stop watch is activated simultaneously with switching operations and records total flow time which, together with the flow rate, defines the volume of fume-laden air that was processed through the impinger. The impinger is then removed to the laboratory for analysis. The welding room is then purged for approximately 5 minutes before the next sample is taken. Normally six samples are acquired for each test condition.

The sampling flowmeter that was used in all of the experiments was calibrated by the manufacturer for standard conditions of temperature and pressure, i.e., 70°F and 29.92 inches Hg. Using the manufacturer's suggested technique for calculating flow rate at non-standard conditions, the calculated flow rate was typically within 1.5 percent of the indicated rate (at standard conditions) which is within the stated reading accuracy of the instrument (2 percent or one division, whichever is greater). One rotameter division at a nominal flow rate of 1.0 cfm corresponds to an accuracy of 2.9 percent. Therefore, it was concluded that the indicated

flow rate did not require adjustment for minor excursions in pressure and temperature from the standard conditions because the correction was significantly less than the accuracy of the instrument.

An integral part of the sampling procedure involved standardizing the position of the welder with respect to the arc. This standardization was accomplished using a T-bar. The horizontal cross-piece on the T-bar could be adjusted vertically depending on the process. Initially, the operator assumed his normal work position. The T-bar was then adjusted so that the forehead portion of his helmet contacted the cross-piece. This cross-piece was then used as a guide to maintain a constant and normal orientation of the welder with respect to the arc as he moved horizontally while laying bead-on-plate. Thus, a consistent operator orientation was achieved within a given test, and this position was repeatable from test to test. For air-carbon arc gouging and shielded manual metal arc welding (electrodes less than 1/4-inch in diameter), the T-bar was positioned 17.5 inches above the work table. Because of the increase in electrode length for the 1/4-inch SMAW electrodes, the T-bar had to be raised to 21 inches above the welding table. For the gas shielded tests, the normal welding position required that the T-bar be adjusted to 11.5 inches above the work level. These T-bar levels were utilized on both the breathing level and breathing zone tests.

Automatic equipment was utilized for the submerged arc welding and oxy-acetylene cutting processes. An operator does not normally wear a standard welding helmet when working with these processes. However, to preserve continuity in the sampling procedure, the instrumented helmet was worn, and the operator moved with the speed of the automatic drive while maintaining an orientation with respect to the arc or flame that was consistent with the process being used.

For the breathing zone experiments, the bifurcated collection tubes were transferred to their corresponding positions on the interior surface of the welding helmet as shown in Figure 4. The welder breathed through a snorkel mouthpiece attached to a breathing tube. Breathing zone fume samples, therefore, were unaffected by the respiratory cycle or dilution because of addition of make-up air.

III.2 Analysis Procedures

Quantitative analysis for metallic fume elements in the impinger solutions was accomplished using a Perkin-Elmer 306 atomic absorption spectrophotometer. The sequence of steps in the sample work-up is as follows:

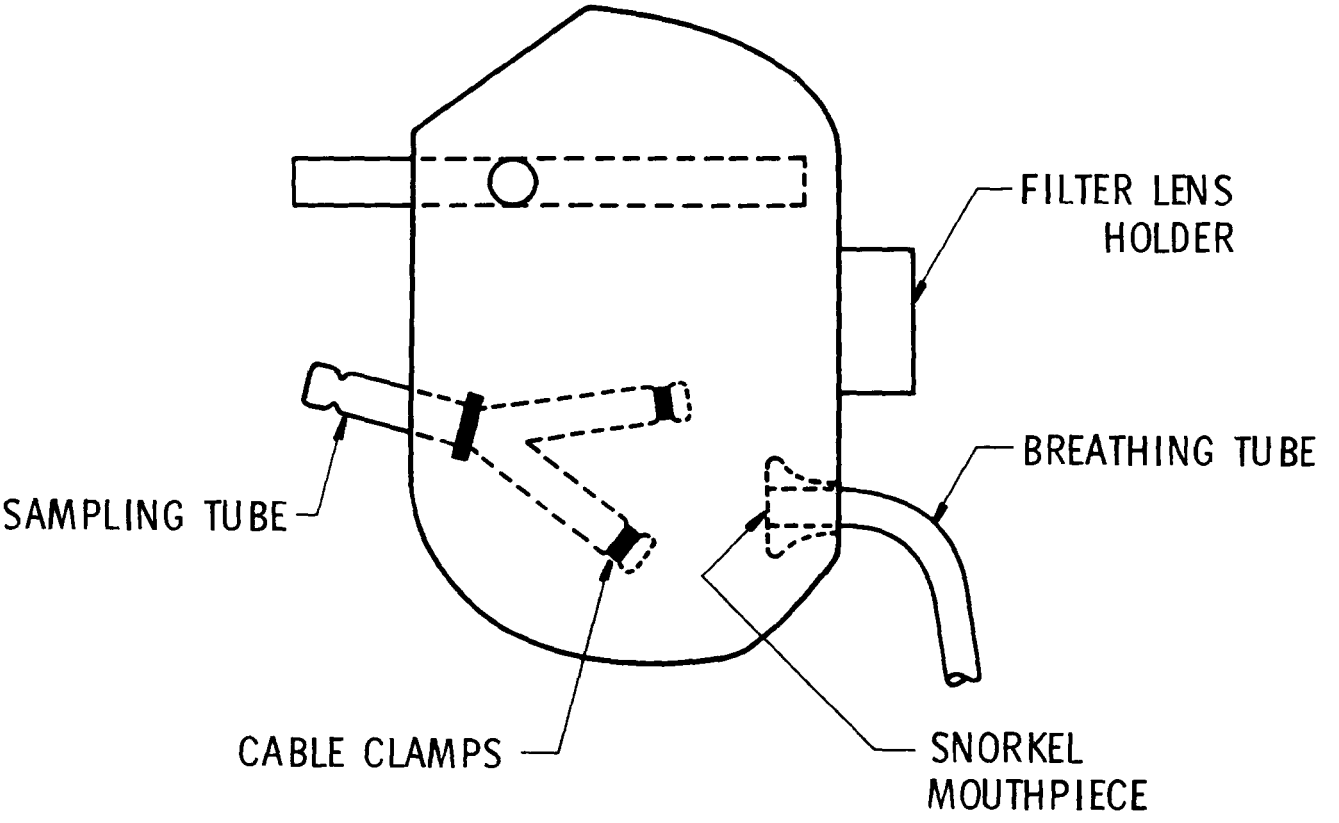

Figure 4. Helmet Configuration for Breathing Zone Sampling

1. Add 10 ml of conc. HCl* to impinger tube thru inlet opening and shake well for several seconds.

2. Pour sample into 250 ml beaker and cover with watch-glass.

3. Add 10 ml of conc. HCl* to impinger tube and shake well. Pour this into the beaker.

4. Rinse the impinger once with 20 ml of deionized water then with 10 ml. Each time adding the rinse to the 250 ml beaker.

5. Cover the beaker with a watch-glass and evaporate on hot plate (under nitrogen) until about 25 ml of sample remains.

6. Add 50 ml conc. HCl* and continue to evaporate until approximately 2-3 ml remains.

7. Remove from hot plate and rinse watch-glass with 10-15 ml of deionized water.

8. Add 10 drops (0.5 ml) of conc. nitric acid* and allow sample to cool to room temperature.

9. Quantatively transfer sample to 50 ml volumetric flask and rinse beaker 3X with deionized water. Add rinses to volumetric flask.

10. QS with deionized water and mix well.

11. Aspirate sample directly from volumetric flask for analysis.

12. An uncontaminated blank of 100 ml of deionized water was carried through the procedure to provide a background or reference level.

During reduction of the AAS data, the background level of the metal in the reagent blank was subtracted from the indicated levels in the impinger solution.

---

* Redistilled acids used.

As described later in this section, a series of tests was conducted using 5μ filters. The work-up procedures for these filters are indicated below.

1. Place filter pad in 250 ml beaker and rinse sample container with 10-15 ml of 1N conc. HCl*. Add rinse to beaker.

2. Add 100 ml of conc. HCl* and cover with watch-glass.

3. Digest for 30 min. on hot plate with low heat.

4. Rinse watch-glass cover with several ml of deionized water. Using teflon-coated forceps, remove the filter pad and rinse well with deionized water. Discard filter.

5. Cover beaker with watch-glass, add nitrogen flow, and evaporate sample on hot-plate to 2-3 ml.

6. Remove from hot-plate, rinse cover with 10-15 ml of deionized water and add 0.5 ml conc. HNO_3*. Allow to cool to room temperature.

7. Quantatively transfer sample to 50 ml volumetric flask and rinse beaker 3X with 5-10 ml of deionized water. Add rinse to volumetric flask.

8. QS volumetric flask with deionized water and mix well.

9. Aspirate directly from volumetric flask for analysis.

10. An unused filter was carried through the procedure and serves as a blank.

The atomic absorption spectrophotometer was calibrated to read out directly in μg of metal per ml of solution. This value was easily converted to mg of metal per cubic meter (m^3) of air sampled by the following equation:

$$\frac{mg}{m^3} = \frac{.035314\ (A)\ (C)}{(B)}$$

* Redistilled acids used.

where 0.035314 is the factor for converting $\mu g/ft^3$ to mg/m^3, A is the concentration of metal ($\mu g/ml$) in aqueous solution, B is the cubic feet of air sampled and C is the total volume in ml (including dilutions) of the aqueous solution that was analyzed.

For those tests in which the elemental concentrations were relatively large, the processed samples were aspirated into a flame. At low concentration levels, a graphite furnace was used as the energy source in place of the flame in order to increase the resolution and sensitivity of the analysis equipment. Typically, these low levels occurred at high ventilation system flow rates.

III.3 Sampling System Performance

An important aspect of the water impingement technique is the impinger performance, i.e., the ability to trap and retain the input contaminants (soluble or insoluble). The measure of this performance is the impinger efficiency which describes the percentage of the input contaminants that are retained in the solution. A knowledge of the efficiency is mandatory for proper interpretation of the fume concentration data. The impinger efficiency is a function of the degree of solubility in water of the medium that is being sampled. Intuitively, it would be expected that trapping efficiency of contaminants that are readily soluble in water, such as soluble aerosols, would be different from the collection efficiency for fumes, which are solid, insoluble particles of metal. Two methods of evaluating the efficiency of fume collection were investigated.

Collection Efficiency: Series Impinger Method

The series method consisted of processing the fume laden air samples through a cascade of impingers. Collection efficiency was determined using two impingers in the sampling train. A larger number of impingers could have been used, but the objective was not total removal of the fume contaminants from the air sample. The fumes generated by 3/16-inch diameter, E-6013 electrodes were collected in the sampling train. Except for the series arrangement of the impingers, all procedures were identical to those that were used in the single impinger baseline tests. All impinger samples were then analyzed by AAS to determine the concentrations of Fe, and collection efficiency was calculated using the mass balance equations outlined in Figure 5.

There were ten efficiency tests conducted using this method. That is, ten electrodes were consumed, and, in each instance, the fumes

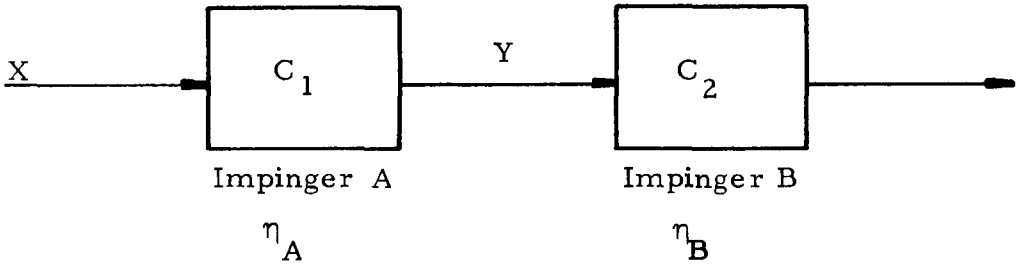

X = CONCENTRATION OF i-TH METALLIC FUME SPECIES AT THE INPUT TO IMPINGER A

Y = CONCENTRATION OF i-TH SPECIES THAT IS NOT TRAPPED IN IMPINGER A

Y = CONCENTRATION INPUT TO IMPINGER B

C_j (j = 1, 2) = CONCENTRATION OF i-TH SPECIES OBTAINED BY AAS

$\eta_A = \eta_B = \eta$ = IMPINGER EFFICIENCY

SYSTEM CONCENTRATION BALANCE

$$\left.\begin{aligned} \eta X &= C_1 \\ Y + C_1 &= X \\ \eta Y &= C_2 \end{aligned}\right\} \quad \text{SOLVE FOR } \eta: \qquad \eta = \frac{C_1 - C_2}{C_1}$$

FIGURE 5. SERIES IMPINGER EFFICIENCY EQUATIONS

were collected in two clean impingers. Application of the mass balance equations yielded an arithmetic mean collection efficiency of 28.8 percent with a standard deviation of 4.3 percent. The calculated efficiency ranged from 19.0 percent to 35.1 percent. This mean collection efficiency, when used in the proper fashion, determines the component concentration at the level of the pick-up ports on the helmet, e.g., by dividing the elemental concentration in the impinger by the calculated efficiency.

Collection Efficiency: Series Filter-Impinger Method

Another series of tests was then conducted to further evaluate the collection efficiency of the water impingement technique. For this the evaluation, breathing level fume samples were obtained from the fume clouds generated by manual metal arc welding of 3/16-inch diameter, E-6013 electrodes on carbon steel using the standard down-hand position. Machine settings, welder position and sampling and welding test procedures were identical to those that were used during the baseline tests for this class of welding electrode.

Two tests were conducted for each of the following filter-impinger configurations:

(1) Filter on impinger exit

(2) Impinger on filter exit.

The impingers were loaded with the usual 100 ml of deionized water. The diameter and pore size of the filter elements were 37mm and 5μ, respectively. The filter holders were commercially available plastic field monitors. The filter deposits as well as the impinger solutions were analyzed by AAS for Fe and Mn. The resulting elemental concentrations were then input to the mass balance equations which are given in Figure 6. Simultaneous solution of these equations yielded the following filter and impinger collection efficiencies:

$$\eta_{I_{Fe}} = 33.6\%$$

$$\eta_{I_{Mn}} = 35.4\%$$

$$\eta_{F_{Fe}} = 99.4\%$$

$$\eta_{F_{Mn}} = 100.0\%$$

FILTER ON IMPINGER EXIT

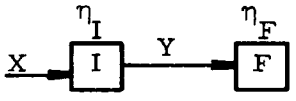

$$\left.\begin{aligned} \eta_I X &= C_i \\ \eta_F Y &= D_i \\ Y + C_i &= X \end{aligned}\right\} \Rightarrow \boxed{\frac{D_i}{\eta_F} + C_i = \frac{C_i}{\eta_I}} \quad (1)$$

IMPINGER ON FILTER EXIT

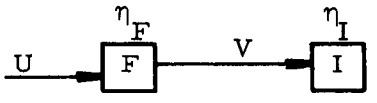

$$\left.\begin{aligned} \eta_F U &= \xi_i \\ \eta_I V &= \delta_i \\ V + \xi_i &= U \end{aligned}\right\} \Rightarrow \boxed{\frac{\delta_i}{\eta_I} + \xi_i = \frac{\xi_i}{\eta_F}} \quad (2)$$

SOLVE EQUATIONS 1 AND 2 SIMULTANEOUSLY

$$\eta_I = \frac{\xi_i C_i - \delta_i D_i}{\xi_i (C_i + D_i)}$$

$$\eta_F = \frac{\xi_i C_i - \delta_i D_i}{C_i (\xi_i + \delta_i)}$$

I = IMPINGER

F = FILTER

η = EFFICIENCY

i = CONCENTRATION OF i-TH FUME COMPONENT

FIGURE 6. SERIES FILTER-IMPINGER EFFICIENCY EQUATIONS

The impinger efficiencies calculated by this procedure fall within the range of the series impinger tests. Therefore, the nominal collection efficiency was 29 percent, and this value was used to generate breathing level and breathing zone concentration data from the contaminant concentration trapped in the impinger.

Various methods of improving the collection efficiency were then investigated. The following factors were theorized to have a significant, positive influence on collection efficiency:

(1) The addition of acid to the water sample would promote increased solubility of the metal fumes, thereby reducing the amount of fume lost through exhaust.

(2) The addition of the surfactant, TMN, would reduce surface tension, bubble size and liquid agitation and thus improve fume retention.

(3) A larger initial liquid volume would give the fumes a longer residence time in the impinger and, therefore, increase the probability of fume retention.

To assess these hypotheses, six impingers were prepared with the following liquid compositions:

Test No.	Liquid Composition
16a	90 ml water + 10 ml HCl
16b	190 ml water + 35 ml TMN + 10 ml HCl
16c	200 ml water + 7.5 ml TMN
16d	180 ml water + 20 ml TMN
16e	100 ml water + 10 ml TMN
16f	100 ml water (reference)

The fumes from six E-6013, 3/16-inch diameter electrodes were collected in each of the six impingers, i.e., one impinger per electrode. These samples were then analyzed by AAS for the presence of Fe. A significant increase in the iron concentration relative to Test No. 16f would indicate a substantial improvement in collection efficiency. The test results, which are shown below, did not support this criterion.

Test No.	% Change in Fe Concentration Relative to Test No. 16f
16a	7.26
16b	-4.81
16c	3.48
16d	6.63
16e	8.57
16f	----

These data indicate that the maximum increase in collection efficiency that could be realized was 8.6 percent relative to the established 29 percent efficiency. That is, if 10 ml of TMN were added to the normal 100 ml of distilled water, the collection efficiency would increase from 29 to 31.4 percent, i.e., 29.0 x 1.086. Therefore, the addition of a surfactant or an acid to the sampling liquid was not justified.

Two important aspects of the collection and analysis procedures are the repeatability and recovery. Repeatability is a measure of the collection system's ability to reproduce a specific result given that the environmental or test conditions remain constant. Recovery, on the other hand, is, to a great extent, a measure of the efficiency of the sample work-up and analysis procedures.

To quantify the system repeatability, three E-6013 electrodes were consumed, and the fumes were collected in separate impingers. These samples were analyzed by atomic absorption spectrophotometry for the presence of Cu, Cr, Fe, Mn and Zn. The results were as follows:

	Element Concentration in mg/m^3				
Sample	Cu	Cr	Fe	Mn	Zn
C-5	0.21	0.	87.88	10.25	.01
C-6	0.17	0.	75.50	9.38	.02
C-7	0.18	0.	85.38	9.88	.03

The concentration levels that are shown for these repeatability tests should not be compared directly with the concentrations that will be presented subsequently for the baseline tests of SMAW. The reason is that the above concentrations are higher than normal because the welder assumed a position closer to the arc than is the usual welding practice. Reduction of the distance between the fume pick-up ports on the helmet and the arc was imposed strictly for the purposes of ascertaining repeatability, i.e., to present a more nearly constant input to the sampling system. The range of scatter for the Zn concentrations is to be expected since these levels are approaching the sensitivity threshold of the atomic absorption instrument. These results indicate that the maximum deviation was approximately 16 percent for Fe, 23 percent for Cu and 9 percent for Mn. This level of repeatability is considered to be quite satisfactory in view of the fact that the spatial location of the fume cloud is a random variable subject to local room air currents. Furthermore, it has been observed that the breathing zone additive effect is reproducible within 6 percent. In accordance with ASTM Standard D-1357[5], the high reproducibility justifies the use of a low collection efficiency.

Recovery was evaluated using the following spiking or loading procedures.

Initially, a blank impinger, carrying 100 ml of deionized water, was spiked with 1 mg of Cu, Ni, Cr, Mn, Fe, Zn, Co and Cd. The spiked blank was then subjected to the normal work-up procedures and subsequently analyzed by AAS. The following percent recoveries were obtained:

	Percent Recovery							
Sample	Cu	Ni	Cr	Mn	Fe	Zn	Co	Cd
S-1	104	110	115	102	88	103	104	100

Recovery represents the ratio of elemental concentration after processing to concentration before processing. The results indicate that good recoveries can be expected using this method and that recovery errors introduced by the analysis procedures should not exceed 15 percent. Deviation of the recovery from the 100 percent level may be due to several factors:

(1) Errors in measuring and manipulating 1 mg of the spiking element.

(2) Loss of solution during the AAS sample processing; for example, through evaporation.

Normal collection procedure involved purging the collection system and the welding room between electrode burns. To purge the collection system, the air motor was permitted to run continuously while the control switch was in the STOP position. Thus, air was drawn continuously from the atmosphere through the pick-up ports on the helmet and through Limb 1 of the collection system. The following test was conducted to assess the effectiveness of the collection system purge routine. An electrode was consumed, the fumes were collected, and then the system was purged. A clean impinger with deionized water was then placed in the collection system, and a volume of air was processed through the impinger to flush the entire system upstream of the impinger (bubbling time equaled previous burn time). The results of an AAS analysis of this blank indicated a completed absence of all elements. The conclusion is that the collection/purge routine was highly effective in that cross-contamination of samples due to residue in the system was non-existent. This result also implies that there was no fallout in the collection line, which further justifies the use of collection efficiency to obtain breathing level or breathing zone concentration.

III. 4 Baseline Breathing Level Fume Composition

This section summarizes the essential experimental results that were obtained in Phase I. At the conclusion of the baseline tests, all of the data were converted to the equivalent breathing level additive effect. In this form, it was possible to determine which process-process variable combinations generated fume concentrations that exceeded the mixture TLV or exposure threshold and the margin by which that level was exceeded, i.e., the processes that appeared to present the greatest potential health hazard were defined. For a 100 percent arc time, the fumes from the following processes exceeded the mixture TLV for all test conditions:

(1) Shielded Manual Metal Arc Welding on Carbon Steel

(2) Shielded Manual Metal Arc Welding on Stainless Steel

(3) Gas Shielded Arc Welding on Carbon Steel.

The average margin by which these three processes exceeded the exposure threshold ranged from approximately 20 to 350. These processes were, therefore, selected for the local exhaust ventilation control studies. The five remaining test matrices were not included in the ventilation study because their fumes did not normally exceed the mixture TLV at the breathing level for 100 percent arc time. In isolated cases where the exposure threshold was exceeded, the margin was minimal compared to the above three processes. Based on the attenuation of fume concentration afforded by the helmet in conjunction with a realistic arc time, it follows that the breathing zone fume concentrations for these five matrices should be well below the mixture TLV. The reader is referred to Reference 1 for a detailed presentation of baseline concentration data for the five excluded processes.

Analysis of the impinger solutions yielded concentrations of unoxidized elements. The concentrations of Fe and Cr were converted to their equivalent oxidized form for use with published TLV's. For example,

Multiply Concentration (mg/m^3) of	by	To Obtain Concentration (mg/m^3) of
Fe	2.86	Fe_2O_3
Cr	1.92	CrO_3

The scale factors represent the ratio of oxidized to unoxidized molecular weights.

In the following discussion of the three dominant process-process variable combinations, C_i denotes the concentration of the i-th fume component trapped in the impinger. These component concentrations were normalized with respect to the appropriate threshold limit values.

Component, C_i	TLV (mg/m^3)
Fe_2O_3	10.0
Cu	0.1
CrO_3	0.1
Mn	5.0 (ceiling)
Ni	1.0

These normalized impinger concentrations were then plotted as a function of electrode diameter, as shown in Appendix A. The basic data from which these curves were derived are also included in Appendix A.

The next step consisted of converting the impinger data to a breathing level additive effect at 100 percent arc time, i.e., by applying the following summation,

$$\frac{\sum_{i=1}^{N} C_i/TLV_i}{\eta_I}$$

where η_I is the impinger collection efficiency. Normally, each C_i is a time-weighted average concentration which reflects the time history of component concentration during a normal work day. However, the data that were obtained on this study are referenced to 100 percent arc time. The additive effect at other arc times can be estimated. The equation for the time-weighted average concentration is

$$C_{i_{TWA}} = \frac{C_{i,1} \times t_1 + C_{i,2} \times t_2 + \ldots\ldots C_{i,j} \times t_j}{\sum_j t_j}$$

where $C_{i,j}$ = Concentration of i-th species during the j-th work task

t_j = Time expended on the j-th work task

$\sum_j t_j$ = Summation of the time expended on all tasks (normally eight hours)

For simplicity, assume that the peripheral activities are conducted during the times for which j is greater than or equal to two and that

$$C_{i,j} = 0 \text{ for } j \geq 2$$

That is, the concentration of the i-th species is non-zero only during arc time, t_1. Then,

$$\frac{t_1}{\sum_j t_j} = \text{fractional arc time}$$

and

$$\left(\frac{C}{TLV}\right)_{i,\,TWA} = \frac{C_i}{TLV_i} \times \frac{t_1}{\sum_j t_j}$$

and

$$\sum_i \frac{(C/TLV)_{i,\,TWA}}{\eta_I} = \left(\sum_i \frac{(C/TLV)_i}{\eta_I}\right)\left(\frac{t_1}{\sum_j t_j}\right)$$

The normalized concentration summation on the right-hand side of the above equation corresponds to a 100 percent arc time. Therefore, the additive effect can be estimated for other arc times by proportionately reducing the normalized concentration summation.

The breathing level additive effect as a function of electrode diameter for 100 percent arc time is shown in Figures 7, 8 and 9. The following observations were derived from the data listed in Appendix A. Note that the breathing level concentration of a particular component is equal to the impinger concentration divided by the collection efficiency. Fume samples from the covered electrodes in Figure 7 were analyzed for Fe, Mn, and Cu. The average breathing level concentrations of manganese and iron oxide exceeded their TLV's in all cases. Breathing level copper concentration exceeded 0.1 mg/m^3 in 25 percent of the tests. In addition, the copper concentration was greater than 80 percent of its TLV on 75 percent of the tests. As indicated, the E-7018 electrode produced the largest breathing level additive effect. The gas shielded processes in Figure 8 were also analyzed for Fe, Mn and Cu. Average breathing level iron oxide and copper concentrations always exceeded their TLV's. Manganese concentration was greater than 5 mg/m^3 on

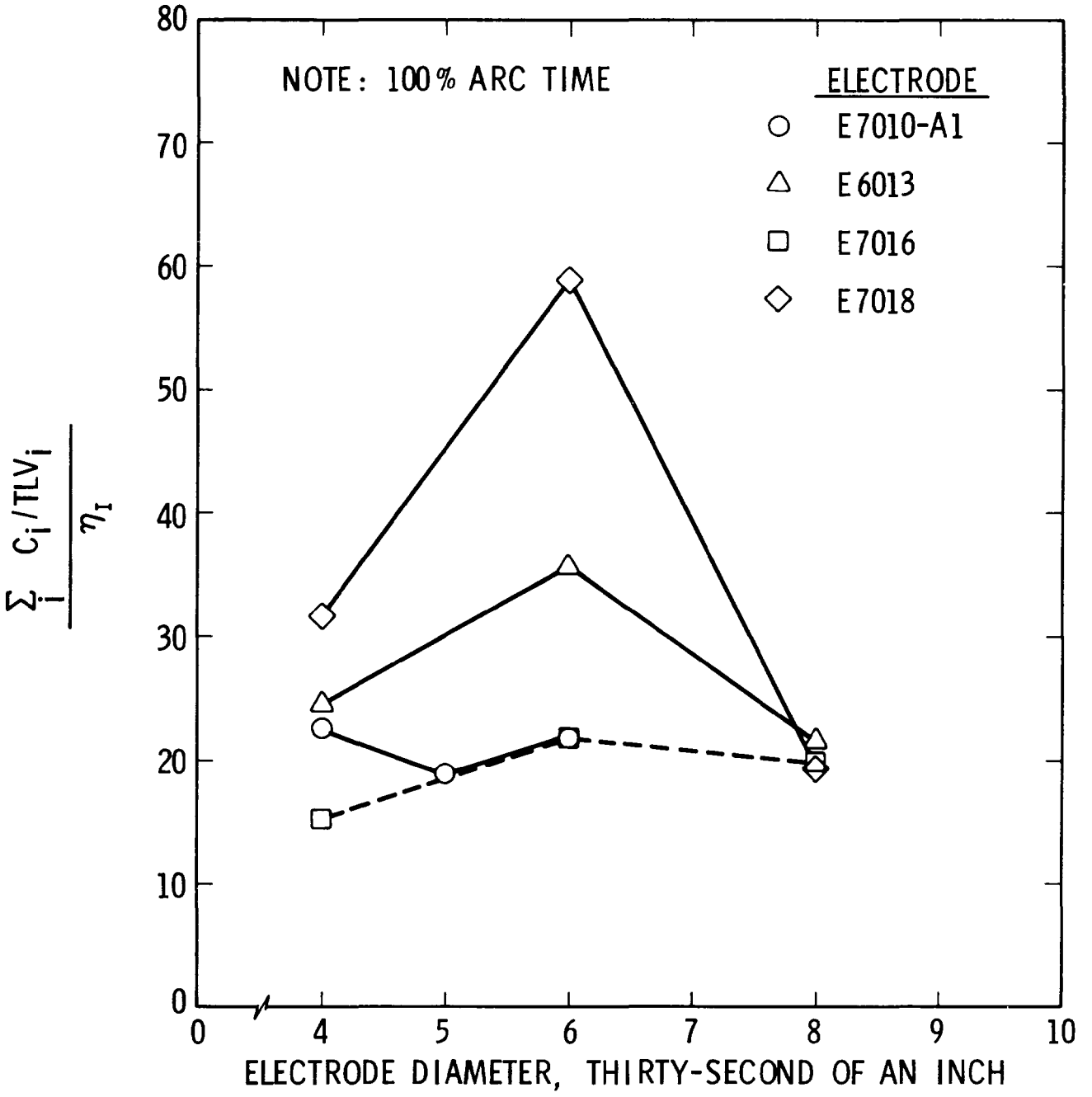

Figure 7. Additive Effect at the Breathing Level for Fumes Generated by Shielded Manual Arc Welding on Cold-Rolled Carbon Steel

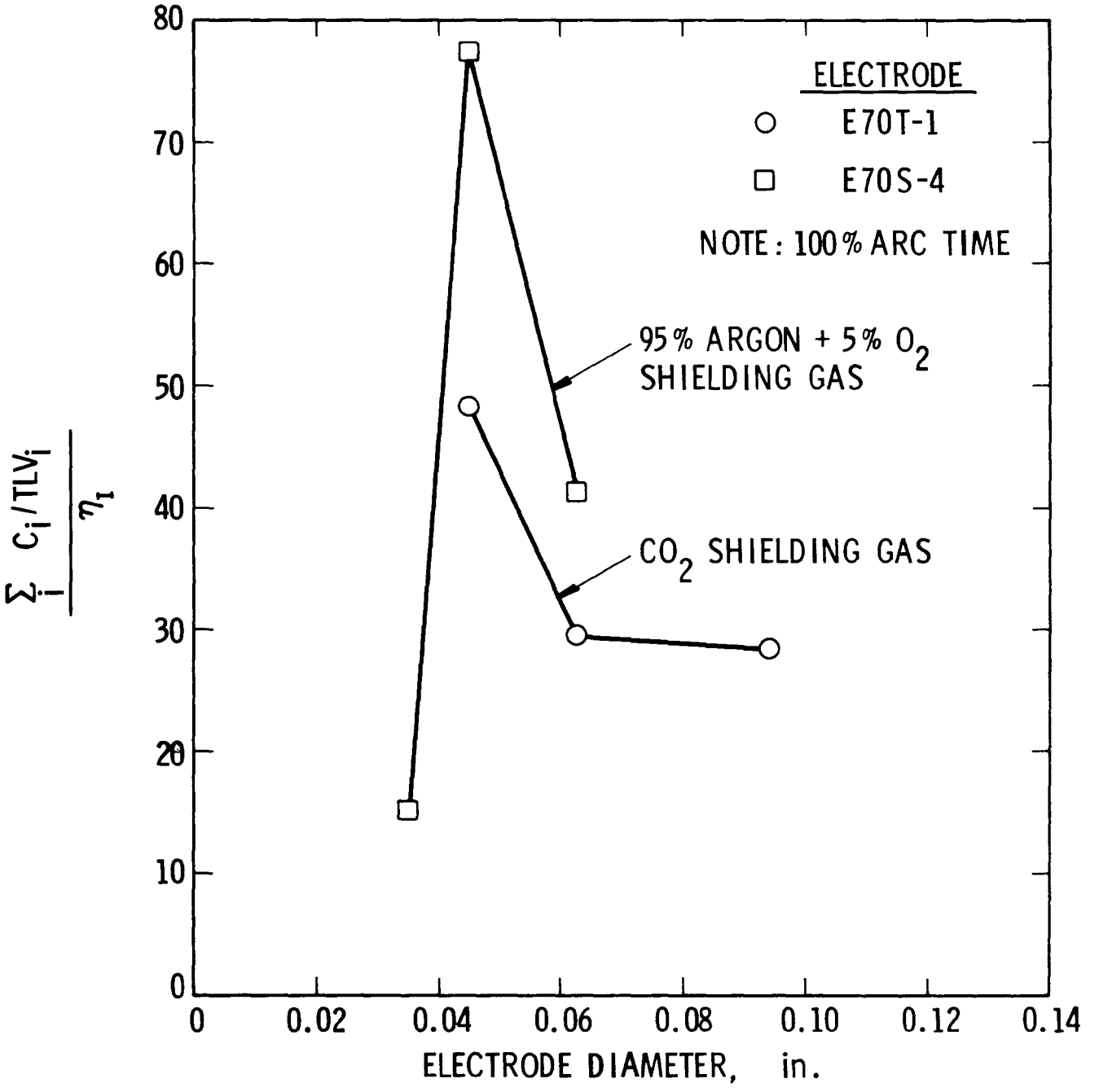

Figure 8. Additive Effect at the Breathing Level for Fumes Generated by Gas Shielded Arc Welding on Cold-Rolled Carbon Steel

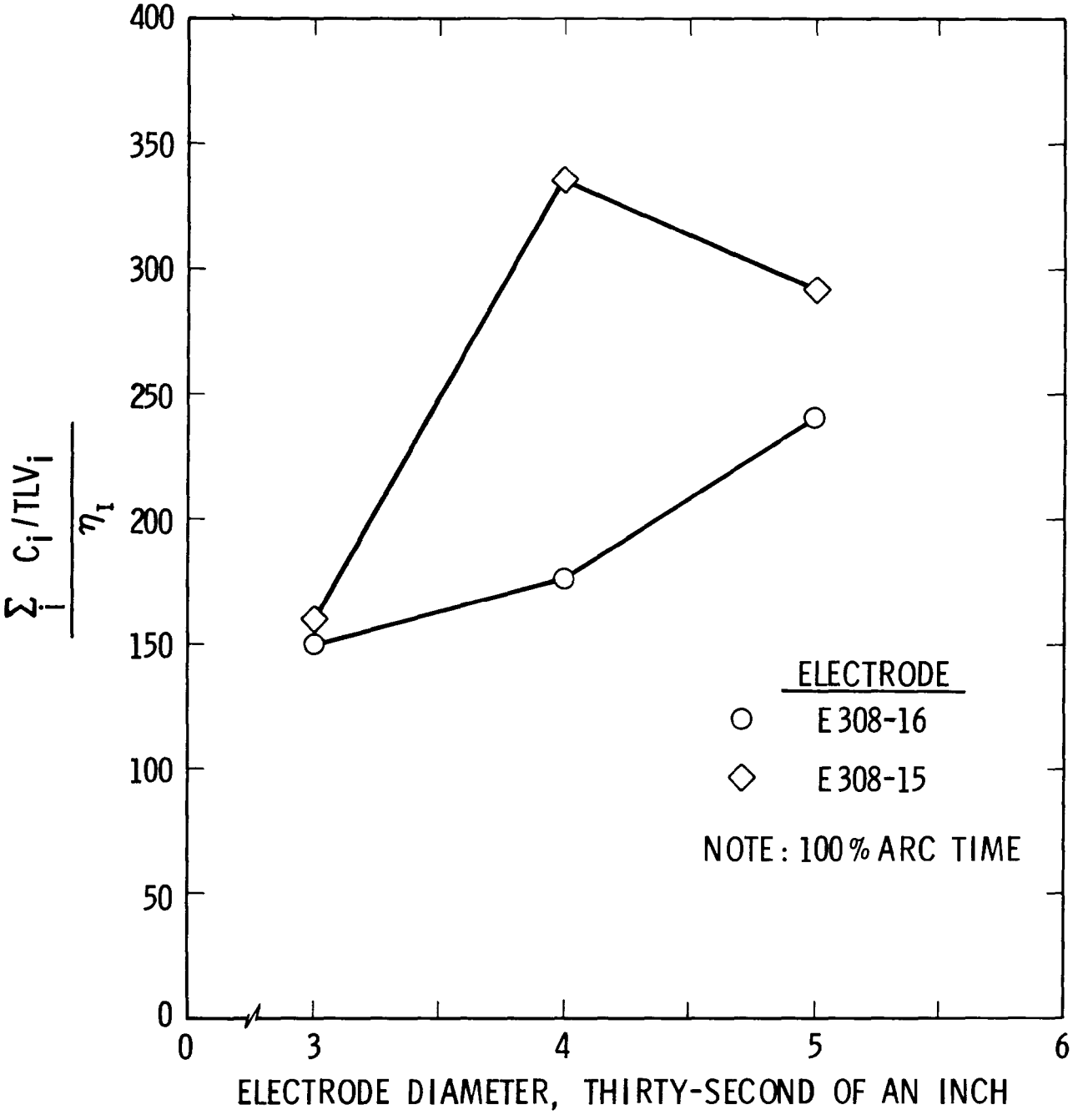

Figure 9. Additive Effect at the Breathing Level for Fumes Generated by Shielded Manual Metal Arc Welding on Stainless Steel

83 percent of the tests. Finally, Figure 9 contains the breathing level additive effect for stainless steel arc welding with covered electrodes. Fumes from this process were analyzed for Fe, Mn, Cu, Cr and Ni. As anticipated, chromic oxide was by far the dominant fume component, and it exceeded the 0.1 mg/m^3 level in all cases. Breathing level concentration of iron oxide also exceeded its TLV in all cases. On 83 percent of the tests, manganese exceeded the TLV of 5 mg/m^3. It is plausible that, under different environmental and experimental conditions, those processes which are not represented in Figures 7 through 9 could result in an additive effect that cannot be neglected.

It is now obvious why these three process-process variable combinations were selected for the local exhaust ventilation control studies. Furthermore, from each of these last three figures, the electrode diameter that produced the largest breathing level additive effect was selected for use in the upcoming ventilation evaluations. It was argued that if the most critical condition can be effectively controlled, then the lower concentration levels will follow suit. The electrode diameters that were used in the ventilation studies are:

Process	Electrode	Diameter (inches)
SMAW on Carbon Steel	E-7018	3/8
SMAW on Stainless Steel	E-308-15	1/8
Gas Shielded Arc Welding	E-70S-4	0.045

IV. VENTILATION SYSTEM DESIGN

The basic ground rules that were followed in the design of local welding ventilation systems were the following:

(1) The system should be tailored to the process, thus taking advantage of the natural motion of the fume cloud.

(2) The evacuation device should be designed so that the fume source is located between the operator and the face of the exhaust system.

(3) The system should be capable of inducing the required capture velocity with a minimal volumetric flow rate.

Candidate systems included crossdraft tables, free-standing hoods, canopy hoods, downdraft tables and low volume-high velocity fume extractors. The canopy hood and the downdraft table were eliminated from further consideration. The former system violates the second ground rule. The latter system violates the third ground rule because (1) the capture velocity vector would be approximately 180 degrees out of phase with the natural vertical motion SMAW fumes and (2) the capture velocity vector would be nearly orthogonal to the shielding gas velocity vector for the MIG process. Consequently, fume extraction by a downdraft table would be inefficient in terms of the size of the exhauster that would be needed to overcome the natural fume motions.

Based on these considerations, a crossdraft table was judged to be the most appropriate system for the gas shielded process, and a free-standing hood was indicated for the covered electrode processes. Each of these systems was fabricated in accordance with the design procedures that are presented in this section. In addition, a commercially available low volume-high velocity fume extraction system for the gas shielded process was evaluated. This system, however, did not require a design analysis.

IV.1 Crossdraft Table for Gas Shielded Arc Welding

Conceptually, the crossdraft table incorporates a flanged slot at the table surface in a manner that is similar to the slotted hood configuration shown in Figure 7 of USAS Z9.2 and Figure 4 -5 of the Industrial

Ventilation Manual. Figure 10 illustrates the conceptual design, as well as the geometric nomenclature. For the analysis, the height, width, and length of the welding bench were standardized as follows:

$$b = 36.5 \text{ in.}$$

$$L = 24 \text{ in.}$$

$$W = 21 \text{ in.}$$

These dimensions are typical of the welding benches that are used at SwRI for small-scale production jobs.

A parametric analysis of this system was then conducted using the performance equations specified in USAS Z9.2 and the Industrial Ventilation Manual. The capture velocity was fixed at 100 fpm at a working distance of 21 inches from the slot. The following equations were used in the analysis:

(1) $Q = K\ L\ W\ v_c$: system flow rate, cfm

where K is a suitable constant, and v_c is the capture velocity in fpm at a distance, W

(2) $V_{SLOT} = Q/(LS)$: slot velocity, fpm

(3) $V_{DUCT} = Q/A_{DUCT}$: duct velocity, fpm

(4) $VP_{SLOT} = \left(\frac{Q}{4005\ LS}\right)^2$: slot velocity pressure, inches of water gage

(5) $VP_{DUCT} = \left(\frac{Q}{4005\ A_{DUCT}}\right)^2$: duct velocity pressure, inches of water gage

(6) $h = S + h_f$: vertical baffle height, in.

where S is the slot height, and h_f is the flange width on the slot which was fixed at 3.0 in.

(7) $h_{e_t} = h_{e_{SLOT}} + h_{e_{TRANSITION}} = 1.78\ VP_{SLOT} + F(\Lambda)\ VP_{DUCT}$

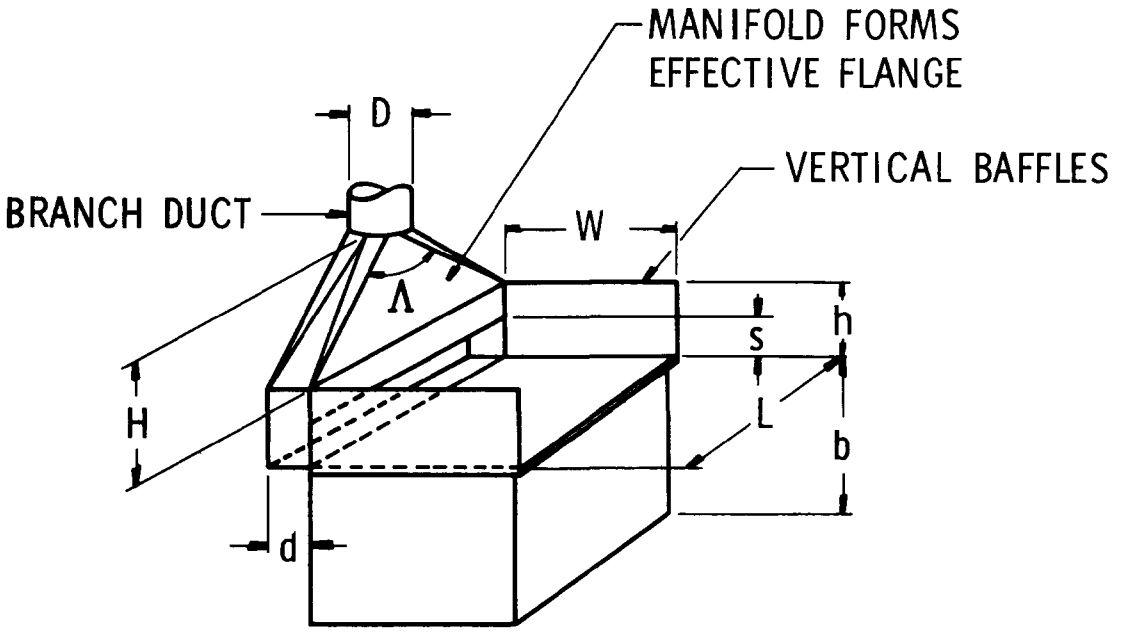

Figure 10. Crossdraft Table Nomenclature

where h_{e_t} is the total entry loss in inches of water gage and $F(\Lambda)$ is the dimensionless entry loss factor for the tapered transition section.

$$(8) \qquad F(\Lambda) = \frac{1 - C_e^2}{C_e^2}$$

where C_e is the coefficient of entry

$$(9) \qquad SP_h = h_{e_t} + VP_{DUCT} \quad : \text{ hood static pressure, inches of water gage}$$

$$(10) \qquad C_{e_{equiv}} = \sqrt{\frac{VP_{DUCT}}{SP_h}}$$

$$(11) \qquad H = \frac{L - D_{DUCT}}{2 \tan (\Lambda/2)} \quad : \text{ hood transition height, in.}$$

The effect of the vertical baffles could not be predicted quantitatively. However, their effect is to prevent entrainment of air from behind the hood and beneath the table. In sizing the flow rate, two values of K were evaluated because the literature does not clearly define the appropriate value for a crossdraft table, i.e., K = 1.6 or 2.8. Initially, all calculations were made for a transition angle, Λ, equal to 90°. The best system was selected for fixed Λ, and then the transition angle was perturbed to assess system sensitivity. The results of these performance calculations are shown in Figures 11, 12, and 13. As shown in Figure 13, hood static pressure is relatively insensitive to changes in the hood transition angle, Λ. This behavior is to be expected since the transition loss, $F(\Lambda)\ VP_{DUCT}$, is small compared to the duct velocity pressure and the slot entry loss. Therefore, a 90° transition angle was chosen. Design point values for system performance and geometry are given in Table IV for the two values of the flow constant, K. A duct diameter of 8 inches was selected because it produced a lower hood static pressure and entry loss than did the 6-inch duct diameter. An 8-inch hood depth, d, was selected because it coincided with the branch duct diameter, thus minimizing design and fabrication costs. A 3-inch slot height was chosen for the K = 1.6 configuration because the average slot velocity of 1120 fpm approximates the 1000-fpm value that is recommended in the Industrial Ventilation Manual. The hood that is shown in Figure 14 was fabricated

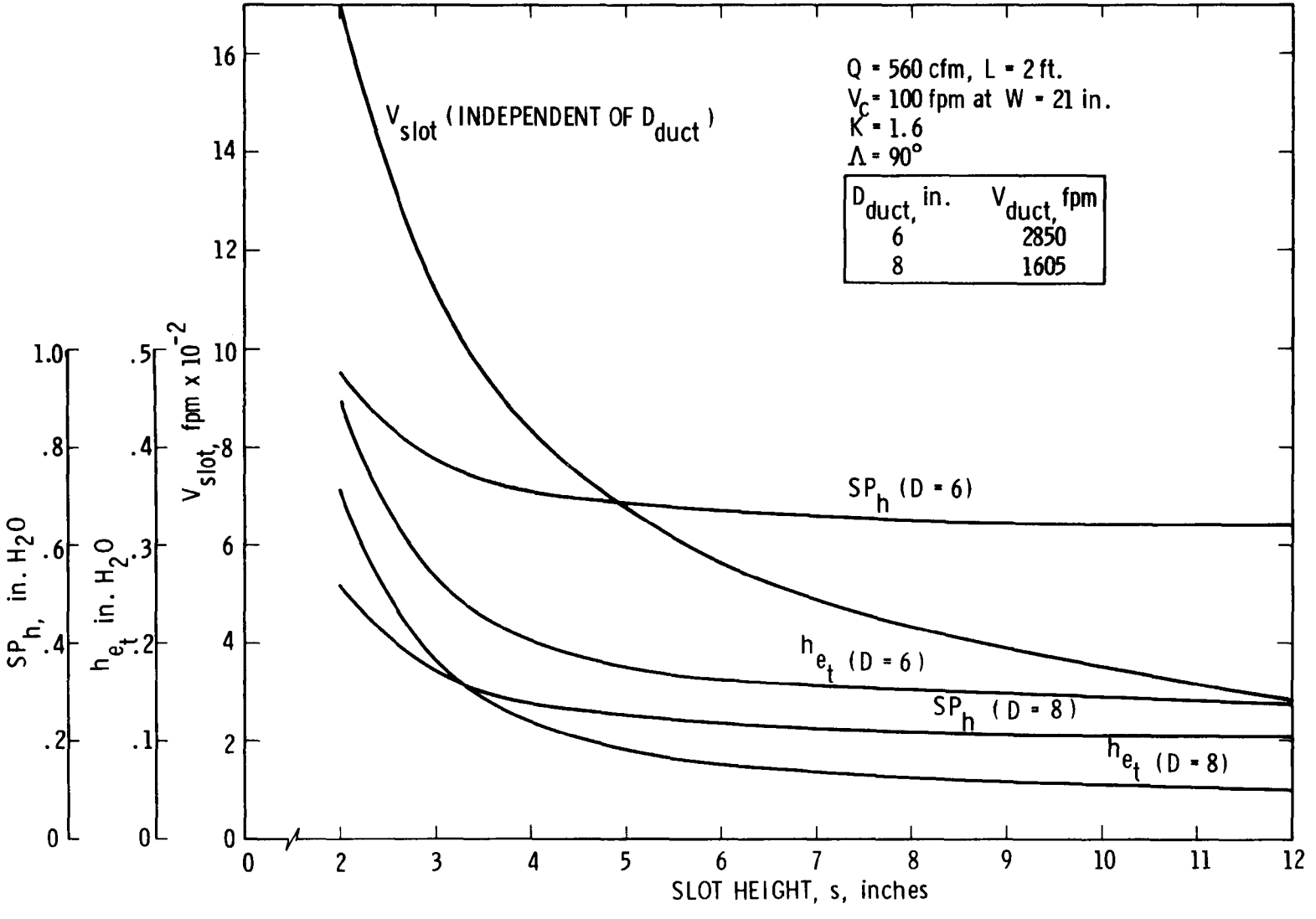

Figure 11. Predicted Crossdraft Table Performance (K = 1.6)

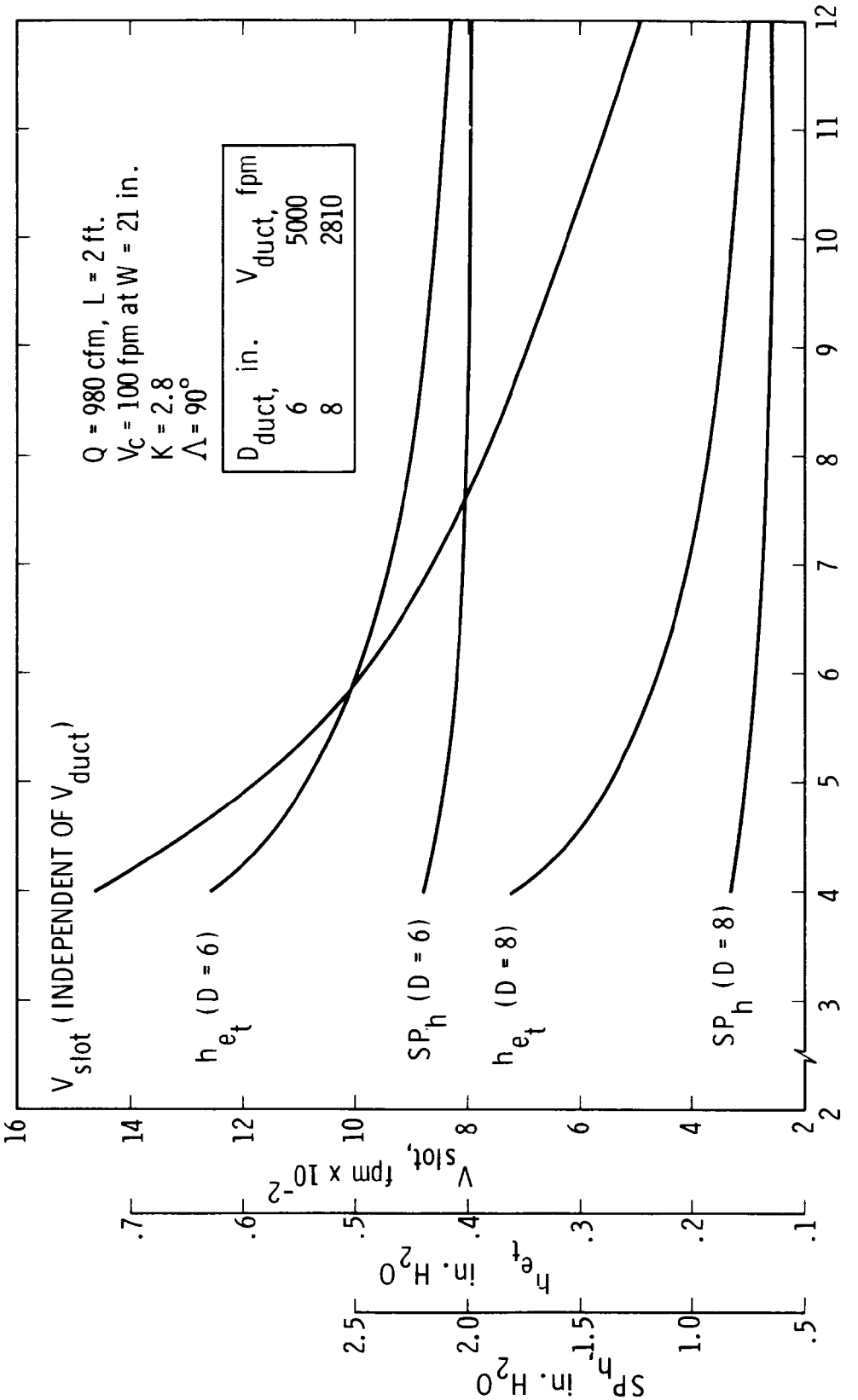

Figure 12. Predicted Crossdraft Table Performance (K = 2.8)

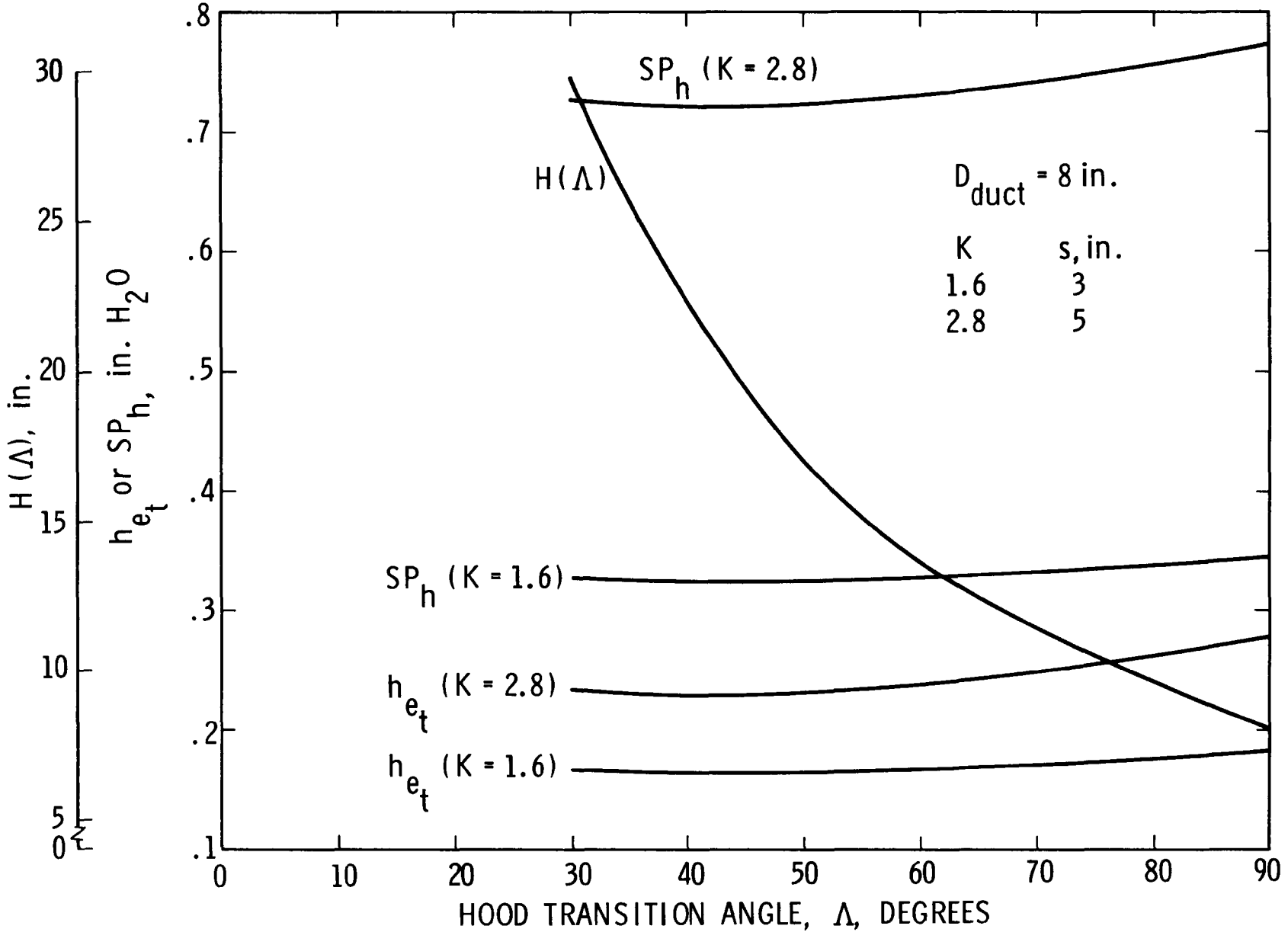

Figure 13. Crossdraft Table Performance As a Function Of Hood Transition Angle, Λ

TABLE IV.

DESIGN POINT PERFORMANCE FOR CROSSDRAFT TABLE

L	= 24 in.	D	= 8 in.
W	= 21 in.	b	= 36.5 in.
Λ	= 90°	d	= 8 in.
H	= 8 in.	V_c	= 100 fpm at W

	K = 1.6	K = 2.8
Q (cfm)	560	980
S (in.)	3	5
V_{SLOT} (fpm)	1120	1180
V_{DUCT} (fpm)	1605	2810
h (in.)	6	8
VP_{SLOT} (in. H_2O)	0.0785	0.0865
VP_{DUCT} (in. H_2O)	0.161	0.493
h_{e_t} (in. H_2O)	0.182	0.277
SP_h (in. H_2O)	0.343	0.770
$C_{e_{equiv}}$	0.685	0.80

Figure 14. Slotted Hood for Crossdraft Table

for the K = 1.6 configuration using galvanized sheet metal with rolled edges and soldered joints. The interior surface is aerodynamically clean. A 12-inch section of 8-inch diameter ducting was soldered to the hood at the transition plane in order to facilitate mating of the hood and branch duct.

During the design analysis, the horizontal and vertical duct transport velocities were calculated using the relationships given on page 21 of USAS Z9.2. The following equations apply:

$$V_{VERTICAL} = 4380 \sqrt{Sd}$$

$$V_{HORIZONTAL} = 6000 \left(\frac{S}{S+1}\right) d^{0.398}$$

where S is the specific gravity relative to air and d is the particle diameter in inches. Prandtl[6] suggests that a specific gravity ratio of 700 to 2400 is appropriate for airborne particles. Welding fumes may be assumed to be airborne particles. For a particle diameter of 1u, the following values were calculated:

	S = 700	S = 2400
V_{VERT} (fpm)	695	1287
V_{HORIZ} (fpm)	102	102

Particle specific gravity has negligible effect on horizontal transport velocity. Comparison of the vertical transport velocities with the design duct velocities indicates that particle settling should not be a problem.

IV.2 Free-Standing Hood for Shielded Manual Metal Arc Welding

A free-standing hood was defined as a local ventilation hood whose longitudinal axis of symmetry is oriented at an oblique angle to the horizontal plane of the welding bench. It is not intended that this class of hood be operated in a canopy mode. In fact, all tests involving this class of hood were conducted at a 45° elevation angle. During the design analysis, both flanged-rectangular and flanged-circular hoods were evaluated. Unflanged concepts were not considered because of the excessive entrainment of air from behind the hood that is associated with such configurations.

The method of predicting the performance of these systems was similar to that which was used on the crossdraft table. The following capture velocity equations from Reference 4 were used:

$$V_{FACE} = V_c \left[\frac{x^{1.5}}{c\, A_H^{0.82}} + 1 \right] \qquad \underline{\text{FLANGED RECTANGULAR}}$$

$$V_{FACE} = V_c \left[\frac{x^{1.91}}{0.0825\, A_H^{1.04}} + 1 \right] \qquad \underline{\text{FLANGED CIRCULAR}}$$

where x is the capture or stand-off distance in inches, A_H is the hood face area in in.^{2}, V_{FACE} is the average hood face velocity which has the same physical units as the capture velocity.

The variable, c, in the rectangular hood equation is a function of hood aspect ratio as given in Reference 4. The following additional changes in the design equations are applicable to the free-standing hood:

(1) $Q = V_{FACE}\, A_H$

(2) $VP_{FACE} = \left(\frac{Q}{4005 A_H} \right)^2$

(3) $h_{e_t} = F(\Lambda)\, VP_{DUCT}$

System performance for the circular hood is shown in Figures 15 and 16. Similar curves for the rectangular hood are included in Figures 17 and 18. The 16 x 16-inch rectangular hood has the same face area as the 18-inch diameter circular hood. For future reference, it should be noted that the design equations are idealistic in that they are based on an unobstructed suction flow field. The implications of this observation are discussed later. The effect of varying the hood transition angle was judged to be insignificant based on the previous analysis. Therefore, Λ was fixed at 90°.

Performance parameters for the most practical circular and rectangular hoods are summarized in Table V. The rectangular design

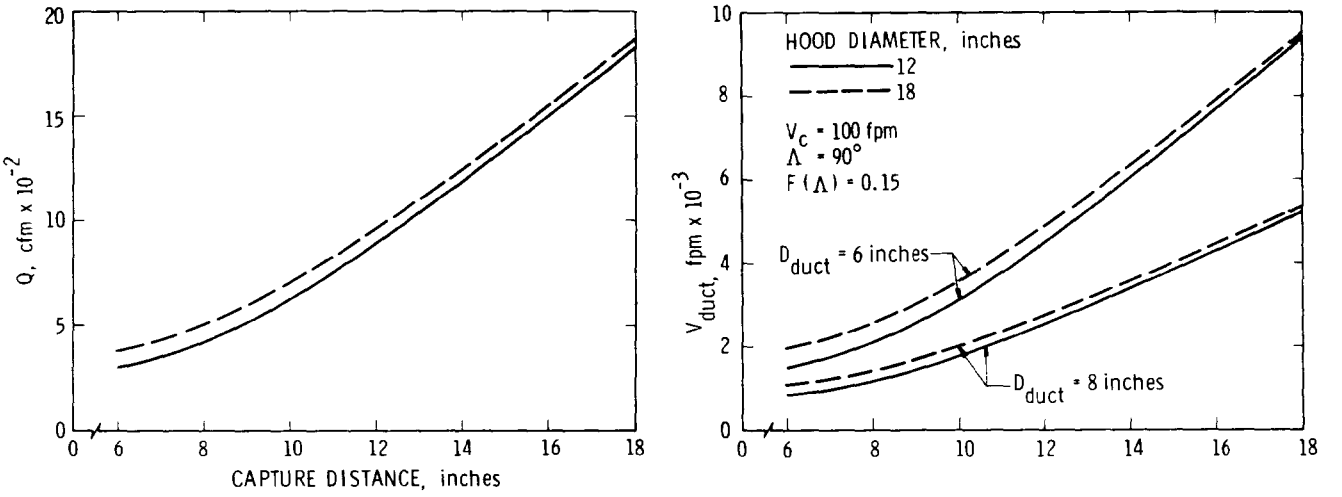

Figure 15. Predicted Performance Of a Round, Flanged Local Hood

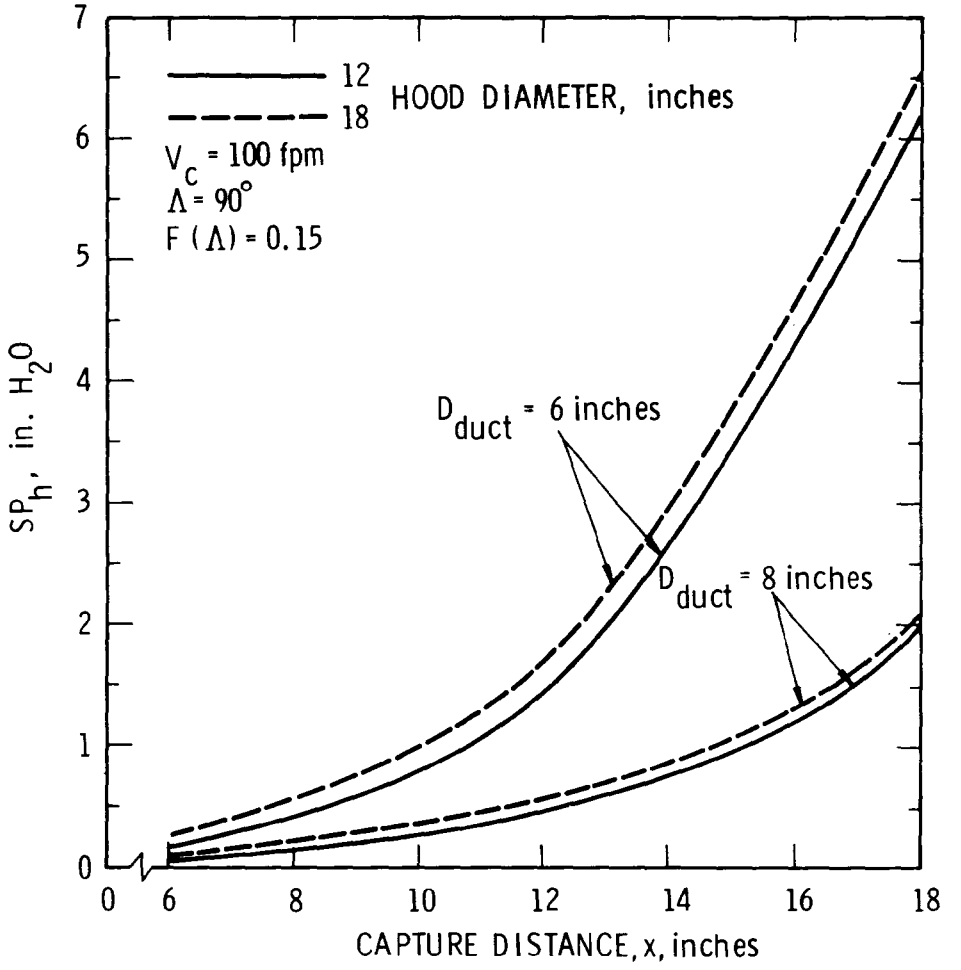

Figure 16. Predicted Performance Of a Round, Flanged Local Hood (Continued)

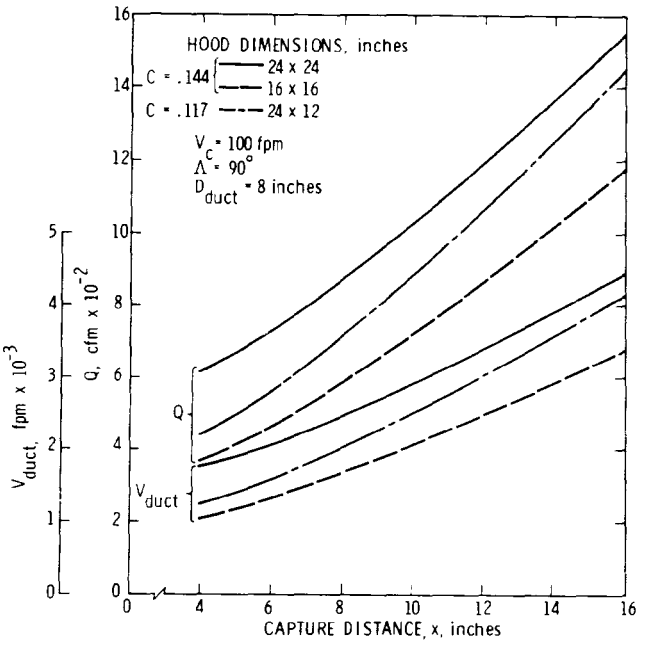

Figure 17. Predicted Performance for a Rectangular, Flanged Local Hood

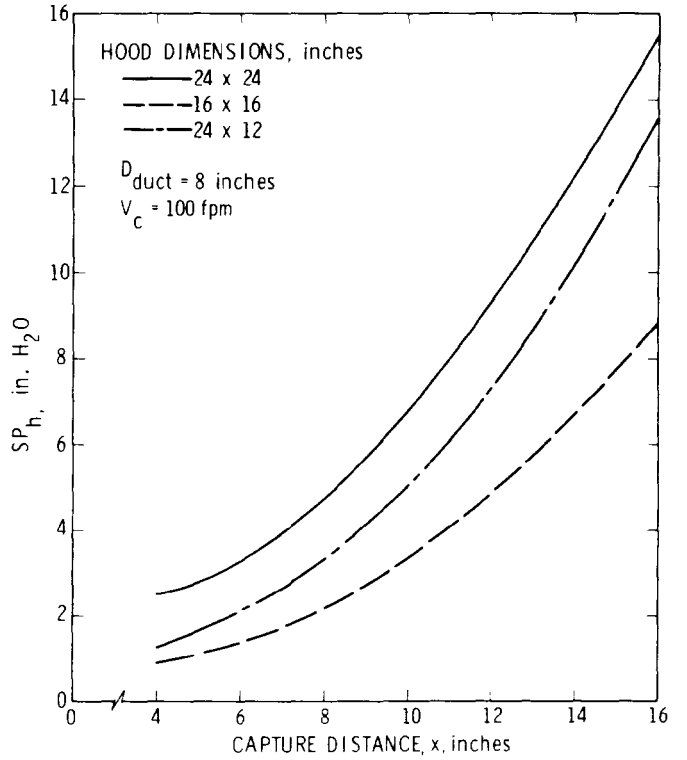

Figure 18. Predicted Performance for a Rectangular, Flanged Local Hood (Continued)

TABLE V.

DESIGN POINT PERFORMANCE FOR
BEST RECTANGULAR AND ROUND HOODS

	Round	Rectangular
V_c (fpm)	100	100
x (in.)	12	12
Face Dimensions (in.)	18	24 x 12
D_{DUCT}	8	8
Q (cfm)	953	884
V_{DUCT} (fpm)	2730	2532
VP_{DUCT} (in. H_2O)	0.466	0.400
V_{FACE} (fpm)	539	442
h_e (in. H_2O)	0.070	0.099
SP_h (in. H_2O)	0.536	0.499
Λ (°)	90	90
H (in.)	5	8
Flange width (in.)	6	6
C_e	0.932	0.896

was selected for testing on the following basis:

(1) The rectangular hood produces the required capture velocity with the smallest air flow rate.

(2) The larger rectangular hood provides ventilation over the entire length of the welding table.

Figure 19 contains a photograph of the rectangular hood. A 6-inch flange borders the 12 x 24-inch hood face. As noted, the major transition angle is 90°. A minor transition angle of approximately 28° was required in order to mate the 12-inch face height with the 8-inch duct diameter in a vertical distance of 8 inches. As before, galvanized sheet metal construction was utilized.

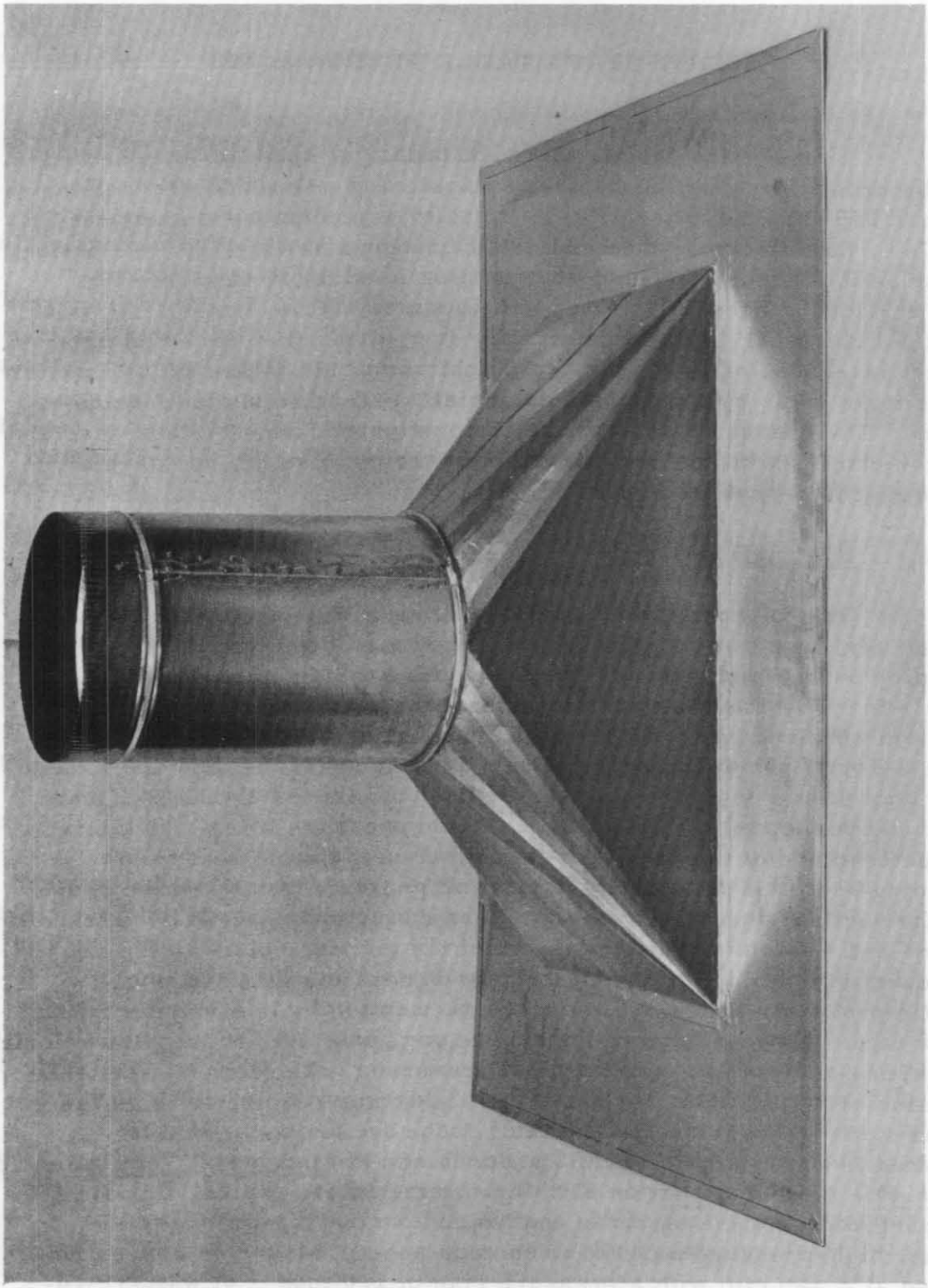

Figure 19. Flanged Rectangular Hood

V. CROSSDRAFT TABLE PERFORMANCE

This section describes the installation, calibration and testing of the crossdraft ventilation table as applied to gas shielded arc welding with 0.045-inch diameter, E-70S-4, solid wire electrodes. As stated earlier, this electrode size and classification was selected for evaluation because it produced the largest breathing level additive effect for the gas shielded processes. It was hypothesized that if the fumes from this critical combination could be effectively controlled, then lower additive effect levels for other size-class combinations would follow suit. Breathing zone fume samples were obtained during all ventilation system evaluations. The exhauster system and calibration procedures that are described in conjunction with the crossdraft table are common to the rectangular hood that is described in Section VI.

V.1 System Installation

The assembled crossdraft table ventilation system (hood plus exhauster) is shown in Figure 20. The slotted hood was mounted on the welding bench, and vertical baffles were added to minimize entrainment of air from behind the hood and underneath the table, thus improving system efficiency by focusing the capture velocity field on the welding site. Four flush-mounted, coplanar hood static pressure taps are located one duct diameter downstream from the hood transition plane. All four of these ports are manifolded into a common pressure line which connects directly to one of the pressure gages located on the table next to the welding bench. Flush-mounted pitot-static pressure ports are located in the vertical ducting, 7.5 duct diameters downstream of the hood transition plane and 3.0 duct diameters upstream of the entrance plane to the 180° elbow at the ceiling. These ports provide access for pitot and pitot-static probe traverses of the duct cross section to obtain a volumetric flow rate. A second differential pressure gage was used to monitor velocity pressure or dynamic head during these traverses. The lengthy vertical section of 8-inch diameter sheet metal ducting was required so that the hood static pressure ports and the pitot probe access port could be located in accordance with ASTM Standards and the Industrial Ventilation Manual. A 10-foot section of 8-inch diameter, fabric coated, flexible ducting connects the output of the branch duct to the input of a radial vane, high-pressure blower. The constant-speed, 3450-rpm blower is rated at 2,140 cfm with a pressure rise of 1.0 inch of water. The shallow head-flow curve declines to 1,620 cfm at 6.0 inches of water.

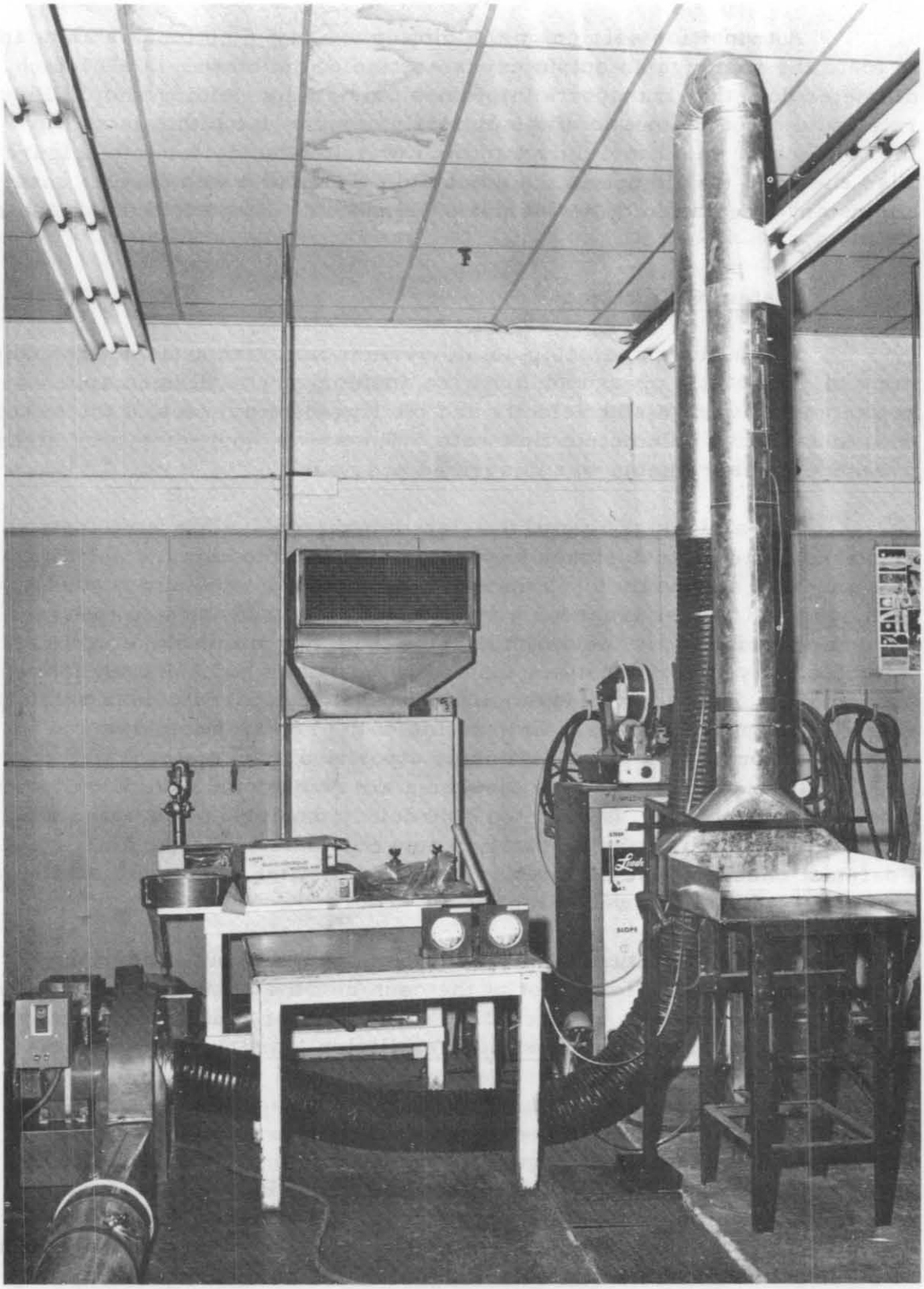

Figure 20. Crossdraft Ventilation System Assembly

A transition section on the blower exhaust functions as an adapter to mate the rectangular output cross section of the blower to a 10-inch diameter duct that transports the fumes outside the welding shop. Flow rate is adjusted by means of the butterfly damper valve that is shown in the circular sheet metal duct in the lower left-hand corner of Figure 20. Also shown in that figure is the adjustable T-bar that was used to ensure a constant orientation of the welder's helmet with respect to the arc during all tests.

V.2 System Calibration

For a given operating point, system calibration included measurement of hood static pressure, hot wire anemometry to define capture velocity and average slot velocity and pitot probe traverses of the branch duct to establish volumetric flow rate. The arrangement for hood static pressure measurements was described previously.

For a given setting of the flow damper valve, hot wire instrumentation, specially designed by SwRI, recorded the capture velocity at a height of approximately 1 inch above the bench level and a working distance of 21 inches from the hood slot. It was necessary to measure capture velocity above the bench surface in order to minimize errors in the velocity reading that are caused by boundary layer and turbulence phenomena. This hot wire system has a proven capability over a velocity range of 20 fpm to 300 fps. Calibration of the hot wire itself was accomplished prior to a given test using a positive displacement water tank. Water entering the tank displaces air through an orifice with known flow characteristics. The hot wire circuit is described in Appendix B. An example of a hot wire calibration curve is shown in Figure 21. Post-test checks of the calibration revealed that the electronic system and probe characteristics were stable.

After the capture velocity had been established, the hot wire was used to probe the hood slot at the center of the 16 equal rectangular areas that are shown in Figure 22. The number of equal area rectangles was determined from the Industrial Ventilation Manual. These areas, which measured 1.5 by 3 inches, were marked off using thin, polyester-coated thread so as not to disturb the flow. Average slot velocity was then obtained from these 16 measurements. An example of a hot wire voltage profile is shown in Figure 23 for a system capture velocity of 100 fpm. Note that the profile is quite uniform. For this case, the maximum and minimum velocity measurements were 1800 and 1550 fpm, respectively. Also evident in Figure 22 is a chalk marker at the center of the bench edge which defines the point at which capture velocity was measured.

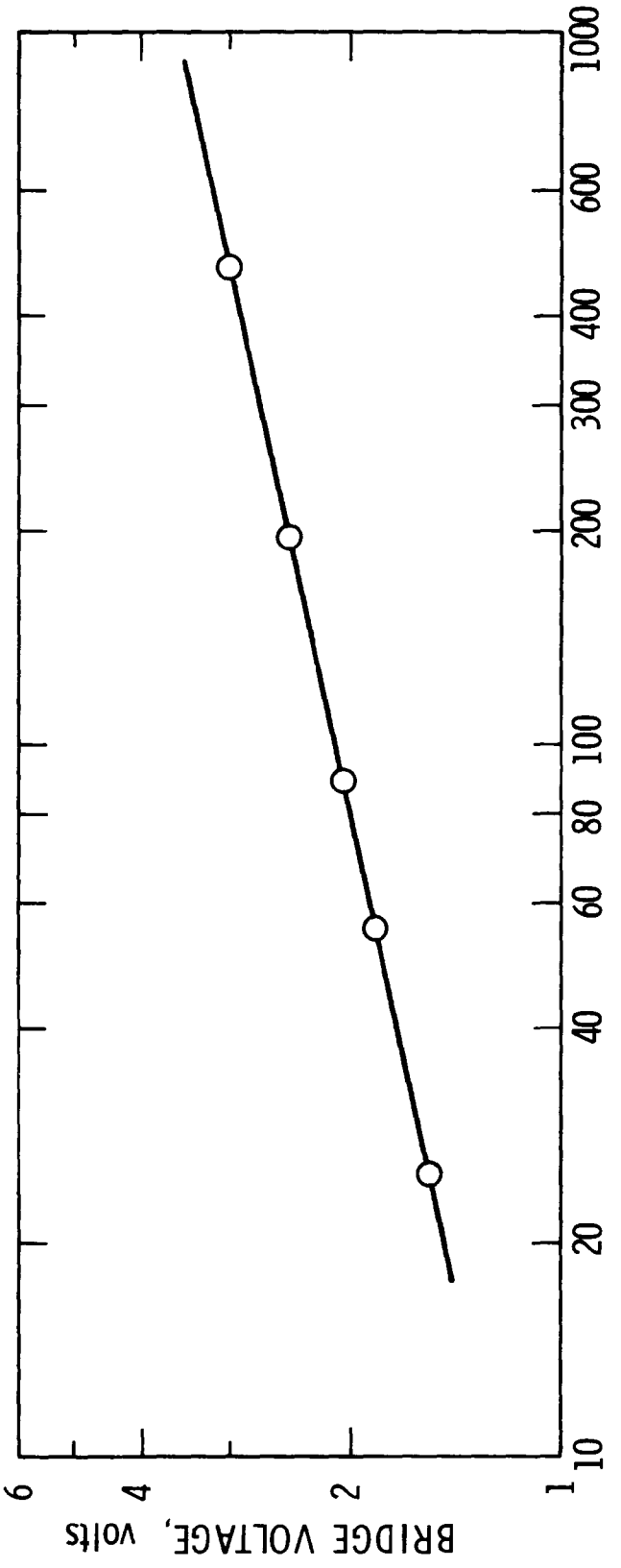

Figure 21. Example Hot Wire Anemometer Calibration Curve

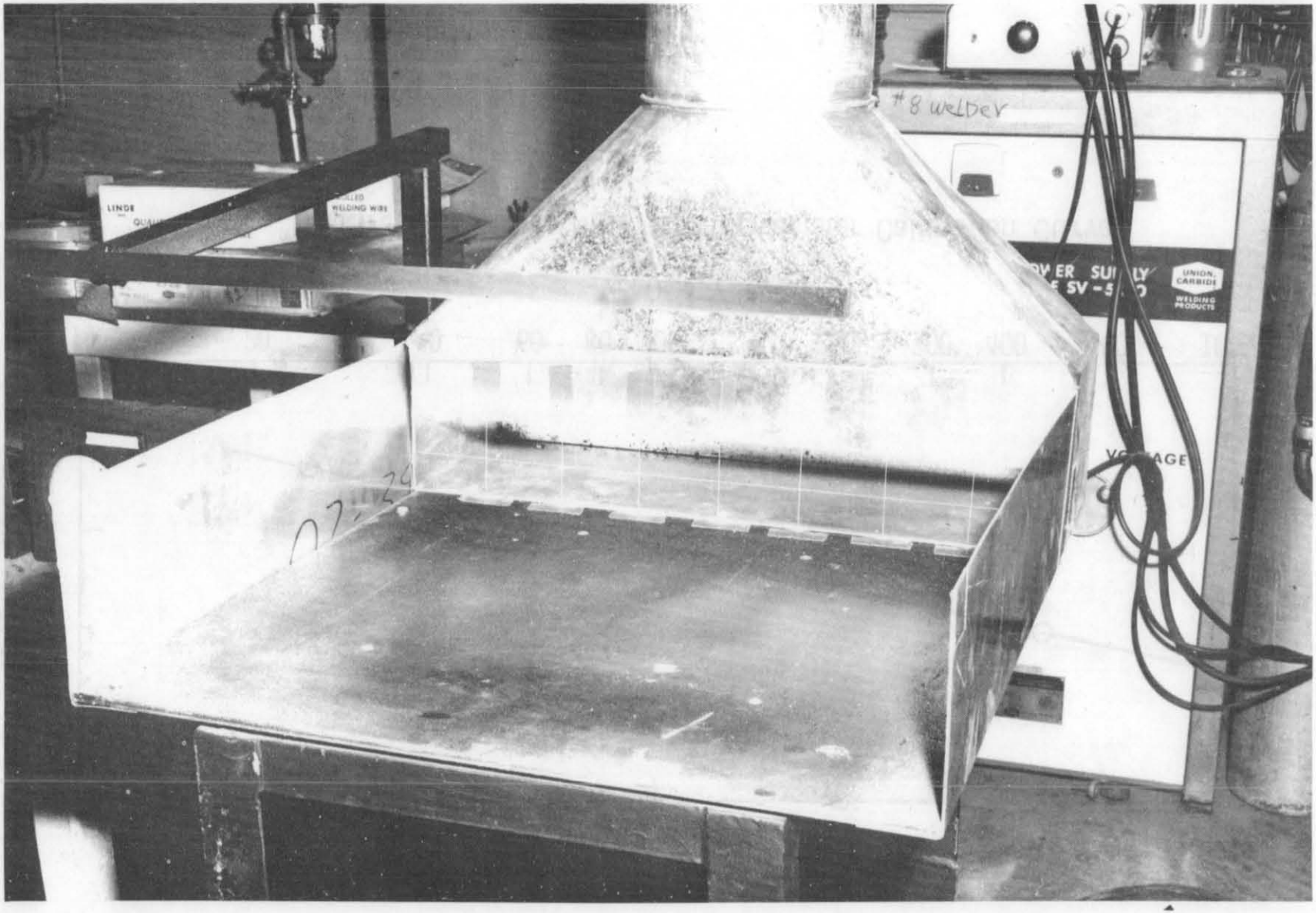

Figure 22. Crossdraft Table With Grid For Hot Wire Traverse

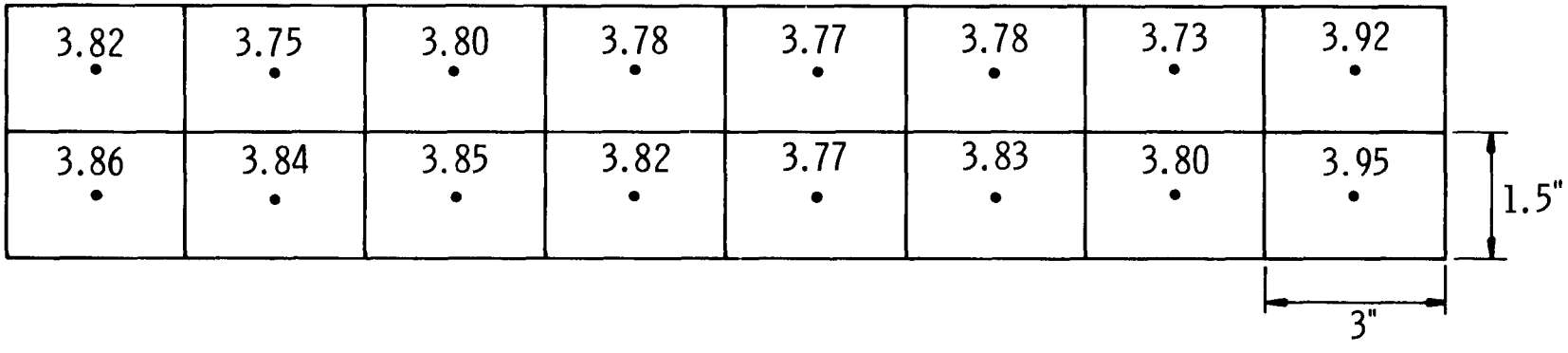

NOTE:

1) NOT TO SCALE
2) AVERAGE VOLTAGE = 3.82 v
3) AVERAGE SLOT VELOCITY = 1650 fpm
4) V_c = 100 fpm

Figure 23. Hot Wire Slot Voltage Profile For The Crossdraft Table

Two methods were utilized to measure flow rate in the branch duct. Both methods were based on the 10-point orthogonal traverse that is given in Table 9-1 of the Industrial Ventilation Manual for an 8-inch duct diameter. Traverse axes were perpendicular and parallel to the hood slot. The first method involved a pitot probe traverse using wall static as reference, while the second method utilized a pitot-static traverse with local flow static pressure as reference. Flow rate, calculated by these two traverse methods, agreed to within 1 percent. The velocity profile parallel to the slot has a high degree of symmetry. There is a slight asymmetry to the velocity profile normal to the slot. Table VI illustrates typical velocity pressure profiles and flow rates that were obtained with these two methods. The fact that the two flow rates are nearly the same indicates that, at the traverse station, the static pressure profile in the duct is highly symmetric. These two values were then averaged to obtain the system flow rate.

The velocity data in Table VI are referred to standard atmospheric conditions since they were derived from the standard velocity pressure equivalence table in the Industrial Ventilation Manual (Figure 6-16). Theoretically, these data should be corrected to the non-standard conditions that existed during the calibration and test. This possibility was evaluated and was found to have negligible impact on the experimental results. For example, during one test, the following atmospheric conditions prevailed:

Local station pressure = 29.65 in. Hg

Dry bulb temperature = 72°F

Relative humidity = 84 percent

The decrease in air density at the non-standard conditions is

$$\frac{\rho}{\rho_{SL}} = \left(\frac{460 + 70}{460 + 72}\right)\left(\frac{29.65}{29.92}\right) = .987$$

For an experimental flow rate of 845 cfm, the weight flow of the air-water mixture is

$$W = 845 \text{ cfm } (0.075 \text{ lb/ft}^3)\ (.987) = 62.55 \text{ lb/min}$$

From a psychrometric chart at the stated conditions, there are 0.0145 pounds of water per pound of dry air. Therefore, the weight flow of dry air is

TABLE VI

BRANCH DUCT FLOW RATE CALIBRATION

Pitot Probe Plus Wall Static

	N-S		E-W	
Point No.	VP (in. H_2O)	V (fpm)	VP (in. H_2O)	V (fpm)
1	.27	2081	.305	2210
2	.37	2436	.40	2533
3	.39	2501	.43	2626
4	.39	2501	.43	2626
5	.39	2501	.415	2579
6	.395	2515	.375	2452
7	.39	2501	.36	2403
8	.39	2501	.34	2335
9	.375	2452	.31	2230
10	.33	2301	.26	2042

V_{ave} = 2414 fpm Q_{ave} = 843 cfm

Pitot-Static

	N-S		E-W	
Point No.	VP (in. H_2O)	V (fpm)	VP (in. H_2O)	V (fpm)
1	.305	2211	.300	2193
2	.380	2469	.400	2533
3	.400	2533	.430	2626
4	.400	2533	.430	2626
5	.400	2533	.425	2610
6	.400	2533	.385	2485
7	.400	2533	.370	2436
8	.400	2533	.350	2369
9	.380	2469	.320	2260
10	.305	2211	.225	1900

V_{ave} = 2430 fpm Q_{ave} = 848 cfm

$$\dot{W}_{\text{dry air}} = \frac{60.55}{1.0145} = 61.66 \text{ lb/min.}$$

The corrected flow rate is

$$Q_{CORR} = \frac{61.66}{0.075} = 822 \text{ cfm}$$

The corrected flow rate is within 2.7 percent of the experimental value. The Industrial Ventilation Manual recommends correcting the flow rate only if the following conditions exist

(1) The air temperature is below 40°F or above 100°F

(2) If the moisture content exceeds 0.02 pounds of water per pound of dry air or

(3) If the local station pressure deviates from 29.92 inches Hg by an equivalent of 1000 ft of altitude.

None of these conditions were encountered during testing; therefore, all ventilation system flow rate data were taken as calibrated.

V.3 Test Protocol and Experimental Results

The strategy for testing the crossdraft system was to obtain breathing zone fume samples in the absence of local ventilation, followed by sample collection in the presence of ventilation at several system operating points. Welding was conducted both perpendicular and parallel to the hood slot to assess the capture efficiency for these two modes.

Reference to Section IV.1 indicates that the preliminary design calculations considered two values of the constant K , i.e., K = 1.6 and 2.8. The system was constructed in accordance with a K of 1.6. However, based on experimentally determined capture velocities and flow rates, this constant was consistently calculated to be 2.42. This discrepancy points out the arbitrary nature of that constant in the design flow rate-capture velocity equation and the necessity to reevaluate empirical constants for each application. Table VII summarizes the actual operating states of this ventilation system.

TABLE VII

CROSSDRAFT TABLE TEST CONDITIONS

V_c (fpm)	62.3	100	116	146.3
Q (cfm)	528	845	983	1239
V_{DUCT} (fpm)	1511	2422	2816	3548
VP_{DUCT} (in. H_2O)	0.143	0.366	0.494	0.785
V_{SLOT} * (fpm)	1056	1690	1966	2478
VP_{SLOT} ** (in. H_2O)	0.070	0.178	0.240	0.384
SP_h (in. H_2O)	0.265	0.670	0.950	1.53
C_e	0.734	0.739	0.719	0.717
h_e (in. H_2O)	0.122	0.304	0.456	0.745

For each of these test conditions, plus the no-ventilation case, a minimum of six fume samples were collected in the breathing zone and analyzed by AAS for Fe, Mn and Cu. The resulting concentrations were expressed in additive form following the procedures that were outlined earlier. The basic concentration data for this system are contained in Appendix C. The effect of the local ventilation rate on the breathing zone fume concentration is shown in Figure 24. The following statements apply to the crossdraft table performance:

(1) System performance reflects 100 percent arc time.

(2) It is well known[7, 8] that the helmet provides a measureable level of protection for the welder by acting as a

---

* Calculated from Q.

** Calculated from V_{SLOT}.

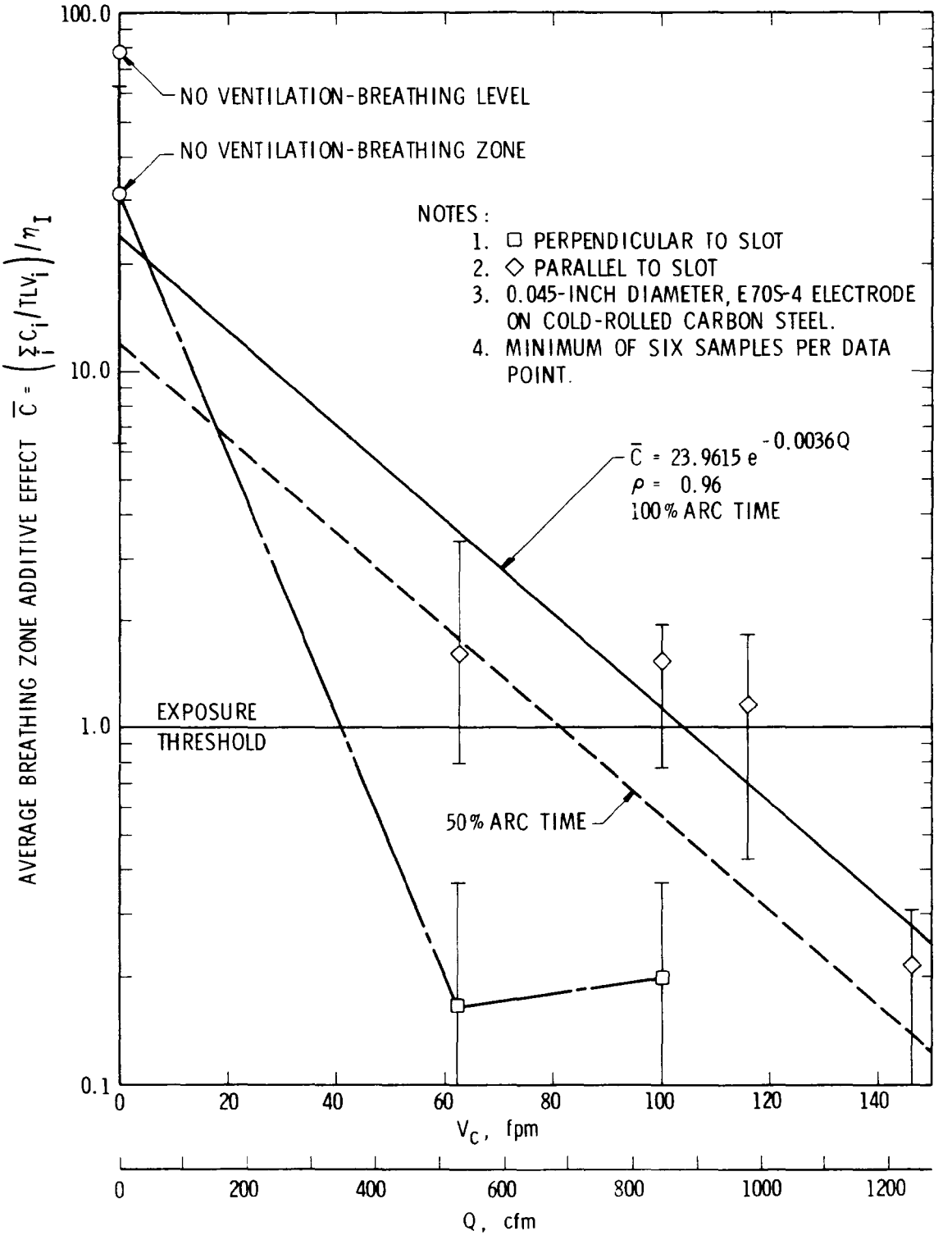

Figure 24. Breathing Zone Additive Effect as a Function of Crossdraft Ventilation Flow Rate

fume attenuator. For this gas shielded process, the ratio of breathing level to breathing zone fume concentration in the absence of local ventilation was approximately 2.50.

(3) For all system operating points, welding perpendicular to the hood slot is more efficient than welding parallel to the slot. This result was anticipated because in the former mode the velocity vector of the shielding gases and fumes are nearly colinear with the capture velocity vector, whereas, in the latter mode these vectors are more nearly orthogonal. An interesting observation was made for the perpendicular mode. While welding toward the slot, a point was reached where the suction flow field had sufficient strength to remove the shielding gas around the arc, thus producing an unacceptable weld bead and an unvalid fume sample. The calculated capture velocity at that point (10 inches from the slot) was approximately 200 fpm which coincides with the maximum capture velocity recommended in USAS Z9.2. This observation should be taken into account on any permanent installation of a crossdraft table. Only valid data points are presented in this report.

(4) For the parallel mode, the data were subjected to regression analysis which yielded an exponential decay of fume concentration with an increasing ventilation rate. The correlation coefficient is 0.96 for the indicated regression equation.

(5) For a 100 percent arc time, a minimum capture velocity of 104 fpm is needed in the parallel mode to reduce breathing zone concentrations below the exposure threshold. This capture velocity is in excellent agreement with the 100 fpm standard recommended in USAS Z49.1[9]. The corresponding flow rate is 882 cfm. A more realistic time of 50 percent indicates that a minimum capture velocity of 80 fpm at 678 cfm may be adequate.

(6) The data in Figure 24 are referenced to the TLV values published by the American Council of Governmental Industrial Hygienists (ACGIH). It is well known that many of these limits are not absolute. The accepted excursion factors for iron oxide and copper are 2.0

and 3.0, respectively. Manganese has no excursion factor since its TLV is a ceiling value. Utilizing these increased TLV's in the analysis would result in a significant reduction in the breathing zone additive effect for 100 percent arc time. For example, at a capture velocity of 100 fpm, the following average breathing zone concentrations were observed:

Element	C_i (mg/m^3)
Fe	0.947
Cu	0.0167
Mn	0.028

Utilizing the excursion factors, the normalized concentration summation becomes

$$\frac{\Sigma \frac{C_i}{TLV_i}}{n_I} = \frac{\frac{0.947 \times 2.86}{2 \times 10} + \frac{0.028}{5} + \frac{0.0167}{3 \times 0.1}}{0.29} = 0.678$$

Compare this figure with the additive effect of 1.53 that was calculated without the use of excursion factors. The point to be made is that the use of excursion factors may result in an underestimate of the flow rate. Flow rates obtained without the use of excursion factors provide a desirable margin of safety.

Figures 25 and 26 illustrate the unquestionable benefit of using the crossdraft ventilation system. In the absence of local ventilation (Figure 25), copious quantities of fume are evident. These fumes not only represent a potential health hazard but their presence also obscures the welder's view of his work. In Figure 26, the ventilation system is shown at an operating point corresponding to a 100-fpm capture velocity in the parallel mode. The ventilation system has eliminated the vertical rise of fumes to the breathing level. Instead, the fumes travel toward the slot in a sheet. This sheet flow behavior was observed at all system operating points; the apparent thickness of the sheet diminishes with increasing flow rate or capture velocity.

Recommendations for any ventilation system must reflect the subjective evaluations of the users, i.e., the welders. Their evaluations were:

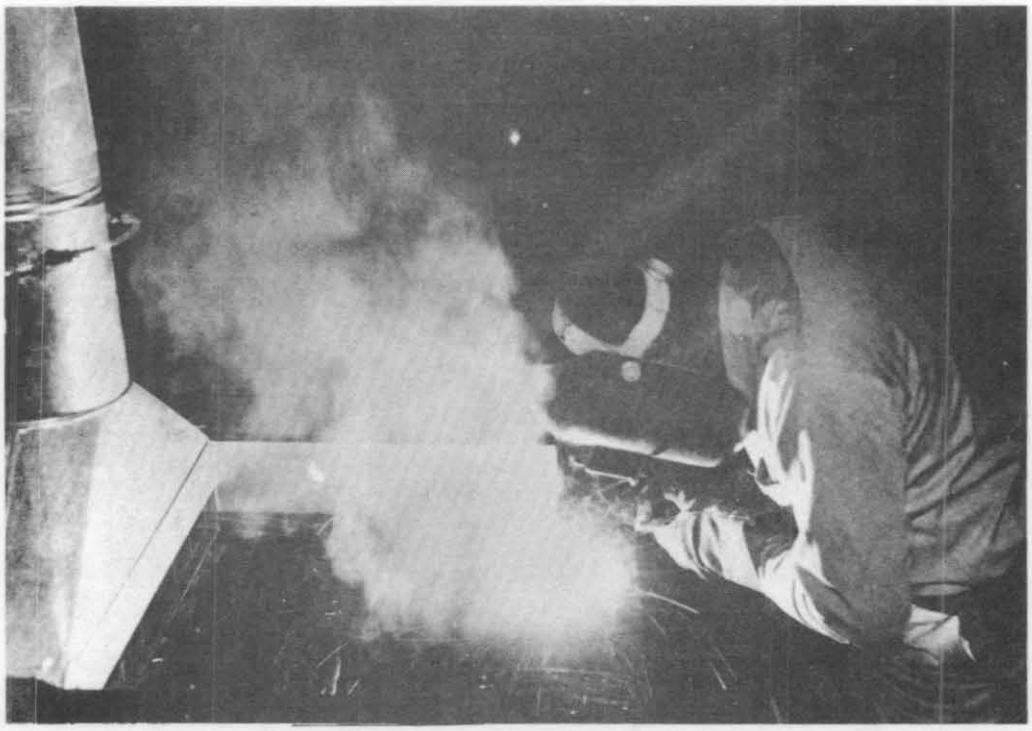

Figure 25. Fume Cloud From Gas Shielded Arc Welding Process

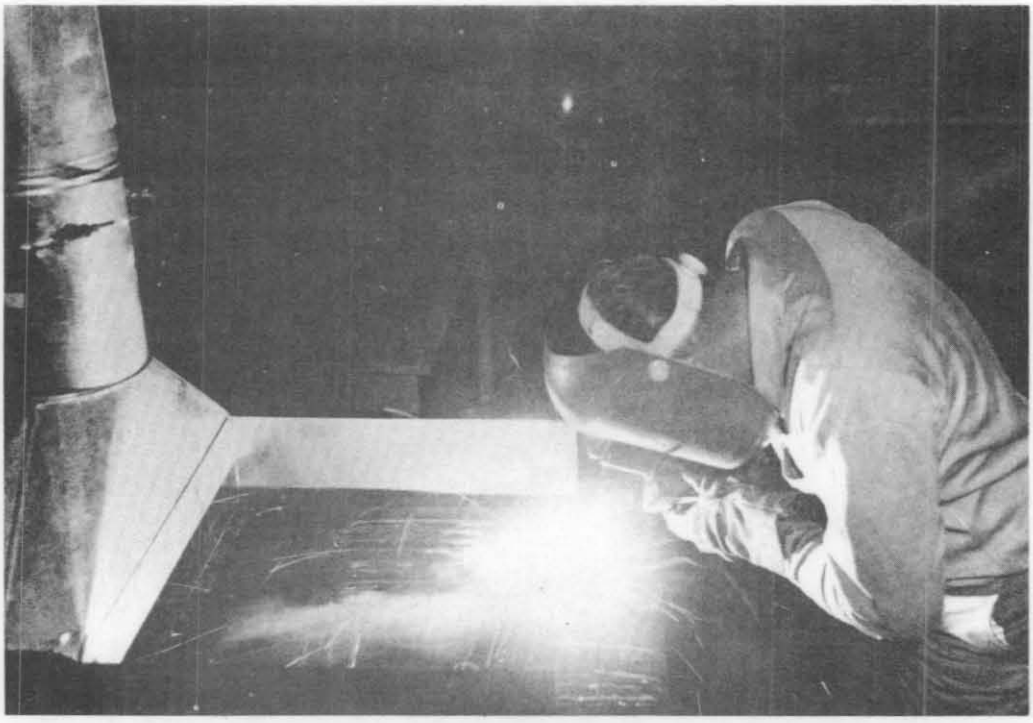

Figure 26. Fume Control With Local Crossdraft Ventilation

(1) This system was convenient to use.

(2) They could not detect the smell of fumes in the breathing zone.

(3) Fume extraction permits an unobscured view of the arc and the metal to be welded.

VI. FREE-STANDING RECTANGULAR HOOD

This section describes the installation and performance testing of the free-standing rectangular hood. The effectiveness of this hood in reducing breathing zone fume concentrations was determined using 3/16-inch diameter, E-7018 electrodes on carbon steel and 1/8-inch diameter, E-308-15 electrodes on stainless steel. The calibration procedures for this system are identical to those that were employed on the crossdraft table. Concentration data for this system are summarized in Appendix D.

VI. 1 System Installation

Figure 27 shows the rectangular hood installed in the test facility. The longitudinal axis of the branch duct was fixed at a 45° angle with respect to the welding bench. In this position, the hood face area is nearly equal to a 45° projection of the table surface onto the hood face. The hood stand-off distance, i.e., the distance between the center of the hood face and the center of the welding bench, was designed to be adjustable. Stand-off distances of 12 and 18 inches were evaluated. The hot wire anemometer instrumentation and calibration tank can be seen on the table to the left of the hood in Figure 27. Figure 28 shows a close-up of the hood face and welding bench. The hood face contains a grid of 16 equal area rectangles (3 by 6 inches) for the hot wire traverses. The chalk marks on the bench define the tack of the welding bead, as well as the point at center of the table where capture velocity was measured. Table VIII summarizes the experimental test conditions for the 12 and 18 inch stand-off distances. The rectangular hood is more efficient aerodynamically than the crossdraft table, as evidenced by the significant reduction in entry loss, h_{et} relative to the crossdraft table. A typical hot wire voltage profile for the hood face is shown in Figure 29.

VI. 2 Hood Performance for E-7018 Electrodes

The performance of this system combination, which was much more efficient than had been anticipated, is shown in Figure 30. Breathing zone additive effect is shown as a function of duct flow rate and stand-off distance for a 100-percent arc time. Note that the welding helmet provides a significant level of protection as indicated by a sevenfold reduction in fume concentration from the breathing level to the breathing zone. The effectiveness of the ventilation system is demonstrated by the fact that,

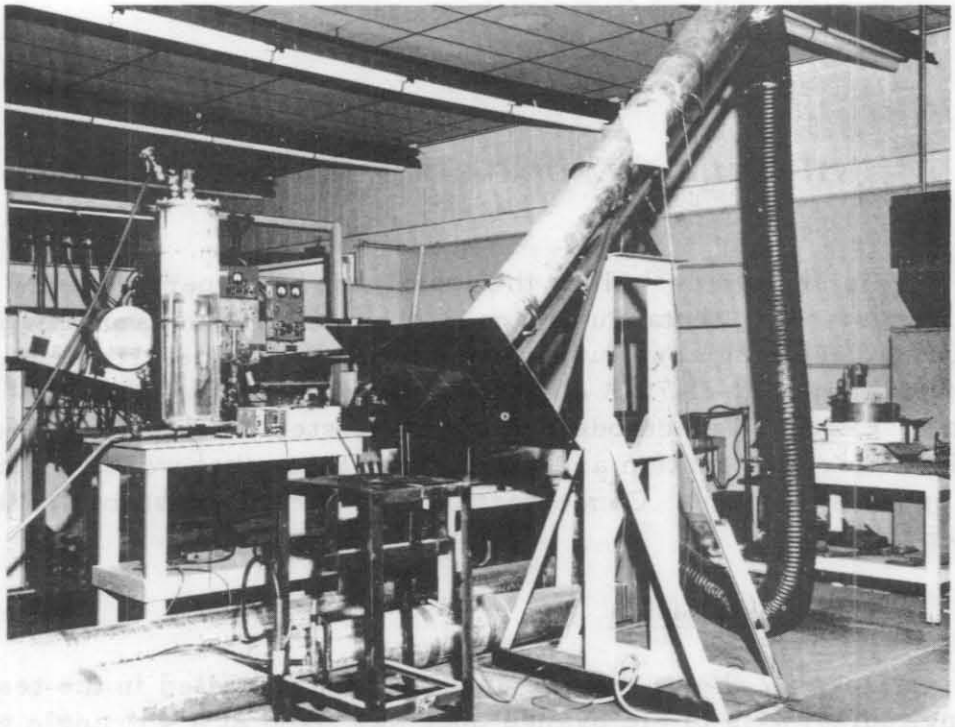

Figure 27. Rectangular Ventilation Hood System Assembly

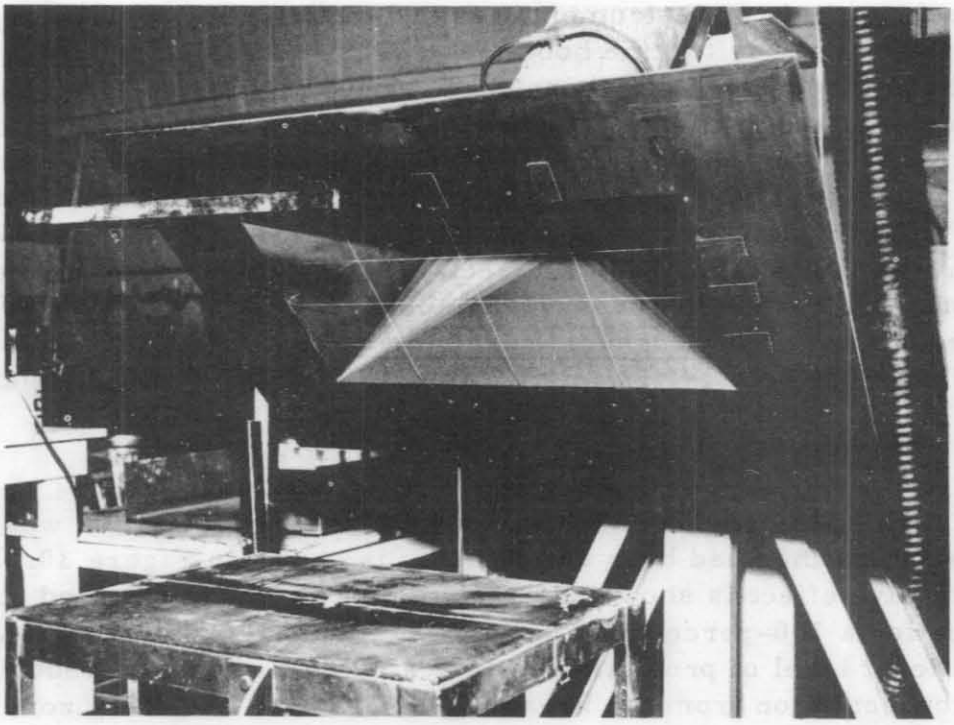

Figure 28. Rectangular Hood Face With Grid For Hot Wire Traverse

TABLE VIII

RECTANGULAR HOOD TEST CONDITIONS

	Stand-Off Distance = 12 inches	
V_c (fpm)	60	105
Q (cfm)	589	915
V_{DUCT} (fpm)	1686	2577
VP_{DUCT} (in. H_2O)	0.177	0.414
SP_h (in. H_2O)	0.19	0.44
C_e^*	0.966	0.970
$h_{e_t}^*$ (in. H_2O)	0.013	0.026
V_{FACE} (fpm)	265	465
VP_{FACE}^* (in. H_2O)	0.004	0.013

	Stand-Off Distance = 12 inches		
V_c (fpm)	20	31	100
Q (cfm)	364	587	1734
V_{DUCT} (fpm)	1042	1681	4949
VP_{DUCT} (in. H_2O)	0.068	0.176	1.53
SP_h (in. H_2O)	0.08	0.20	1.72
C_e^*	0.922	0.938	.943
$h_{e_t}^*$ (in. H_2O)	0.012	0.024	0.19
V_{FACE} (fpm)	182	290	870
VP_{FACE}^* (in. H_2O)	.002	.005	.047

* Calculated.

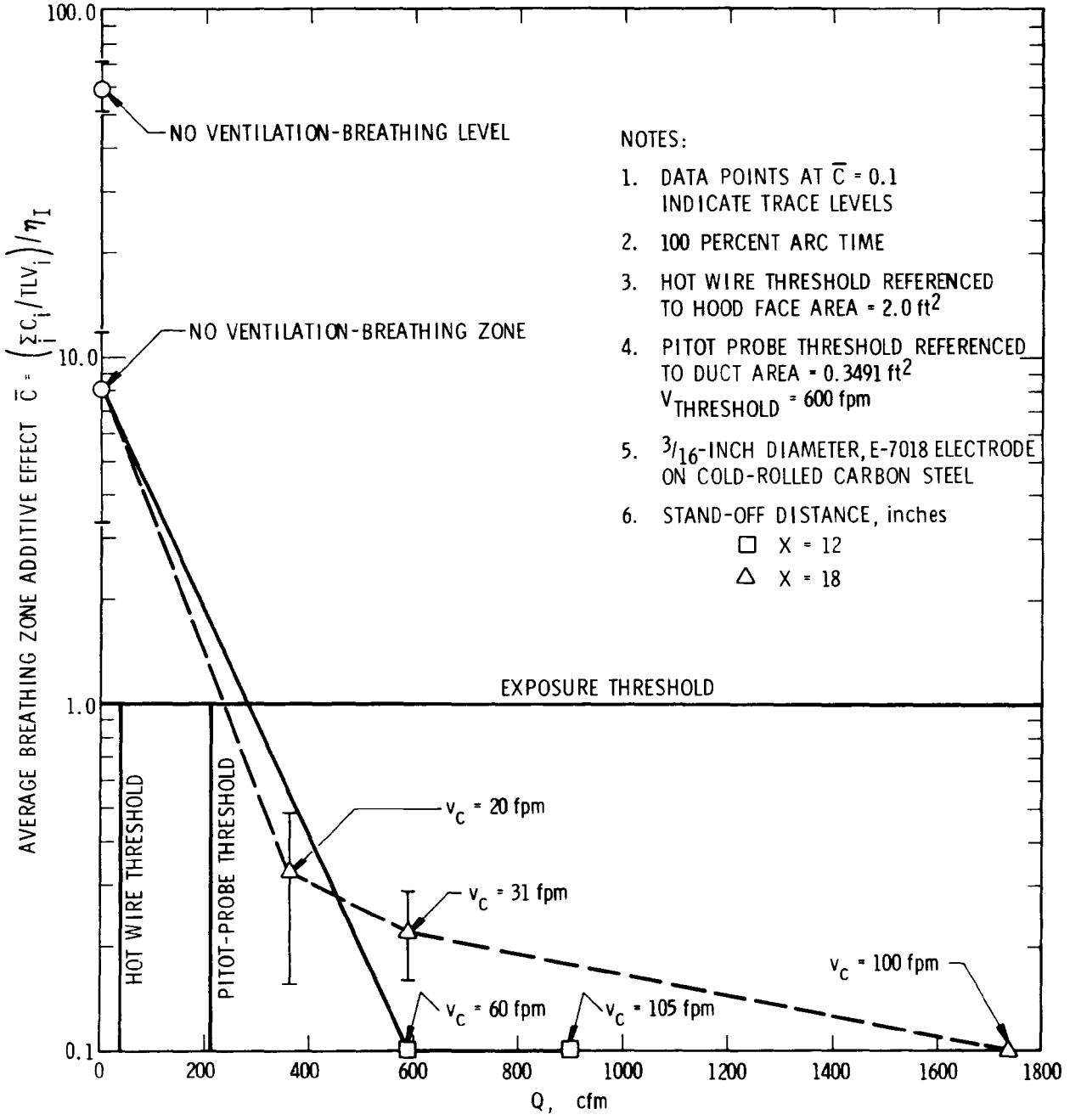

Figure 30. Breathing Zone Additive Effect as a Function of Rectangular Hood Ventilation Rate for Arc Welding on Cold-Rolled Carbon Steel

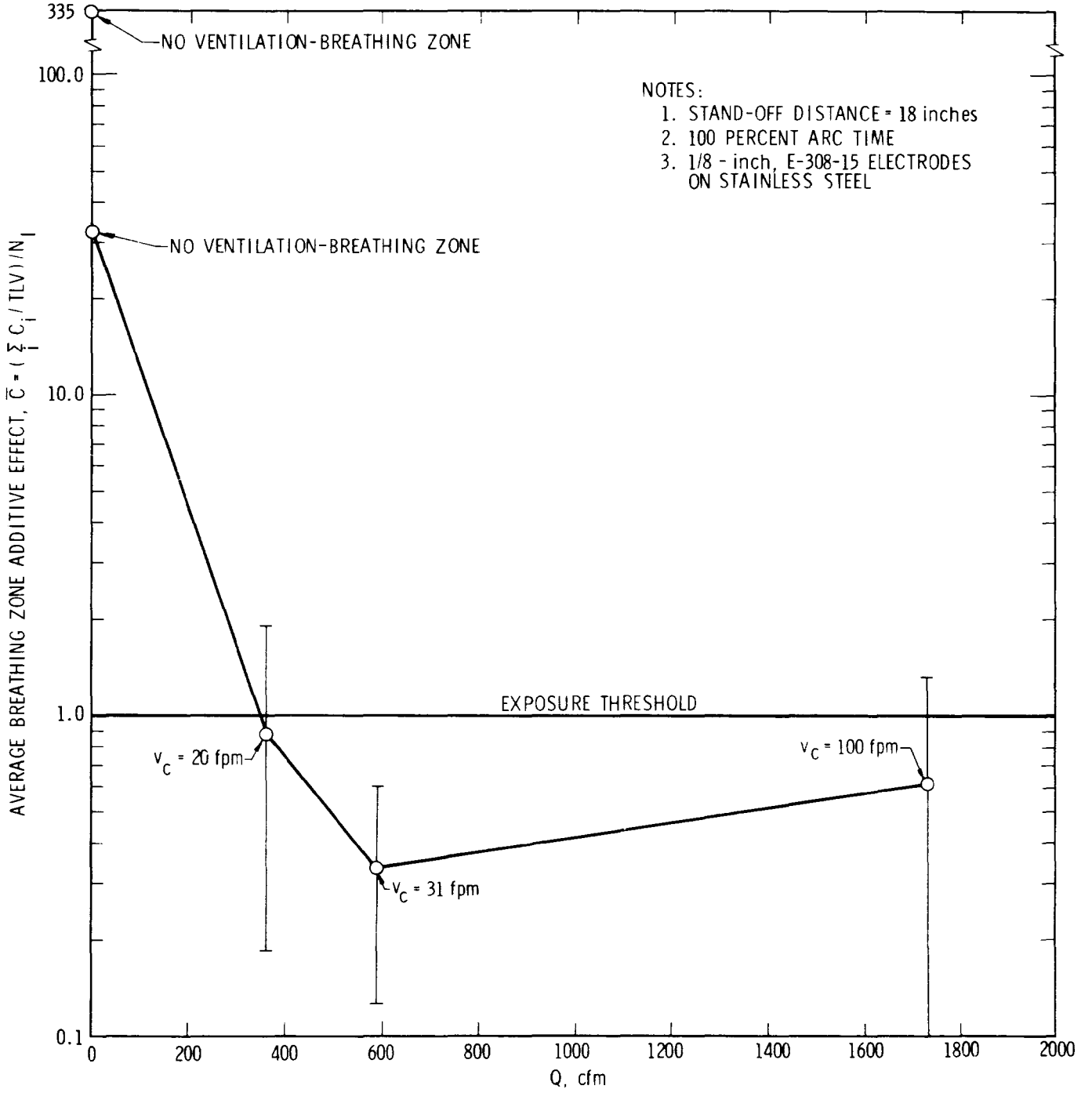

Figure 31. Breathing Zone Additive Effect As a Function Of Rectangular Hood Ventilation Rate For Arc Welding On Stainless Steel

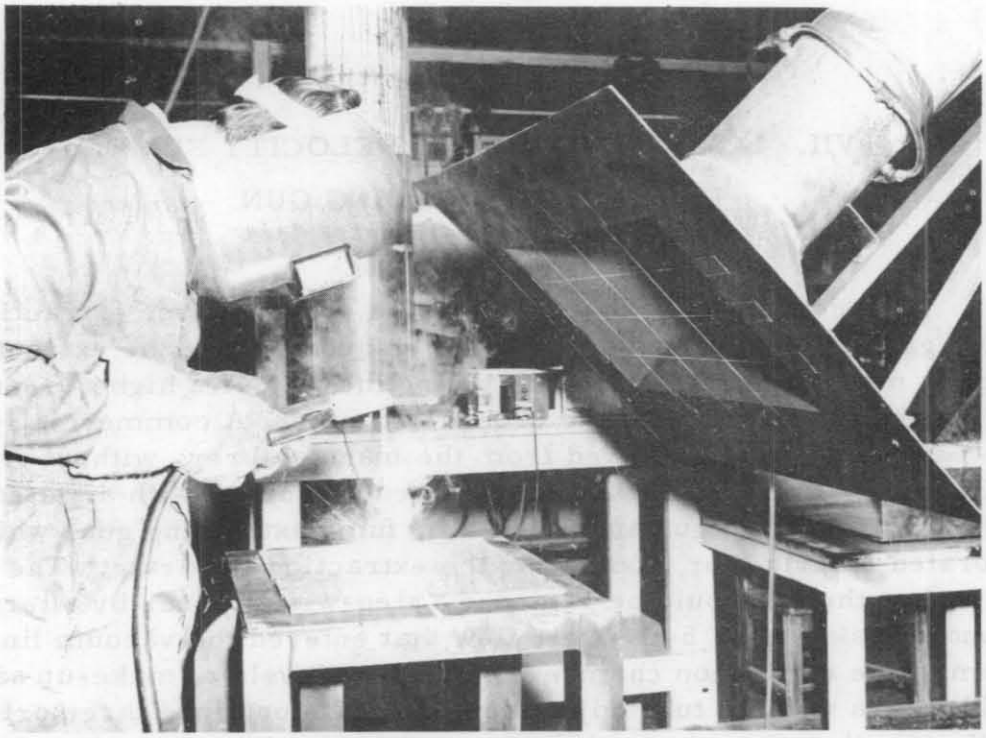

Figure 32. Fume Cloud From Shielded Manual Metal Arc Welding Process - No Ventilation

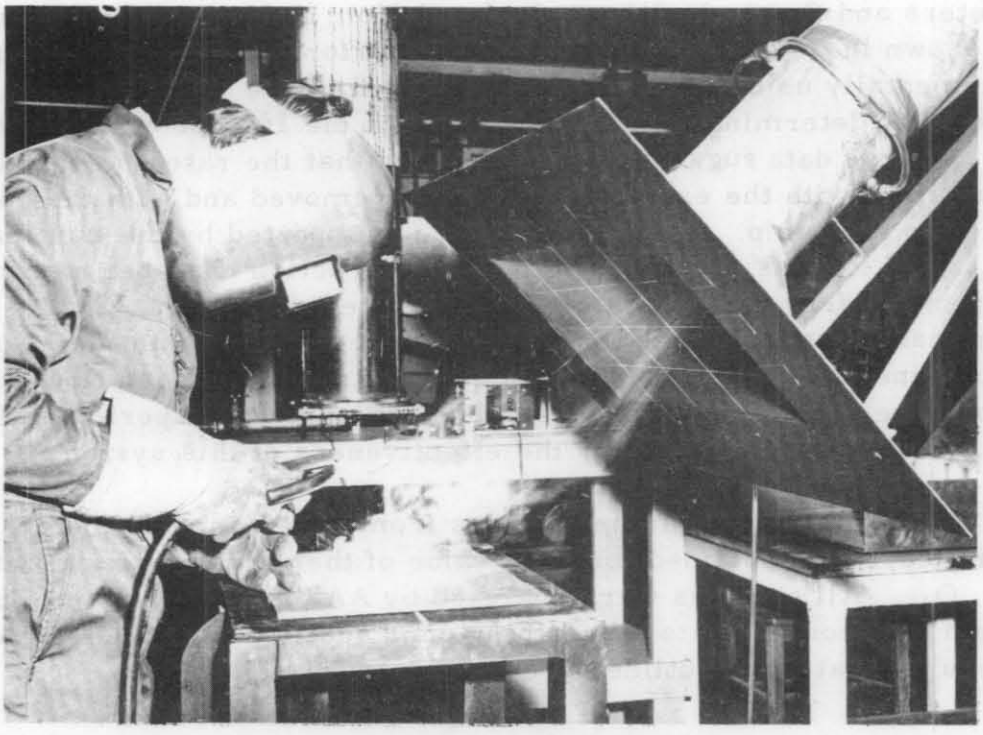

Figure 33. Fume Control With Local Rectangular Hood Ventilation

VII. LOW VOLUME, HIGH VELOCITY FUME EXTRACTING WELDING GUN

The concept of a low volume, high velocity fume extracting welding gun for gas shielded processes is quite unique because the extraction device is mounted on the gun, thus giving the welder a higher degree of mobility than is afforded by the crossdraft table. A commercially-available unit was evaluated as-received from the manufacturer, without structural modification. The unit consisted of a vacuum source with a stated rating of 60 cfm through the gun and a 400-amp fume extracting gun, which incorporated a device for modulating the extraction flow rate. The suction flow rate at the gun could be varied in a step-wise manner by altering the amount of make-up or bypass air flow that entered the vacuum line downstream of the extraction chamber. Different levels of make-up air were provided by a vacuum tube adjustment nut that contained three orifices of differing diameters located on the periphery of the nut. The desired orifice could be selected by rotating the nut over a 1/2-inch, pre-drilled hole in the main vacuum tube on the gun.

Table IX contains flow rate specifications, measured orifice diameters and flow velocities calculated from these specifications. Also shown in Table IX is the pneumatic performance as determined experimentally using the calibrated, SwRI hot wire anemometer. All air velocity determinations were made with the 10-foot vacuum line in place. These data suggest that it is possible that the rated performance was obtained with the extraction chamber removed and with the gun short-coupled to the pump. This observation is supported by the fact that Q_{1max}, which was obtained without the extraction chamber, approximates the specified flow rate (60 cfm). The difference between Q_{1max} and 60 cfm can be attributed to the frictional pressure drop in the 10-foot vacuum line, which would result in a decrease in the mean flow velocity or flow rate. As a result of these observations, the experimental values of Q_1 were used in assessing the effectiveness of this system.

Breathing zone fume samples from 0.045-inch diameter, E70S-4 electrodes, were obtained for each value of the nozzle extraction flow rate, Q_1. All samples were analyzed by AAS for Fe, Mn and Cu, and the data was converted to a breathing zone additive effect using the procedures that were outlined previously.

TABLE IX

PNEUMATIC PERFORMANCE OF LOW VOLUME-HIGH VELOCITY FUME EXTRACTION SYSTEM

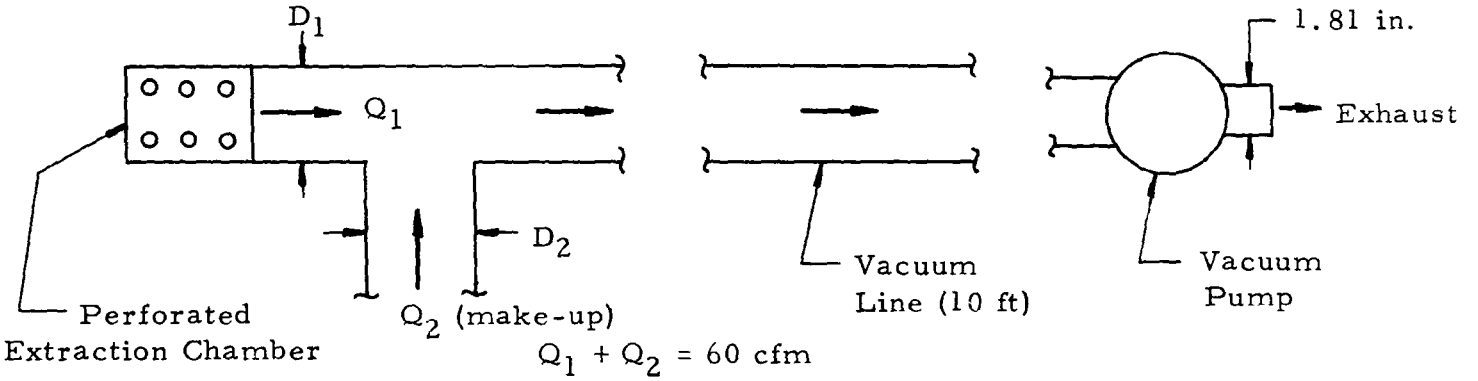

$Q_1 + Q_2 = 60$ cfm

Rated Performance

Q_1 (cfm)[+]	Q_2 (cfm)[+]	D_1 (in.)[*]	D_2 (in.)[*]	V_1 (fps)[**]	V_2 (fps)[**]
60	0	0.75	0	326	0
53	7	0.75	0.25	288	342
45	15	0.75	0.375	244	326
30	30	0.75	0.50	163	367

[+] Manufacturer's specifications.

[*] Measured.

[**] Calculated from continuity.

Experimental Performance

Q_1 (cfm)	Q_2[*] (cfm)	V_2[+] (fps)	D_2 (in.)
32.16[**]	0	0	0
28.70	3.46	169	0.25
23.00	9.16	199	0.375
17.27	14.89	182	0.50

[+] Obtained from hot wire with extraction chamber and vacuum line intact.

[*] Calculated from V_2 and D_2.

[**] Calculated from pump exhaust velocity (30 fps) with extraction chamber and vacuum line intact.

Q_{1max} = 50.62 cfm with extraction chamber removed, D_2 = 0.0 and vacuum line intact.

The experimental results obtained with this class of ventilation system are shown in Figure 34. Note that the shielding gas flow rate had to be increased according to the extraction flow rate in order to maintain an acceptable quality weld bead.

The breathing zone additive effect profile followed the anticipated trend up to an extraction flow rate of 28.70 cfm. The increase in average concentration at the maximum flow rate, 32.16 cfm, was unexpected even for a sample size of two. One plausible explanation is that the mandatory increase in shielding gas flow rate was sufficient to accelerate the fume particles beyond the effective capture velocity range of the perforated nozzle. Consequently, these fumes would rise into the breathing zone.

A proportionate reduction in the additive effect for a 50 percent arc time would result in data points which exceed the mixture TLV or Exposure Threshold at the maximum and minimum nozzle extraction flow rates. These data suggest an optimum extraction flow rate in the 23 to 29 cfm range for the 0.045-inch diameter, E70S-4 electrode.

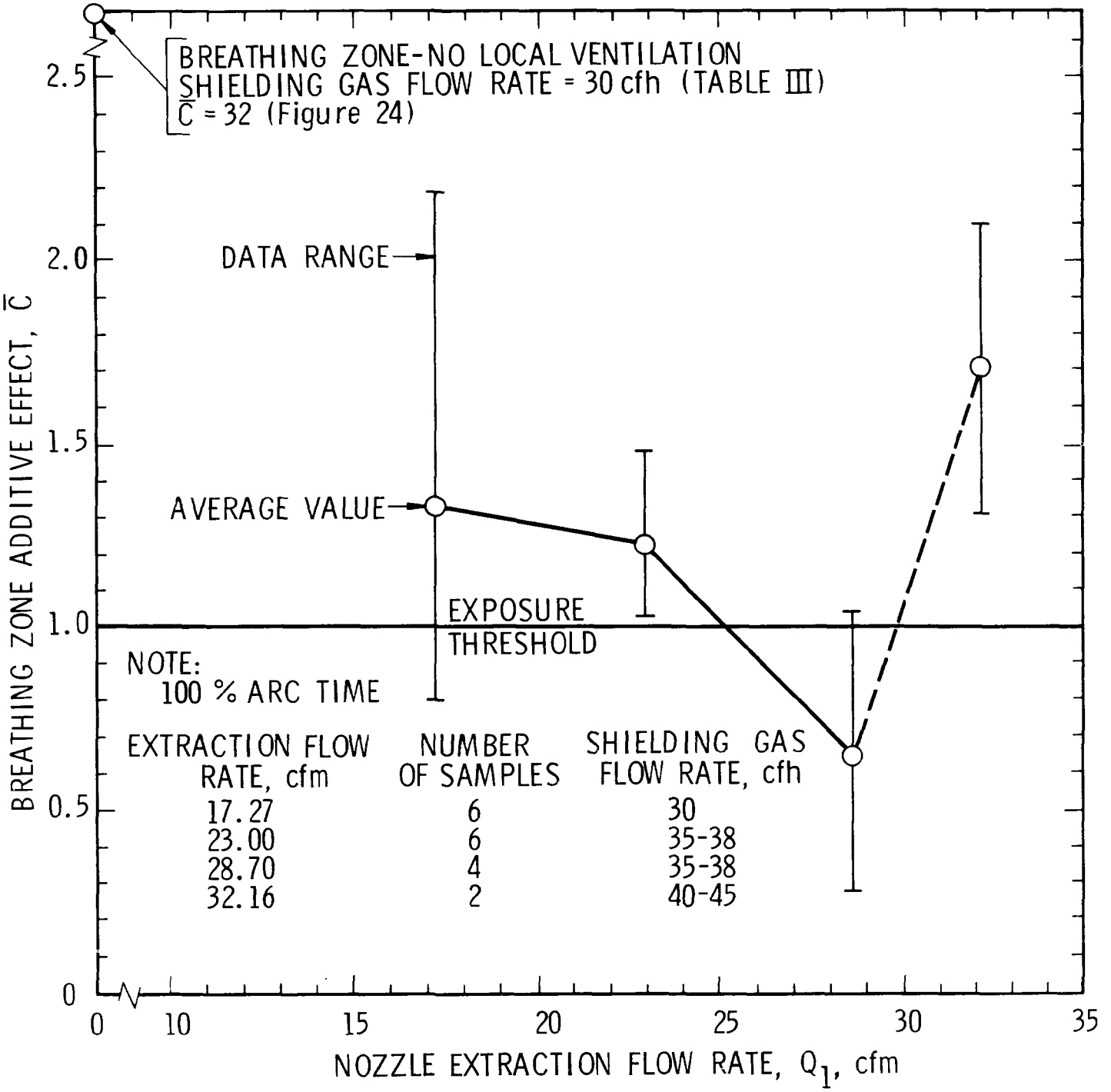

Figure 34. Breathing Zone Additive Effect As a Function Of Low Volume, High Velocity Extraction Flow Rate

VIII. FLUORIDE ANALYSIS

A separate task effort was designed and executed to determine if the particulate and gaseous fluorides that are generated by shielded manual metal arc welding were amenable to control by local exhaust ventilation. In the absence of local ventilation, breathing zone samples were collected for the following electrodes.

Electrode	Diameter (inch)
E-7018	3/16
E-7016	3/16
E-6013	3/16
E-308-15	1/8

These samples were then analyzed for total fluoride concentration. Local ventilation control was then applied to the E-7018 electrode because it had produced the highest indicated fluoride concentration in the no-ventilation tests. The validity of a true breathing zone determination is discussed later.

Except for determinative steps, the method of sampling and analyzing for inorganic fluorides was taken from ASTM Standard D-1606-60.[10] To accomplish the collection of gaseous and particulate fluorides, the sampling train was modified as shown in Figure 35. Inorganic particulate fluorides were collected on Gelman Metricel VM-1, 5u filters, and gaseous fluorides were collected in an impinger that contained 75 ml of NaOH solution (5 gm/liter). Sampling rate was nominally 1.0 cfm as specified in this standard. The sample work-up procedure involved a predistillation preparation of both the filter and the impinger solution. This operation destroyed organic matter in the samples and reduced the sample size to a suitable volume. The samples were then steam distilled from a perchloric acid mixture, and fluoride determinations were made on the distillate. For each test condition, an uncontaminated filter and 75 ml of uncontaminated NaOH solution were also subjected to the same work-up and analysis procedures to establish a reference or background concentration level. This background level was then subtracted from the fluoride concentrations that were obtained from the test samples.

The determination of fluoride content was accomplished using an Orion fluoride ion specific electrode and meter instead of the

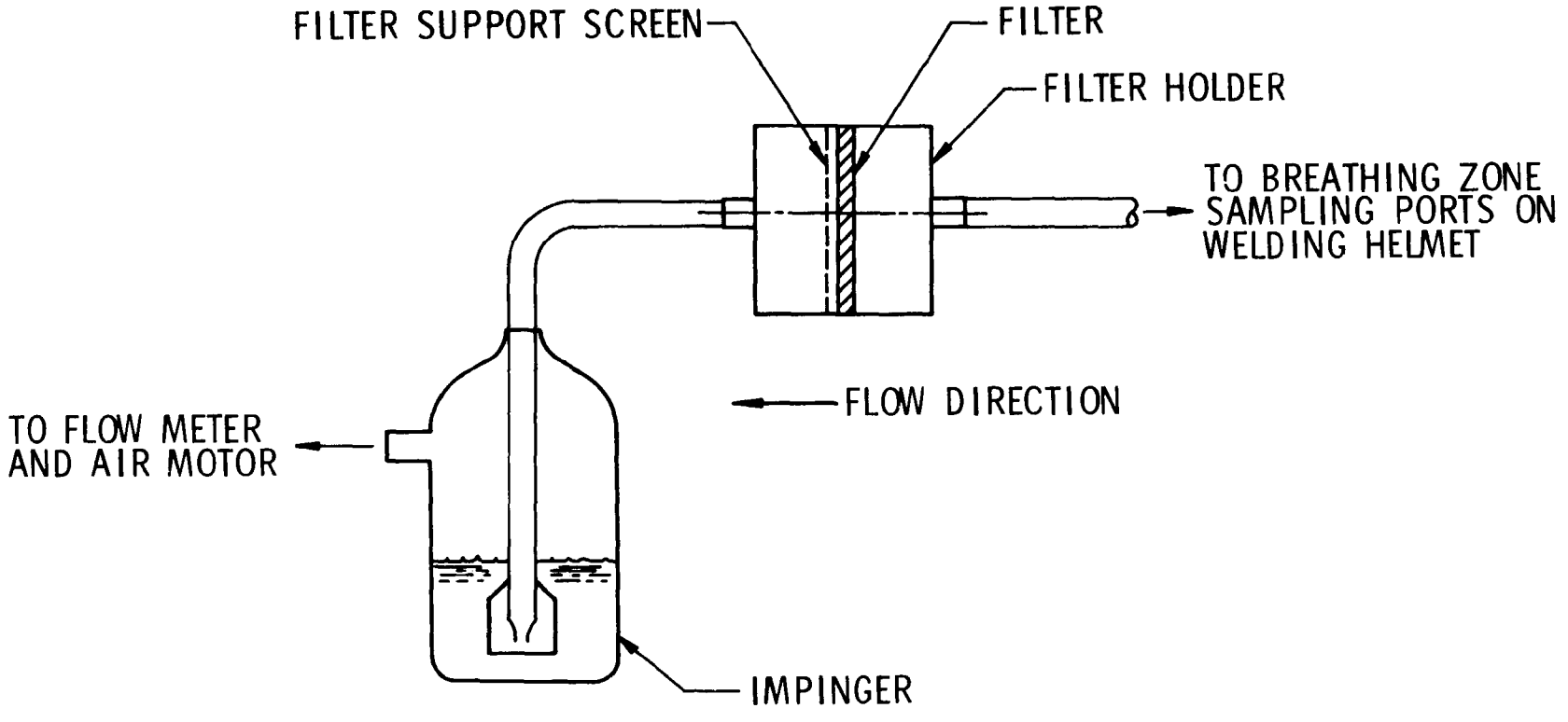

Figure 35. Total Fluoride Sampling Apparatus

colorimetric procedure contained in the ASTM Standard. A 2.5-ml volume of Orion total ionic strength buffer was added to each sample prior to the fluoride determination to insure that the pH of the solution fell between 5.0 and 6.0. The ion specific meter was standardized with 1.0 and 0.1-ppm fluoride solutions, and a direct readout of fluoride concentration in ppm was obtained. The results were then converted to mg/m^3 by the same procedure that was used for metallic fumes.

The sample work-up and analysis procedures in ASTM Standard D-1606-60 were extremely time consuming. Consequently, only three samples were taken at each test condition, and fluoride collection efficiency was not evaluated.

The fluoride data, which are presented below, should be interpreted on a trend or relative basis rather than on an absolute basis because:

(1) A true breathing zone concentration cannot be inferred from the trapped concentration without a knowledge of the collection efficiency. The fact that the no-ventilation fluoride concentrations agree quite closely with the data of Alpaugh[7], Jones [11], Smith [12] and Steel [13] indicates that high trapping efficiencies should be expected.

(2) The sample work-up and analysis procedures generate total fluoride ion concentration. Hence, a comparison with separate particulate and gaseous fluoride concentration data in the literature is not feasible.

The total fluoride ion concentrations for the no-ventilation tests are summarized in Table X. As anticipated, the low hydrogen, E-7018, electrode produced the largest fluoride ion concentration. Table XI summarizes the variation of trapped fluoride ion concentration with the operating state of the rectangular hood. The data for this electrode appear to follow the same concentration-capture velocity trend that was exhibited by the breathing zone concentration of metallic fumes (see Figure 30). As in the latter case, the fluoride concentration falls below its threshold limit value (2.5 mg/m^3) at a capture velocity of 20 fpm. This observation indicates that the rectangular hood is effective in reducing contaminant concentrations to an acceptable level. Furthermore, this reduction in fluoride and metallic fume concentration apparently can be accomplished at the same ventilation system operating point.

TABLE X

TOTAL FLUORIDE ION CONCENTRATION
NO LOCAL VENTILATION

Electrode Classification		F^- (mg/m^3)
E-7018		4.5
		2.0
		1.5
	AVERAGE	2.7
E-7016		1.5
		1.7
		0.6
	AVERAGE	1.3
E-6013		0.2
		N.D.*
		N.D.
	AVERAGE	TRACE
E-308-15		2.6
		2.2
		1.1
	AVERAGE	2.0

* Not detectable.

TABLE XI

EFFECT OF LOCAL VENTILATION ON TOTAL
FLUORIDE ION CONCENTRATION
FOR E-7018 ELECTRODES

Capture Velocity (fpm)		F^- (mg/m^3)
0		4.5
		2.0
		1.5
	AVERAGE	2.7
20		0.6
		N.D.*
		N.D.
	AVERAGE	0.2
100		0.2
		0.2
		N.D.
	AVERAGE	0.1

NOTE: Rectangular hood with 18-inch stand-off distance.

*Not detectable.

IX. CONCLUSIONS AND RECOMMENDATIONS

An experimental investigation was conducted to define satisfactory criteria for the control of welding and cutting fumes using local exhaust ventilation methods. The criteria for the effectiveness of a system was its ability to reduce the additive effect of the breathing zone metallic fume concentrations below the mixture exposure limit ($\sum_i C_i/TLV_i \leq 1$).

Breathing level fume samples were obtained for several combinations of welding or cutting processes and process variables. These samples reflected a 100 percent arc time and no local ventilation. Environmental conditions were representative of in-door, job-shop production operations in an unconfined space, and crossdrafts were negligible. No other processes were operated simultaneously with the test process. Therefore, cross-contamination due to mixed facilities or to concurrent operations of the same process was eliminated. Based on these tests, the following processes were judged to constitute the greatest potential health hazard and were, therefore, selected for local exhaust ventilation control studies.

(1) Shielded Manual Metal Arc Welding (E-7018, 3/8 in.) on Carbon Steel,

(2) Shielded Manual Metal Arc Welding (E308-15, 1/8 in.) on Stainless Steel, and

(3) Gas Shielded Arc Welding (E705-4, 0.045 in.) on Carbon Steel.

Although the breathing level additive effect for other electrode diameters also exceeded the mixture TLV, the electrode diameters for the above three conditions generated the largest additive effect. Those conditions representing lesser levels of additive effect can be controlled effectively by defining the ventilation requirements for the most severe conditions.

A crossdraft ventilation table was designed and fabricated for use with the gas shielded process. In addition, a low volume-high velocity fume extracting welding gun was evaluated in conjunction with this process A free-standing rectangular hood was applied to the covered electrode pro cesses. Based on the analysis of breathing zone fume samples, the prevailing standard on capture velocity, i.e., 100 fpm per Reference 9, is extremely effective in controlling fume concentrations, and, under certair conditions, namely those defined in the second paragraph above, the requirements on capture velocity and system flow rate may be relaxed and still provide a suitable margin of safety (see Figures 24, 30 and 31).

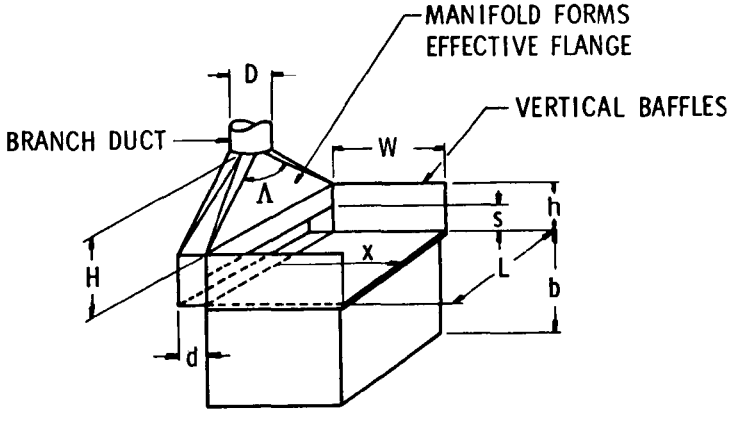

L = 24 in.
W = 21 in.
H = 8 in.
S = 3 in.
h = 6 in.
D = 8 in.
b = 36.5 in.
Λ = 90°
d = 8 in.
100 percent arc time

$$Q = 2.42\ L\ W\ V_c$$

	Welding Direction	
	Parallel to Slot	Perpendicular to Slot
V_c (fpm) at x = W	104	62
Q (cfm)	882	528
V_{SLOT} (fpm)	1764	1056
VP_{SLOT} (in. H_2O gage)	0.19	0.07
V_{DUCT} (fpm)	2526	1511
VP_{DUCT} (in. H_2O gage)	0.40	0.14
Entry loss, h_e (in. H_2O gage)	← 1.13 VP_{DUCT} →	

Figure 36. Recommended Crossdraft Table Performance for Gas Shielded Arc Welding

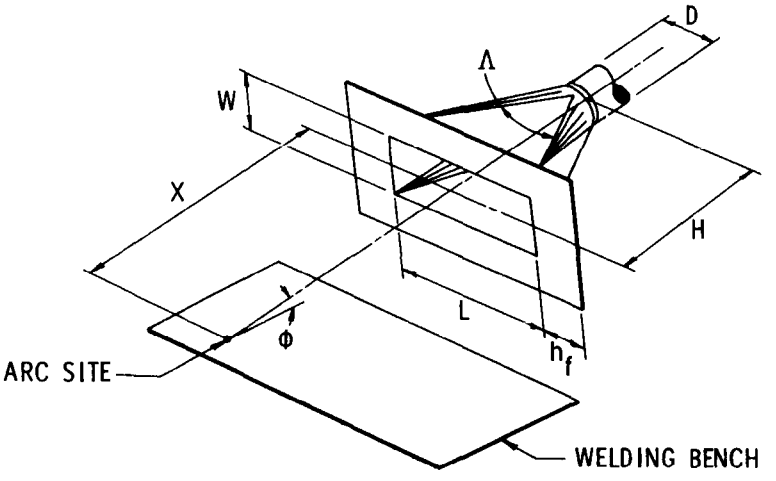

L = 24 in.
W = 12 in.
H = 8 in.
Φ = 45°
Λ = 90°
D = 8 in.
h_f = 6 in.
X = 18 in.
100 percent arc time

	Base Metal	
	Carbon Steel	Stainless Steel
V_c (fpm) at x	20	100
Q (cfm)	364	1734
V_{FACE} (fpm)	182	870
VP_{FACE} (in. H_2O gage)	not measurable	0.05
V_{DUCT} (fpm)	1042	4949
VP_{DUCT} (in. H_2O gage)	0.07	1.53
Entry loss, h_e (in. H_2O gage)	0.17 VP_{DUCT}	0.12 VP_{DUCT}

Figure 37 Recommended Rectangular Hood Performance for Shielded Manual Metal Arc Welding

A schematic drawing showing performance recommendations for the crossdraft table and the rectangular hood are presented in Figures 36 and 37, respectively. These performance recommendations represent minimum system operating states which resulted in a breathing zone additive effect that was equal to or less than the mixture TLV or Exposure Threshold at 100 percent arc time. The results of the fluoride tests of SMAW electrodes indicate that effective control of fluoride compounds and metallic fumes can be achieved at the same operating point with the free-standing rectangular hood.

These ventilation system requirements were derived on the basis of a given set of ground rules which included the environmental conditions and base materials that were stated at the beginning of this report. Extrapolation of system performance to other situations is not recommended. The next logical step is to develop local ventilation system design criteria for different environmental conditions and surface treatments of the base metal in order to provide acceptable ventilation requirements for an even larger portion of the welding community. To this end, recommendations for future research include the development of ventilation criteria for

(1) Welding in confined spaces such as ship bulkheads and nuclear reactor pressure vessels. The buildup of fume concentrations with time becomes an important factor in sizing the volumetric flow rate requirements.

(2) Welding with mixed facilities. The cross-contamination due to simultaneous operation of different processes in close proximity to each other and its effect on single-process ventilation requirements should be evaluated.

(3) Welding on paint-primed and zinc-coated base metals.

REFERENCES

1. Astleford, W. J., "Engineering Control of Welding Fumes," Interim Technical Report No. 1, Contract No. HSM 99-72-76, Southwest Research Institute, January 1973.

2. Industrial Ventilation - A Manual of Accepted Practice, Committee on Industrial Ventilation, Lansing, Michigan, 1972.

3. Fundamentals Governing the Design and Operation of Local Exhaust Systems, USA Standard Z9.2-1960.

4. Handbook of Air Conditioning, Heating and Ventilation, Second Edition, Industrial Press, 1965.

5. "Standard Recommended Practice for Planning the Sampling of the Atmosphere," ASTM Standard Designation D-1357-57 (Reapproved 1967).

6. Prandtl, L., Essentials of Fluid Dynamics, Hafner Publishing Company, 1952.

7. Alpaugh, E. L. et al, "Ventilation Requirements for Gas-Metal-Arc Welding versus Covered-Electrode Welding," American Industrial Hygiene Association Journal, Vol. 29, No. 6, 1968.

8. Johnson, W. S., "An Investigation into the True Exposure of Arc Welders by Means of Simultaneous Sampling Procedures," American Industrial Hygiene Association Journal, Vol. 20, No. 3, June 1959.

9. Safety in Welding and Cutting, USA Standard Z49.1-1957.

10. "Standard Method of Test for Inorganic Fluoride in the Atmosphere," ASTM Standard Designation D-1606-60 (Reapproved 1967).

11. Jones, R. C., "Selective Tests for Contaminants in Welding Fumes from Electric Arc Welding - An Environmental Assessment," Ann. Occup. Hyg., Vol. 10, 1967.

REFERENCES (CONCLUDED)

12. Smith, K. W., "Fume Exposures from Welding with Low Hydrogen Electrodes," Ann. Occup. Hyg., Vol. 10, 1967.

13. Steel, J., "Respiratory Hazards in Shipbuilding and Shiprepairing," Ann. Occup. Hyg., Vol. II, 1968.

APPENDIX A

BASELINE FUME CONCENTRATION DATA

TABLE A 1

Fume Component Concentrations for Shielded Manual Metal Arc Welding of E-7010-A1 Electrodes on Carbon Steel

Electrode Diameter: 1/8 Inch

Sample No.	Impinger Concentration (mg/m^3)			$(\Sigma C_i/TLV_i)/\eta_I$*
	Cu	Fe	Mn	
SMAW1-a	0.07	23.84	2.96	27.97
-b	0.06	16.29	1.81	19.38
-c	0.10	26.97	3.13	32.20
-d	0.07	22.60	2.87	26.68
-e	0.04	12.14	1.32	14.26
-f	0.04	12.14	1.41	14.32
Average	0.063	18.99	2.25	22.45
	Cu	Fe_2O_3	Mn	
C_i/TLV_i max	1.00	7.71	0.63	
C_i/TLV_i ave	0.63	5.43	0.45	
C_i/TLV_i min	0.40	3.47	0.26	

Electrode Diameter: 5/32 Inch

Sample No.	Impinger Concentration (mg/m^3)			$(\Sigma C_i/TLV_i)/\eta_I$
	Cu	Fe	Mn	
SMAW2-a	0.02	12.36	1.94	25.07
-b	0.04	25.94	4.72	30.22
-c	0.03	13.99	2.76	16.73
-d	0.02	11.75	2.31	13.87
-e	0.03	17.20	2.89	19.99
-f	0.02	15.60	2.72	17.95
Average	0.027	16.14	2.89	18.84
	Cu	Fe_2O_3	Mn	
C_i/TLV_i max	0.40	7.42	0.94	
C_i/TLV_i ave	0.27	4.62	0.58	
C_i/TLV_i min	0.20	3.36	0.39	

Electrode Diameter: 3/16 Inch

Sample No.	Impinger Concentration (mg/m^3)			$(\Sigma C_i/TLV_i)/\eta_I$
	Cu	Fe	Mn	
SMAW3-a	0.03	13.01	2.85	15.83
-b	0.04	17.31	3.89	21.13
-c	0.04	17.04	3.88	20.86
-d	0.05	20.77	4.79	25.51
-e	0.04	15.89	3.78	19.66
-f	0.06	22.84	5.12	28.12
Average	0.043	17.81	4.05	21.84
	Cu	Fe_2O_3	Mn	
C_i/TLV_i max	0.60	6.55	1.02	
C_i/TLV_i ave	0.43	5.09	0.81	
C_i/TLV_i min	0.30	3.72	0.57	

* Iron converted to iron oxide for summation

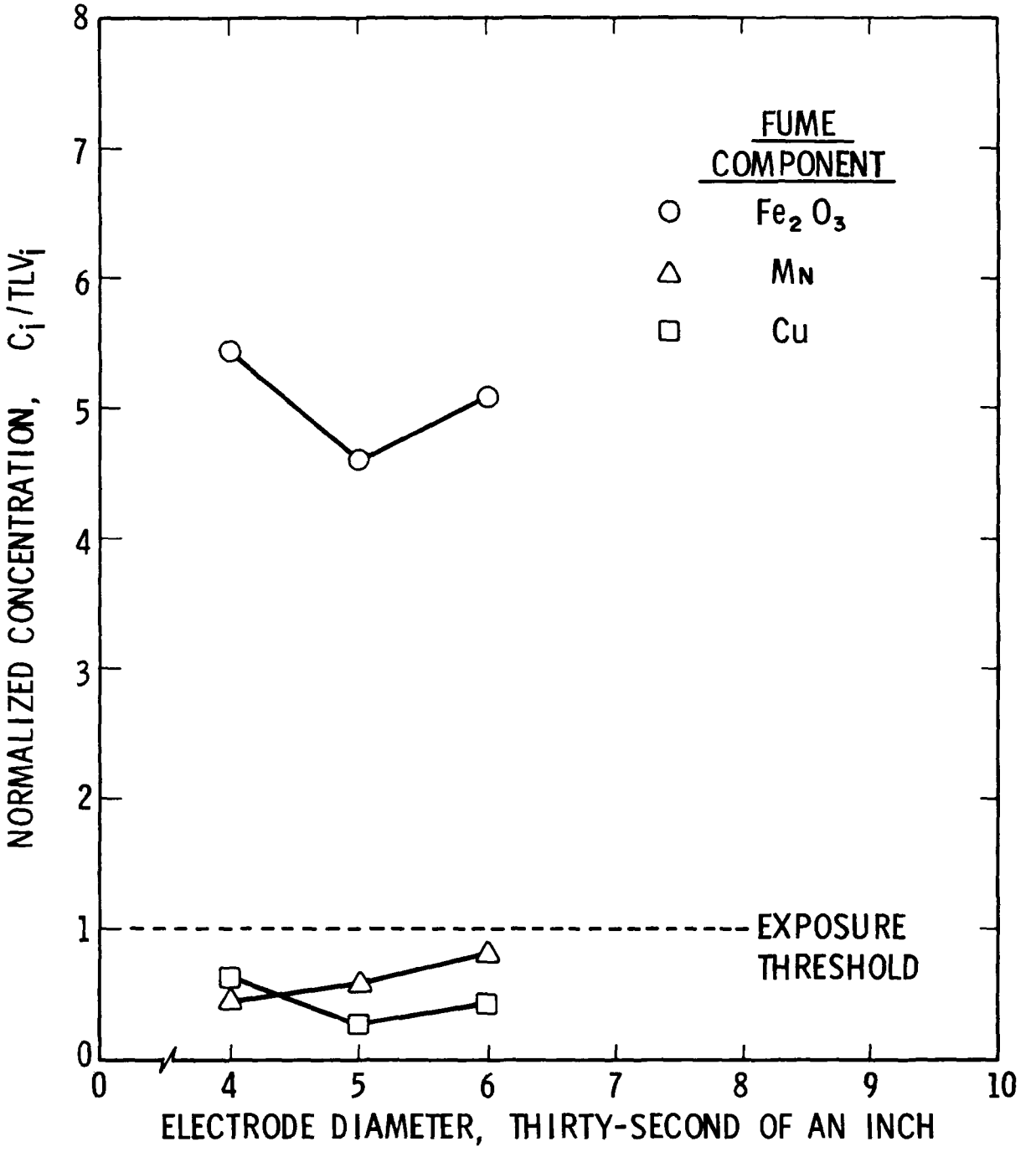

Figure A1. Normalized Impinger Concentrations Obtained from Welding E-7010-A1 Electrodes on Cold-Rolled Carbon Steel

TABLE A2

Fume Component Concentrations for Shielded Manual Metal Arc Welding on E-6013 Electrodes on Carbon Steel

Electrode Diameter: 1/8 Inch

Sample No.	Impinger Concentration (mg/m^3)			$(\Sigma C_i/TLV_i)/\eta_{II}$
	Cu	Fe	Mn	
SMAW4-a	0.03	24.98	2.84	27.63
-b	0.05	29.79	3.52	33.53
-c	0.03	30.03	3.72	33.22
-d	0.03	28.81	3.61	31.94
-e	0.03	20.47	2.82	23.17
-f	0.03	13.93	1.76	15.99
Average	0.033	24.67	2.88	27.48
	Cu	Fe_2O_3	Mn	
C_i/TLV_i max	0.50	8.59	0.74	
C_i/TLV_i ave	0.33	7.06	0.58	
C_i/TLV_i min	0.30	3.98	0.35	

Electrode Diameter: 3/16 Inch

Sample No.	Impinger Concentration (mg/m^3)			$(\Sigma C_i/TLV_i/\eta_{II}$
	Cu	Fe	Mn	
SMAW5-a	0.04	28.96	3.59	32.81
-b	0.07	47.03	6.37	53.19
-c	0.04	31.69	3.98	35.38
-d	0.05	28.42	3.65	32.27
-e	0.05	38.46	5.75	43.62
-f	0.03	14.98	2.39	17.46
Average	0.047	31.59	4.29	35.73
	Cu	Fe_2O_3	Mn	
C_i/TLV_i max	0.70	13.45	1.27	
C_i/TLV_i ave	0.47	9.03	0.86	
C_i/TLV_i min	0.30	4.28	0.48	

Electrode Diameter: 1/4 Inch

Sample No.	Impinger Concentration (mg/m^3)			$(\Sigma C_i/TLV_i/\eta_{II}$
	Cu	Fe	Mn	
SMAW6-a	0.02	11.52	1.78	13.28
-b	0.02	12.70	2.81	15.15
-c	0.03	25.05	4.58	28.90
-d	0.02	14.80	2.38	16.93
-e	0.03	29.82	4.21	33.35
-f	0.02	19.02	3.08	21.57
Average	0.023	18.82	3.08	21.47
	Cu	Fe_2O_3	Mn	
C_i/TLV_i max	0.30	8.53	0.92	
C_i/TLV_i ave	0.23	5.38	0.63	
C_i/TLV_i min	0.20	3.29	0.36	

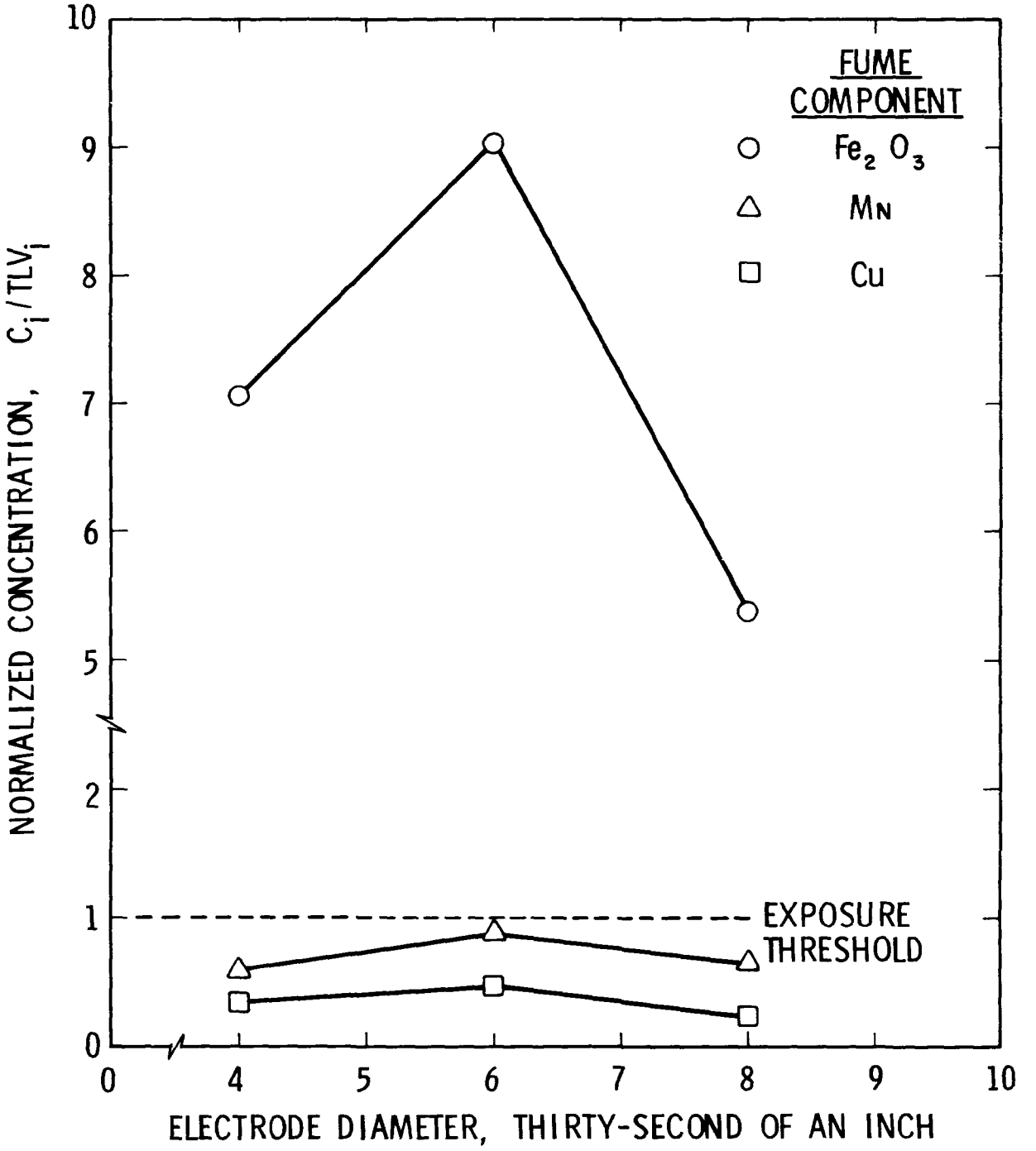

Figure A2. Normalized Impinger Concentrations Obtained from Welding E-6013 Electrodes on Cold-Rolled Carbon Steel

TABLE A3

Fume Component Concentrations for Shielded Manual Metal Arc Welding of E-7016 Electrodes on Carbon Steel

Electrode Diameter: 1/8 Inch

Sample No.	Impinger Concentration (mg/m^3)			$(\Sigma C_i/TLV_i)/\eta_T$
	Cu	Fe	Mn	
SMAW7-a	0.01	12.11	2.75	14.18
-b	0.01	6.84	1.17	7.90
-c	0.02	17.11	4.02	20.34
-d	0.01	15.11	3.52	17.67
-e	0.01	10.75	2.49	12.66
-f	0.02	15.75	4.10	19.05
Average	0.013	12.95	3.01	15.30
	Cu	Fe_2O_3	Mn	
C_i/TLV_i max	0.20	4.89	0.82	
C_i/TLV_i ave	0.13	3.69	0.60	
C_i/TLV_i min	0.10	1.96	0.23	

Electrode Diameter: 3/16 Inch

Sample No.	Impinger Concentration (mg/m^3)			$(\Sigma C_i/TLV_i)/\eta_T$
	Cu	Fe	Mn	
SMAW8-a	0.02	17.14	5.45	21.35
-b	0.01	6.02	1.88	7.58
-c	0.05	37.55	11.81	46.90
-d	0.03	21.18	6.51	26.41
-e	0.02	8.01	2.66	10.42
-f	0.04	13.64	5.27	18.47
Average	0.028	17.26	5.60	21.85
	Cu	Fe_2O_3	Mn	
C_i/TLV_i max	0.50	10.74	2.36	
C_i/TLV_i ave	0.28	4.94	1.12	
C_i/TLV_i min	0.10	1.72	0.38	

Electrode Diameter: 1/4 Inch

Sample No.	Impinger Concentration (mg/m^3)			$(\Sigma C_i/TLV_i)/\eta_T$
	Cu	Fe	Mn	
SMAW9-a	0.00	25.18	5.23	28.44
-b	0.00	21.35	4.62	24.24
-c	0.01	15.42	3.53	17.64
-d	0.00	15.69	3.60	17.96
-e	0.05	16.73	3.63	20.73
-f*	0.00	8.83	2.16	10.20
Average	0.01	17.20	3.80	19.93
	Cu	Fe_2O_3	Mn	
C_i/TLV_i max	0.50	7.20	1.05	
C_i/TLV_i ave	0.10	4.92	0.76	
C_i/TLV_i min	0.00	2.52	0.43	

* This sample went to dryness during evaporation procedure and would, therefore, lose some of the more volatile metals.

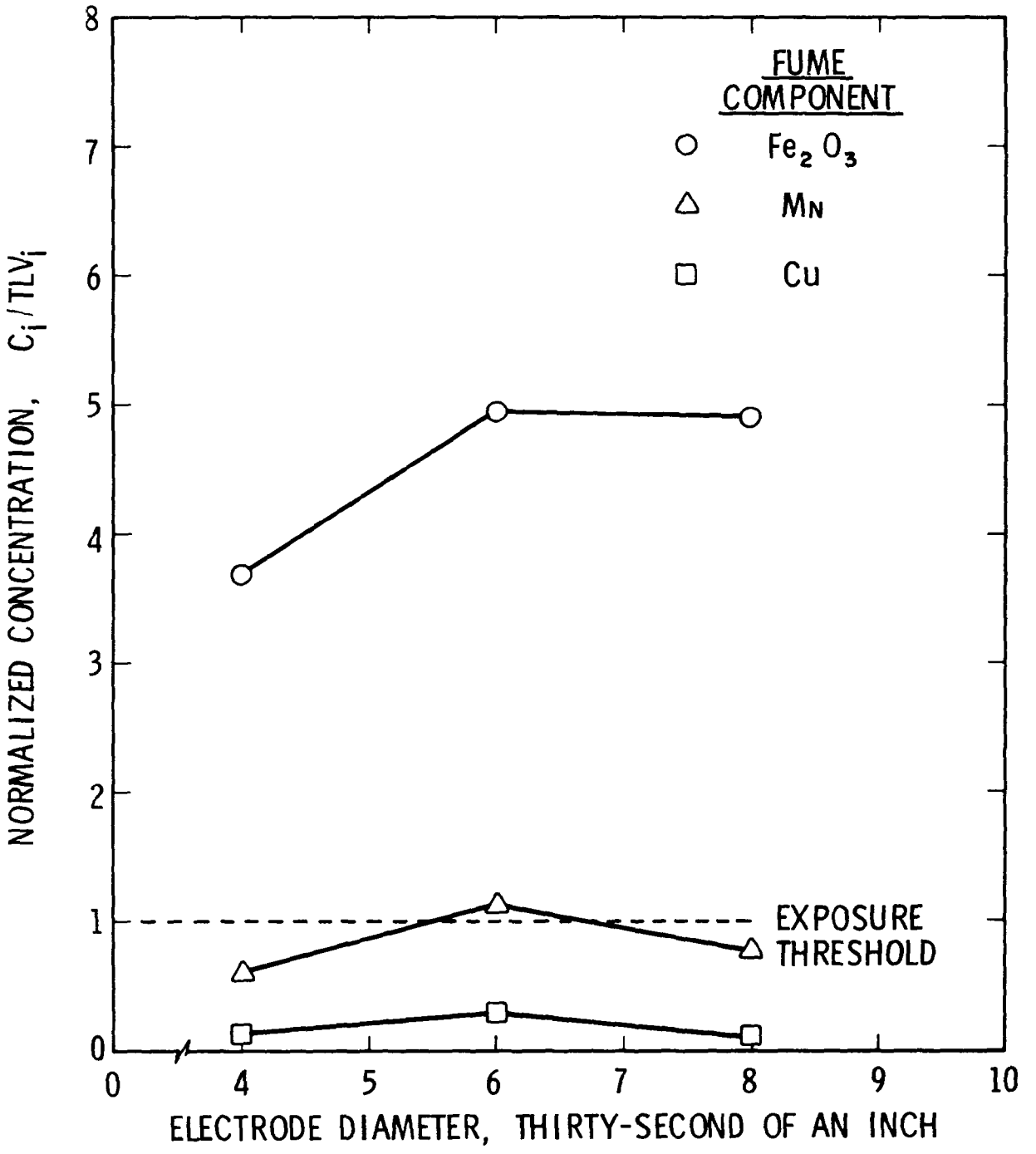

Figure A3. Normalized Impinger Concentrations Obtained from Welding E-7016 Electrodes on Cold-Rolled Carbon Steel

TABLE A4

Fume Component Concentrations for Shielded Manual Metal Arc Welding of E-7018 Electrodes on Carbon Steel

Electrode Diameter: 1/8 Inch

Sample No.	Impinger Concentration (mg/m^3)			$(\Sigma C_i/TLV_i)/\eta_I$
	Cu	Fe	Mn	
SMAW10-a	0.04	43.28	10.14	51.06
-b	0.03	18.16	4.11	21.78
-c	0.02	21.20	5.01	25.05
-d	0.03	18.82	4.50	22.70
-e	0.04	37.12	8.88	44.11
-f	0.02	20.28	4.68	23.92
Average	0.03	26.48	6.22	31.44
	Cu	Fe_2O_3	Mn	
C_i/TLV_i max	0.40	12.38	2.03	
C_i/TLV_i ave	0.30	7.57	1.24	
C_i/TLV_i min	0.20	5.19	0.82	

Electrode Diameter: 3/16 Inch

Sample No.	Impinger Concentration (mg/m^3)			$(\Sigma C_i/TLV_i)/\eta_I$
	Cu	Fe	Mn	
SMAW11-a	0.06	47.79	9.56	55.79
-b	0.04	46.28	10.02	53.93
-c	0.00	45.08	9.42	50.95
-d	0.04	58.08	11.97	66.91
-e	0.01	47.67	10.71	54.74
-f	0.01	61.89	14.31	71.25
Average	0.027	51.13	10.99	58.94
	Cu	Fe_2O_3	Mn	
C_i/TLV_i max	0.60	17.70	2.86	
C_i/TLV_i ave	0.27	14.62	2.20	
C_i/TLV_i min	0.10	12.89	1.88	

Electrode Diameter: 1/4 Inch

Sample No.	Impinger Concentration (mg/m^3)			$(\Sigma C_i/TLV_i)/\eta_I$
	Cu	Fe	Mn	
SMAW12-a	0.02	11.88	3.05	14.51
-b	0.02	13.71	4.48	17.30
-c	0.04	25.27	6.35	30.68
-d	0.03	20.80	4.87	24.91
-e	0.02	6.97	2.65	9.39
-f	0.03	14.47	4.95	18.72
Average	0.027	15.52	4.39	19.26
	Cu	Fe_2O_3	Mn	
C_i/TLV_i max	0.40	7.23	1.27	
C_i/TLV_i ave	0.27	4.44	0.88	
C_i/TLV_i min	0.20	1.99	0.53	

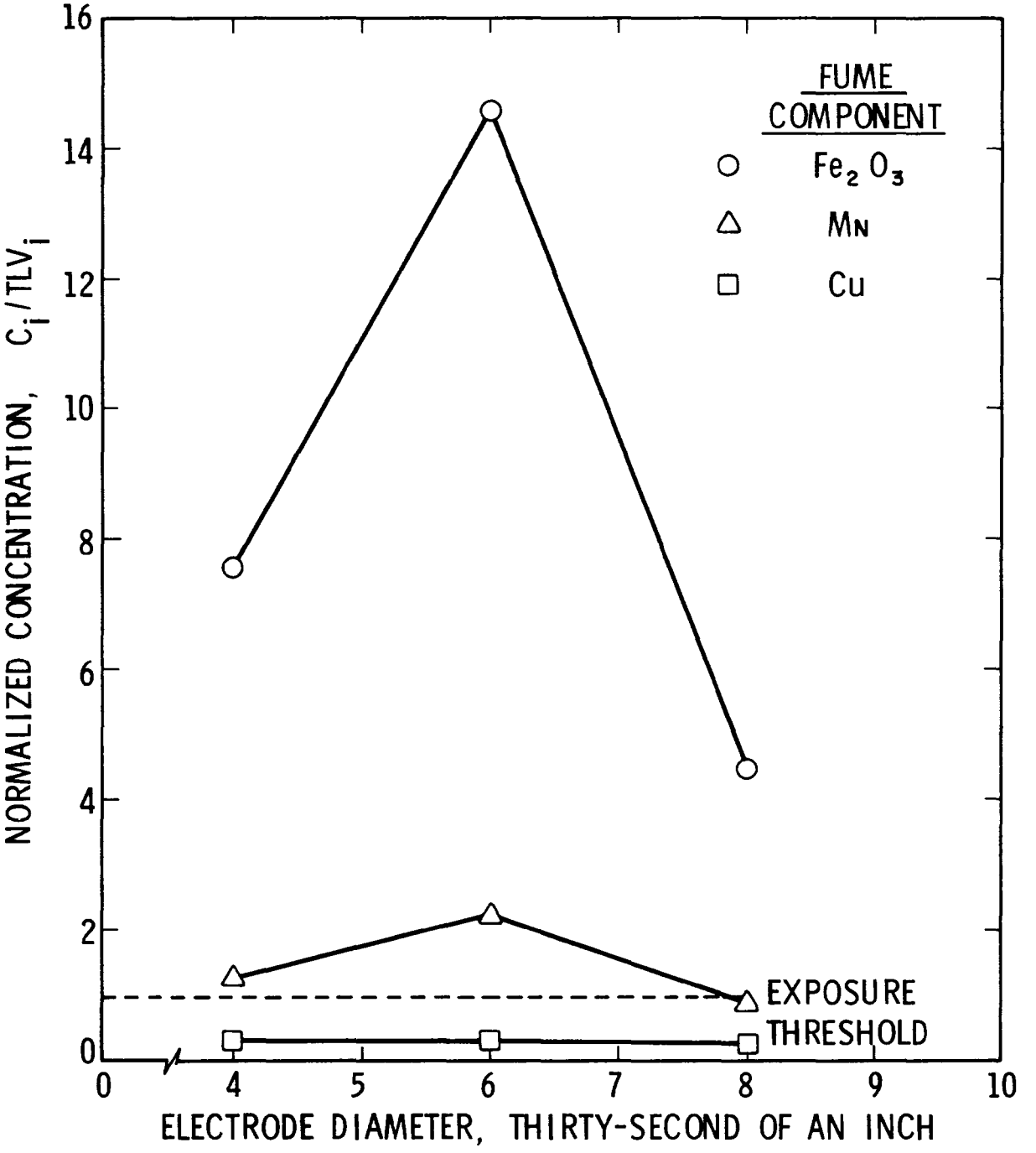

Figure A4. Normalized Impinger Concentrations Obtained from Welding E-7018 Electrodes on Cold-Rolled Carbon Steel

TABLE A5

Fume Component Concentrations for Gas Shielded Arc Welding of E70T-1 Electrodes on Carbon Steel

Electrode Diameter: 1/16 Inch

Sample No.	Impinger Concentration (mg/m^3)			$(\Sigma C_i/TLV_i)/\eta_I$
	Cu	Fe	Mn	
GMAW1-a	0.07	13.45	1.91	17.00
-b	0.08	27.41	4.65	33.00
-c	0.13	44.27	8.89	54.27
-d	0.07	24.12	4.31	29.17
-e	0.05	14.67	3.81	18.82
-f	0.06	19.77	3.65	24.08
Average	0.077	23.95	4.54	29.41
	Cu	Fe_2O_3	Mn	
C_i/TLV_i max	1.30	12.66	1.78	
C_i/TLV_i ave	0.77	6.85	0.91	
C_i/TLV_i min	0.50	3.85	0.38	

Electrode Diameter: 3/32 Inch

Sample No.	Impinger Concentration (mg/m^3)			$(\Sigma C_i/TLV_i)/\eta_I$
	Cu	Fe	Mn	
GMAW2-a	0.12	14.44	3.00	20.45
-b	0.13	16.99	2.68	23.09
-c	0.15	25.72	4.79	33.84
-d	0.22	32.41	6.68	44.16
-e	0.12	17.84	3.81	24.36
-f	0.12	17.67	4.48	24.65
Average	0.142	20.85	4.24	28.38
	Cu	Fe_2O_3	Mn	
C_i/TLV_i max	2.20	9.27	1.34	
C_i/TLV_i ave	1.42	5.96	0.85	
C_i/TLV_i min	1.20	4.86	0.54	

Electrode Diameter: 0.045 Inch

Sample No.	Impinger Concentration (mg/m^3)			$(\Sigma C_i/TLV_i)/\eta_I$
	Cu	Fe	Mn	
GMAW3-a	0.19	42.70	8.35	54.42
-b	0.15	33.50	4.57	41.36
-c	0.22	48.00	8.92	61.08
-d	0.10	25.30	3.21	30.61
-e	0.18	41.90	7.99	53.04
-f	0.17	38.80	6.78	48.80
Average	0.168	38.37	6.63	48.21
	Cu	Fe_2O_3	Mn	
C_i/TLV_i max	2.20	13.73	1.78	
C_i/TLV_i ave	1.68	10.97	1.33	
C_i/TLV_i min	1.00	7.24	0.64	

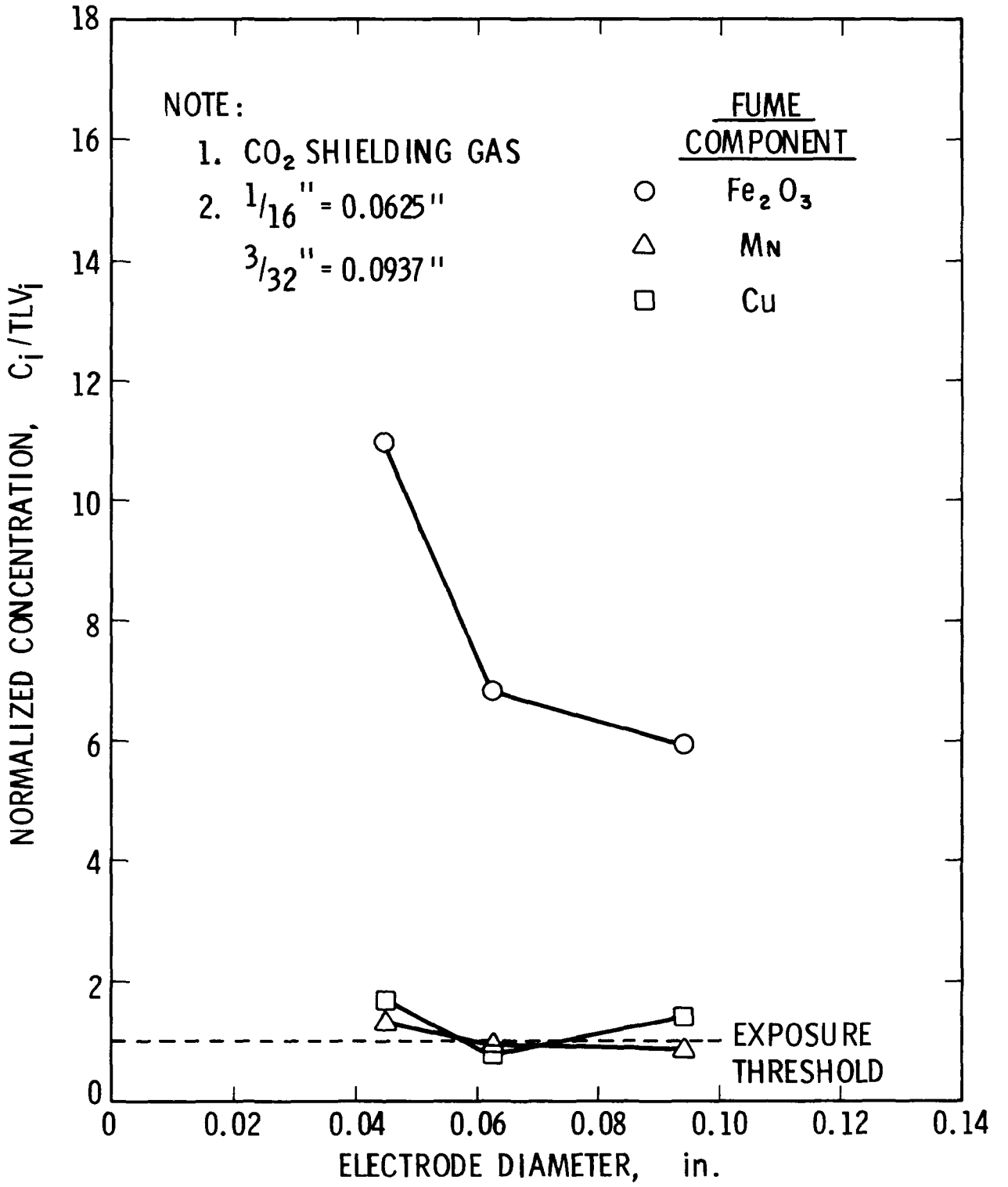

Figure A5. Normalized Impinger Concentrations Obtained from Welding E70T-1 Electrodes on Cold-Rolled Carbon Steel

TABLE A6

Fume Component Concentrations for Gas Shielded Arc Welding of E70S-4 Electrodes on Carbon Steel

Electrode Diameter: 0.035 Inch

Sample No.	Impinger Concentration (mg/m^3)			$(\Sigma C_i/TLV_i)/\eta_T$
	Cu	Fe	Mn	
GMAW4-a	0.14	4.55	0.69	9.79
-b	0.32	14.20	2.43	26.71
-c	0.15	4.95	0.92	10.69
-d	0.21	6.52	1.23	14.52
-e	0.17	5.44	0.98	11.90
-f	0.23	8.03	1.48	16.87
Average	0.203	7.28	1.29	15.07
	Cu	Fe_2O_3	Mn	
C_i/TLV_i max	3.20	4.06	0.49	
C_i/TLV_i ave	2.03	2.08	0.26	
C_i/TLV_i min	1.40	1.30	0.14	

Electrode Diameter: 0.045 Inch

Sample No.	Impinger Concentration (mg/m^3)			$(\Sigma C_i/TLV_i)/\eta_T$
	Cu	Fe	Mn	
GMAW5-a	0.63	74.71	8.28	101.11
-b	0.47	58.67	6.07	78.25
-c	0.59	64.38	7.24	88.83
-d	0.41	44.51	5.05	61.52
-e	0.40	46.36	4.43	62.57
-f	0.46	54.32	5.43	73.18
Average	0.493	57.16	6.08	77.56
	Cu	Fe_2O_3	Mn	
C_i/TLV_i max	6.30	21.37	1.66	
C_i/TLV_i ave	4.93	16.34	1.22	
C_i/TLV_i min	4.0	12.73	0.89	

Electrode Diameter: 1/16 Inch

Sample No.	Impinger Concentration (mg/m^3)			$(\Sigma C_i/TLV_i)/\eta_T$
	Cu	Fe	Mn	
GMAW6-a	---	---	---	---
-b	0.25	10.62	1.50	20.13
-c	0.40	24.29	2.59	39.53
-d	0.47	29.74	2.96	47.58
-e	0.64	37.89	4.14	62.29
-f	0.36	23.09	2.18	36.69
Average	0.424	25.13	2.67	41.24
	Cu	Fe_2O_3	Mn	
C_i/TLV_i max	6.40	10.84	0.83	
C_i/TLV_i ave	4.24	7.19	0.53	
C_i/TLV_i min	2.50	3.04	0.30	

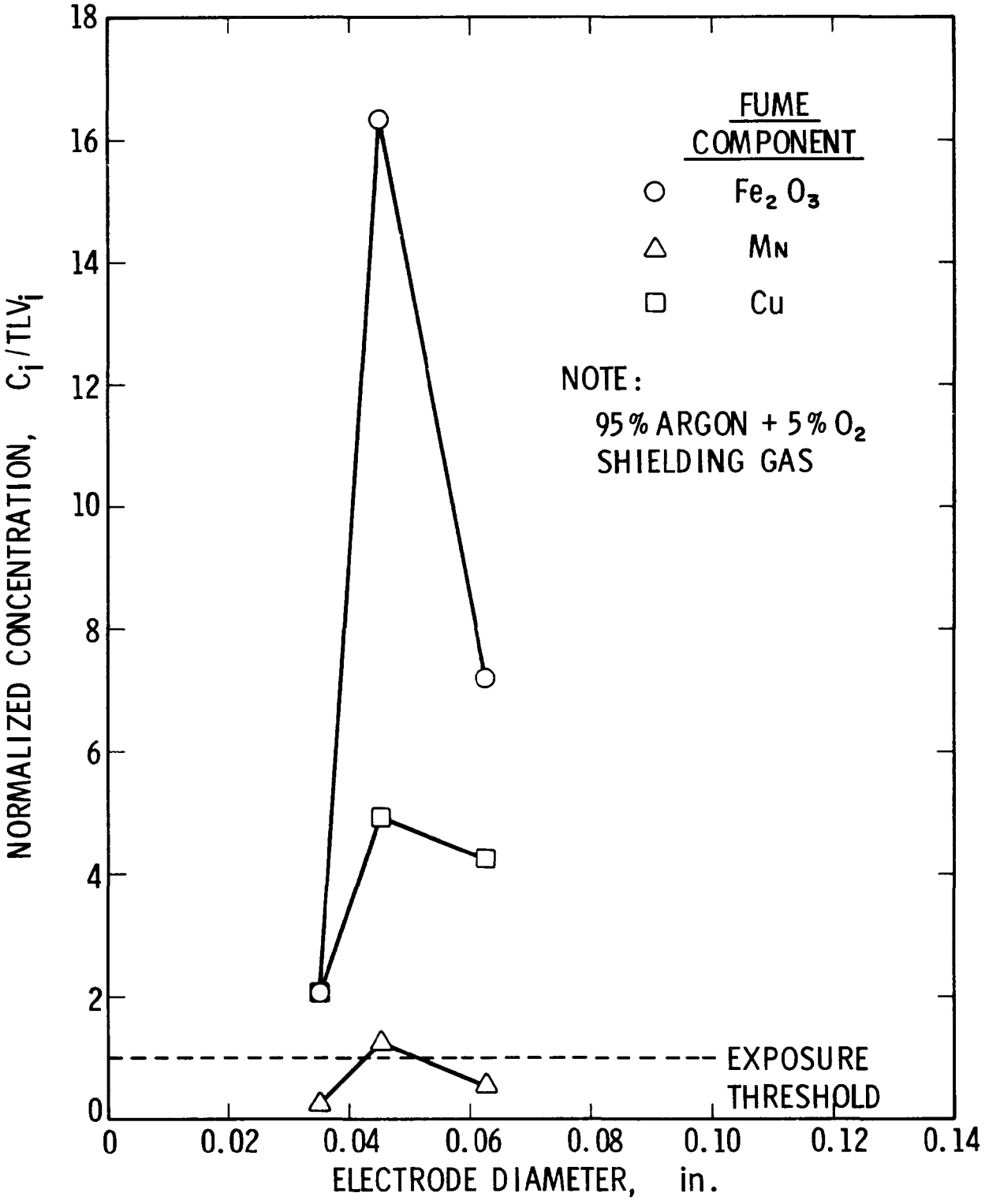

Figure A6. Normalized Impinger Concentrations Obtained from Welding E70S-4 Electrodes on Cold-Rolled Carbon Steel

TABLE A7

Fume Component Concentrations for Shielded Manual Metal Arc Welding of E308-16 Electrodes on Stainless Steel

Electrode Diameter: 1/8 Inch

Sample No.	Impinger Concentration (mg/m^3)					$(\Sigma C_i/TLV_i)/\eta_I$*
	Cu	Fe	Mn	Cr	Ni	
SMAWSS1-a	0.00	3.92	3.55	2.33	0.21	161.30
-b	0.00	1.91	2.13	1.14	0.06	79.04
-c	0.04	5.46	5.82	4.68	0.32	321.73
-d	0.04	4.11	4.47	2.65	0.31	185.03
-e	0.05	4.36	4.32	2.66	0.26	186.01
-f	0.04	2.87	3.21	1.74	0.24	122.45
Average	0.028	3.77	3.96	2.53	0.23	175.93
	Cu	Fe_2O_3	Mn	CrO_3	Ni	
max	0.50	1.56	1.16	89.99	0.32	
C_i/TLV_i ave	0.28	1.08	0.79	48.65	0.23	
min	0.00	0.55	0.43	21.92	0.06	

Electrode Diameter: 3/32 Inch

Sample No.	Impinger Concentration (mg/m^3)					$(\Sigma C_i/TLV_i)/\eta_I$
	Cu	Fe	Mn	Cr	Ni	
SMAWSS2-a	0.00	1.38	0.69	0.82	0.09	56.44
-b	0.01	1.39	0.68	0.79	0.10	54.83
-c	0.01	3.83	2.36	2.71	0.29	186.17
-d	0.02	2.89	1.65	1.94	0.15	133.64
-e	0.01	1.45	0.67	0.76	0.13	53.00
-f	0.04	1.09	2.66	6.26	0.35	419.95
Average	0.015	2.00	1.45	2.21	0.19	150.46
	Cu	Fe_2O_3	Mn	CrO_3	Ni	
max	0.40	1.09	0.53	120.38	0.35	
C_i/TLV_i ave	0.15	0.57	0.29	42.50	0.18	
min	0.00	0.31	0.13	14.61	0.09	

Electrode Diameter: 5/32 Inch

Sample No.	Impinger Concentration (mg/m^3)					$(\Sigma C_i/TLV_i)/\eta_I$
	Cu	Fe	Mn	Cr	Ni	
SMAWSS3-a	0.02	1.80	1.36	1.23	0.14	85.32
-b	0.04	2.23	2.22	1.63	0.19	113.68
-c	0.05	3.29	2.58	2.23	0.29	155.39
-d	0.06	5.94	3.37	5.73	0.28	390.58
-e	0.04	3.47	1.91	2.39	0.20	165.04
-f	0.07	6.27	4.70	7.84	0.41	532.31
Average	0.047	3.83	2.69	3.51	0.25	240.50
	Cu	Fe_2O_3	Mn	CrO_3	Ni	
max	0.70	1.79	0.94	150.76	0.41	
C_i/TLV_i ave	0.47	1.09	0.54	67.50	0.25	
min	0.20	0.52	0.39	23.65	0.14	

* Iron and chrome converted to oxidized form for summation

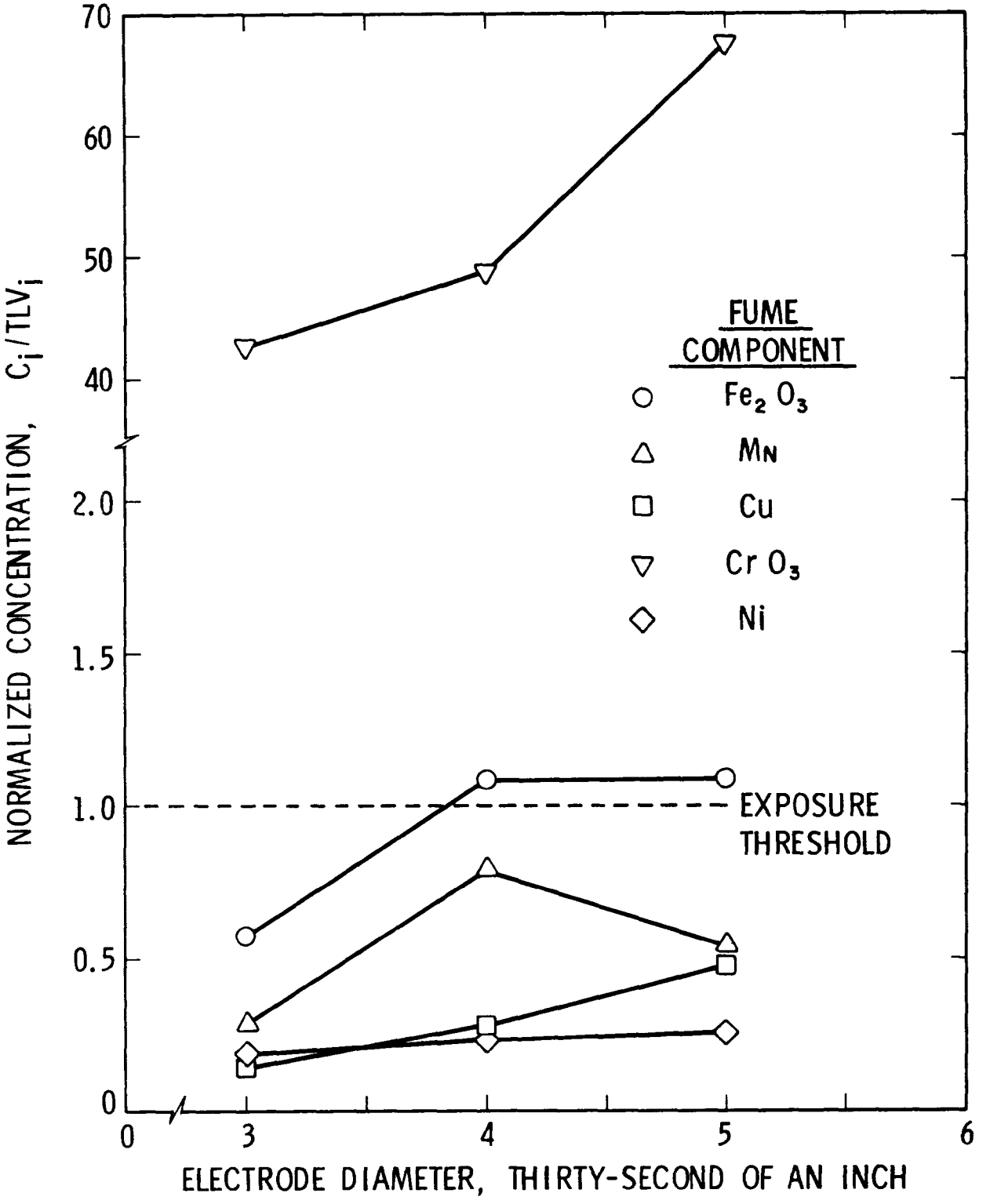

Figure A7. Normalized Impinger Concentrations Obtained from Welding E308-16 Electrodes on Type 304 Stainless Steel

TABLE A8

Fume Component Concentrations for Shielded Manual Metal Arc Welding of E308-15 Electrodes on Stainless Steel

Electrode Diameter: 1/8 Inch

Sample No.	Impinger Concentration (mg/m^3)					$(\Sigma C_i/TLV_i)/\eta_I$
	Cu	Fe	Mn	Cr	Ni	
SMAWSS4-a	0.08	3.00	2.58	2.31	0.29	161.43
-b	0.15	3.83	3.33	3.20	0.31	224.18
-c	0.18	5.64	5.19	4.38	0.37	303.83
-d	0.21	6.90	5.71	5.96	0.46	414.16
-e	0.26	9.37	7.81	8.04	0.64	558.10
-f	0.19	6.38	4.97	4.96	0.40	346.04
Average	0.178	5.85	4.93	4.81	0.41	335.18
	Cu	Fe_2O_3	Mn	CrO_3	Ni	
C_i/TLV_i max	2.60	2.68	1.56	154.61	0.64	
C_i/TLV_i ave	1.78	1.67	0.99	92.50	0.41	
C_i/TLV_i min	0.80	0.86	0.52	44.42	0.29	

Electrode Diameter: 3/32 Inch

Sample No.	Impinger Concentration (mg/m^3)					$(\Sigma C_i/TLV_i)/\eta_I$
	Cu	Fe	Mn	Cr	Ni	
SMAWSS5-a	0.00	1.46	1.09	1.11	0.00	75.68
-b	0.03	0.72	0.43	0.46	0.00	32.50
-c	0.08	6.19	5.04	4.96	0.43	342.21
-d	0.05	3.34	2.56	2.64	0.22	182.33
-e	0.08	4.15	3.19	3.07	0.31	213.38
-f	0.05	2.08	1.62	1.67	0.11	115.84
Average	0.048	2.99	2.32	2.32	0.18	160.42
	Cu	Fe_2O_3	Mn	CrO_3	Ni	
C_i/TLV_i max	0.80	1.77	1.01	95.38	0.43	
C_i/TLV_i ave	0.48	0.86	0.46	44.61	0.18	
C_i/TLV_i min	0.30	0.21	0.09	8.85	0.00	

Electrode Diameter: 5/32 Inch

Sample No.	Impinger Concentration (mg/m^3)					$(\Sigma C_i/TLV_i)/\eta_I$
	Cu	Fe	Mn	Cr	Ni	
SMAWSS6-a	0.03	2.45	2.67	2.86	0.18	195.26
-b	0.04	5.23	3.25	4.17	0.40	286.24
-c	0.06	5.00	6.83	5.13	0.48	353.01
-d	0.04	3.66	4.84	4.36	0.33	298.13
-e	0.07	5.86	6.80	6.19	0.37	423.98
-f	0.02	2.67	3.06	2.88	0.26	197.00
Average	0.043	4.15	4.58	4.27	0.34	292.61
	Cu	Fe_2O_3	Mn	CrO_3	Ni	
C_i/TLV_i max	0.70	1.68	1.37	119.03	0.48	
C_i/TLV_i ave	0.43	1.19	0.92	82.11	0.34	
C_i/TLV_i min	0.20	0.70	0.53	55.00	0.18	

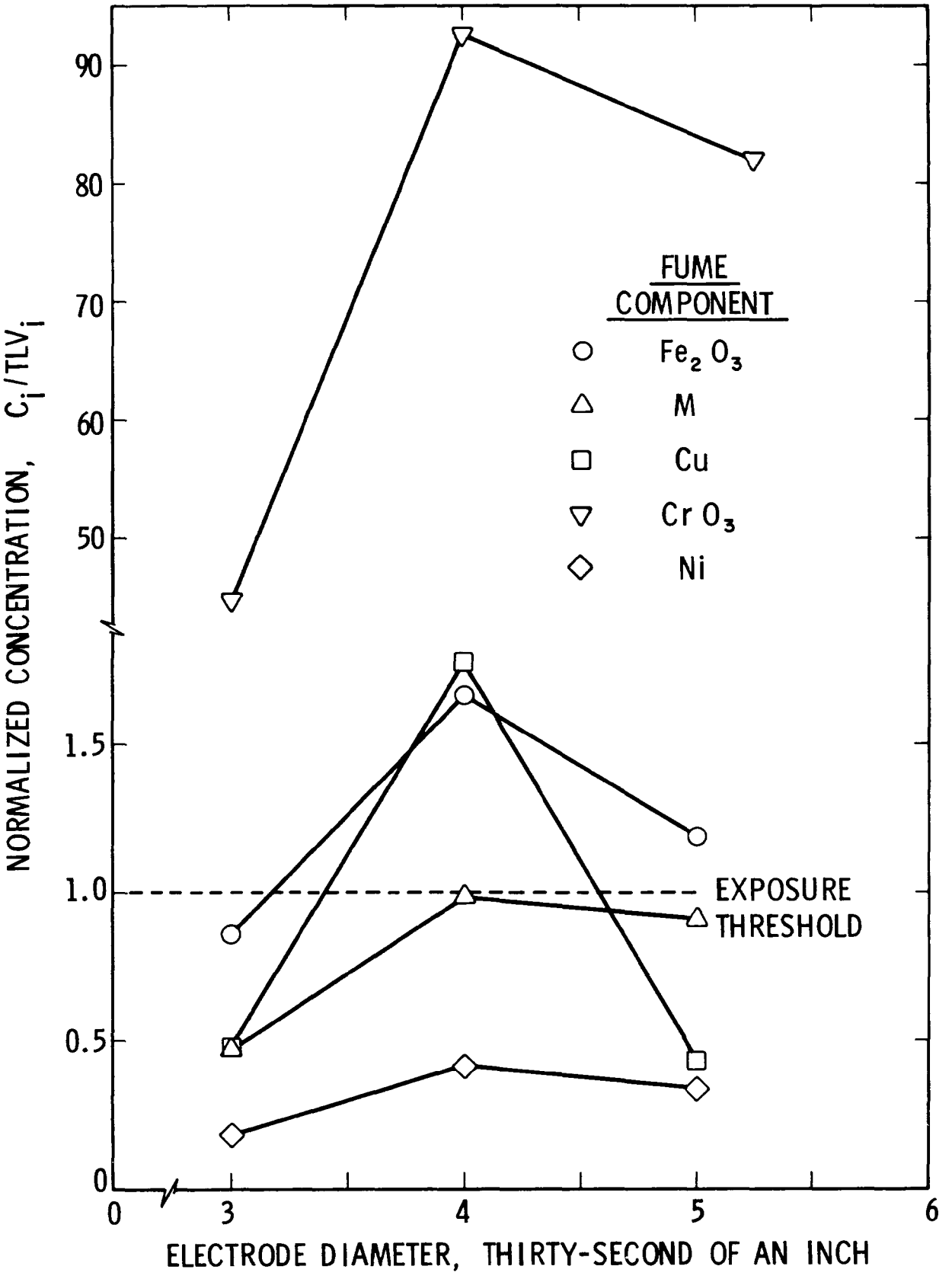

Figure A8. Normalized Impinger Concentrations Obtained from Welding E308-15 Electrodes on Type 304 Stainless Steel

APPENDIX B

HOT WIRE ANEMOMETER SYSTEM

A constant temperature, hot wire anemometer system, which was originally designed and fabricated at SwRI for use in mapping exit velocity profiles on ceiling vents of air conditioning systems, was utilized in establishing capture velocities and face or slot velocity profiles for the various local exhaust ventilation systems. The merits of this system include a broad velocity measurement range, good repeatability over long periods of time, compact design and simplicity of operation.

A hot wire or film system is basically a device which provides an electrical output proportional to the thermal energy that is convected, conducted, and radiated from the heated wire or film placed to a fluid stream. The quantity of heat transferred per unit time is dependent on the flow velocity, the difference in temperature between the wire and the fluid, the physical properties of the fluid as well as the dimensions and physical properties of the wire.

Normally, radiation effects are negligible if the wire is operated at temperatures less than approximately 575°F. Also, whenever the wire length is much greater than the diameter, as is the usual case, the heat conducted into the wire supports is negligible. Therefore, convection is the primary heat transfer mechanism from the wire to the fluid, and for Reynolds numbers greater than 0.5 the convection is predominantly forced, with the contribution from free convection being negligible.

A schematic of the circuit that was used to measure the energy output of the wire is shown in Figure B-1. The hot wire circuit was fabricated using integrated circuits in conjunction with a medium power transistor, which permitted electronic simplification and a higher packing density. This particular circuit is known as a constant temperature circuit because it employs negative feedback techniques to maintain the wire at a constant temperature.

Basically, the circuit functions in the following manner. A slight change in the resistance of the hot wire relative to its no-flow operating point is detected by the bridge circuit and the first stage amplifier. The signal is conditioned and subsequently used as the voltage control signal for a voltage-controlled current source and a transistor in an emitter-follower configuration. This action increases the current flow into the load and the bridge circuit. Therefore, the wire resistance increases to the point previously established for the no-flow case, i.e., its original temperature. The output voltage is proportional to the energy required to maintain the wire at constant temperature.

One aspect of the probe design, which permits rugged use in an industrial environment, is the increased wire diameter. Given two wires

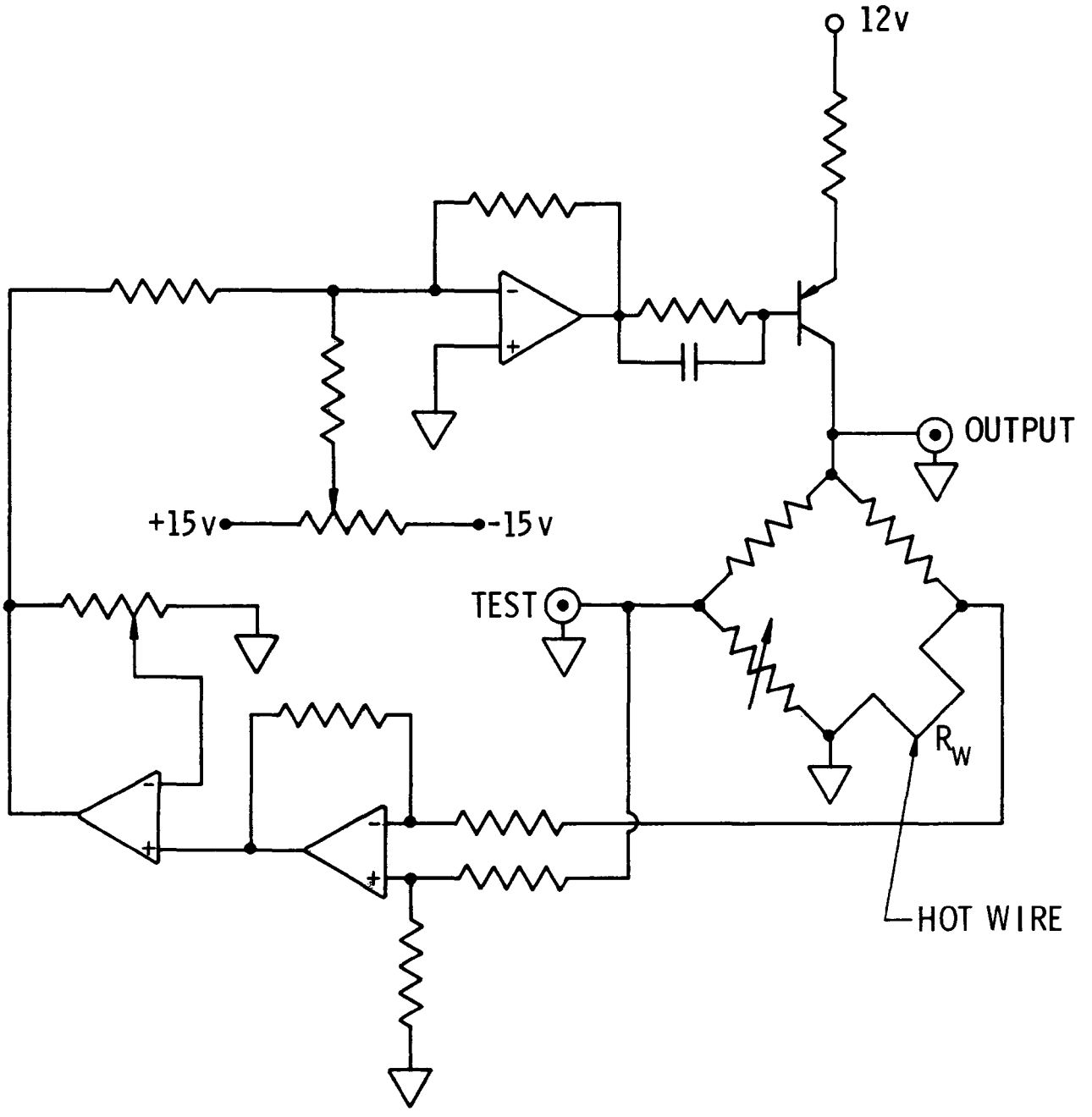

Figure B-1. Hot Wire Circuit Diagram

of equal length, the larger diameter wire will have a larger thermal inertia. The effect of increasing thermal inertia is to produce a reduction in the frequency response of the instrument. However, a high frequency response is generally not needed in industrial applications. Therefore, in the original design, frequency response was compromised in favor of ruggedness. The SwRI system has a frequency response of about 5 K Hz. The wire is made of gold-plated tungsten with a diameter of 0.0007 inch.

APPENDIX C

BREATHING ZONE FUME CONCENTRATIONS FOR THE CROSSDRAFT TABLE

Table C1

Breathing Zone Fume Concentrations for the Crossdraft Table

No ventilation

Sample No.	Impinger Concentration (mg/m^3)			$(\Sigma C_i/TLV_i)/n_I$ *
	Cu	Fe	Mn	
GMAW-MS1-a	0.38	26.86	2.17	41.09
-b	0.05	4.51	0.21	6.32
-c	0.26	26.60	2.55	36.96
-d	0.52	41.28	5.54	62.46
-e	0.14	11.02	0.98	16.37
-f	0.16	15.98	1.41	22.25
Average	0.25	21.04	2.14	30.85

Perpendicular: capture velocity = 62 fpm

Sample No.	Impinger Concentration (mg/m^3)			$(\Sigma C_i/TLV_i)/n_I$
	Cu	Fe	Mn	
GMAW-MS7-a	--	0.17	--	0.17
-b	--	0.15	--	0.15
-c	--	--	--	--
-d	--	0.18	--	0.18
-e	--	0.38	--	0.38
-f	--	0.12	--	0.12
Average	0.0	0.17	0.0	0.17

Perpendicular: capture velocity = 100 fpm

Sample No.	Impinger Concentration (mg/m^3)			$(\Sigma C_i/TLV_i)/n_I$
	Cu	Fe	Mn	
GMAW-MS3-a	0.001	0.22	0.022	0.267
-b	--	0.13	0.011	0.136
-c	--	0.36	0.007	0.360
-d	--	0.11	0.018	0.121
-e	--	0.11	0.014	0.118
-f	--	0.23	0.025	0.244
Average	0.0	0.19	0.016	0.200

Parallel: capture velocity = 62 fpm

Sample No.	Impinger Concentration (mg/m^3)			$(\Sigma C_i/TLV_i)/n_I$
	Cu	Fe	Mn	
GMAW-MS4-a	0.014	1.24	0.043	1.74
-b	0.001	0.76	0.028	0.80
-c	0.019	0.98	0.039	1.65
-d	0.004	1.09	0.039	1.24
-e	0.004	0.81	0.029	0.96
-f	0.005	3.17	0.045	3.29
Average	0.008	1.34	0.037	1.62

* Iron concentration converted to iron oxide for summation.

Table C1

Breathing Zone Fume Concentrations for the Crossdraft Table

No ventilation

Sample No.	Impinger Concentration (mg/m^3)			$(\Sigma C_i/TLV_i)/n_I$ *
	Cu	Fe	Mn	
GMAW-MS1-a	0.38	26.86	2.17	41.09
-b	0.05	4.51	0.21	6.32
-c	0.26	26.60	2.55	36.96
-d	0.52	41.28	5.54	62.46
-e	0.14	11.02	0.98	16.37
-f	0.16	15.98	1.41	22.25
Average	0.25	21.04	2.14	30.85

Perpendicular: capture velocity = 62 fpm

Sample No.	Impinger Concentration (mg/m^3)			$(\Sigma C_i/TLV_i)/n_I$
	Cu	Fe	Mn	
GMAW-MS7-a	--	0.17	--	0.17
-b	--	0.15	--	0.15
-c	--	--	--	--
-d	--	0.18	--	0.18
-e	--	0.38	--	0.38
-f	--	0.12	--	0.12
Average	0.0	0.17	0.0	0.17

Perpendicular: capture velocity = 100 fpm

Sample No.	Impinger Concentration (mg/m^3)			$(\Sigma C_i/TLV_i)/n_I$
	Cu	Fe	Mn	
GMAW-MS3-a	0.001	0.22	0.022	0.267
-b	--	0.13	0.011	0.136
-c	--	0.36	0.007	0.360
-d	--	0.11	0.018	0.121
-e	--	0.11	0.014	0.113
-f	--	0.23	0.025	0.244
Average	0.0	0.19	0.016	0.200

Parallel: capture velocity = 62 fpm

Sample No.	Impinger Concentration (mg/m^3)			$(\Sigma C_i/TLV_i)/n_I$
	Cu	Fe	Mn	
GMAW-MS4-a	0.014	1.24	0.043	1.74
-b	0.001	0.76	0.028	0.80
-c	0.019	0.98	0.039	1.65
-d	0.004	1.09	0.039	1.24
-e	0.004	0.81	0.029	0.96
-f	0.005	3.17	0.045	3.29
Average	0.008	1.34	0.037	1.62

* Iron concentration converted to iron oxide for summation.

APPENDIX D

BREATHING ZONE FUME CONCENTRATIONS FOR THE RECTANGULAR HOOD

Table D1

E-7018 Electrodes

No ventilation

Sample No.	Impinger Concentration (mg/m^3)			$(\Sigma C_i/TLV_i)/\eta_I$ *
	Cu	Fe	Mn	
SMAW-RH1-a	0.014	10.36	1.76	11.90
-b	0.018	9.28	1.86	11.07
-c	0.007	6.05	0.96	6.86
-d	0.006	2.88	0.44	3.34
-e	0.009	3.64	0.50	4.24
-f	0.026	9.11	1.50	10.93
Average	0.013	6.89	1.17	8.06

Capture velocity = 60 fpm: Stand-off distance = 12 inches

Sample No.	Impinger Concentration (mg/m^3)			$(\Sigma C_i/TLV_i)/\eta_I$
	Cu	Fe	Mn	
SMAW-RH3-a	--	0.07	--	0.07
-b	--	0.06	--	0.06
-c	--	0.07	--	0.07
-d	--	0.02	--	0.02
-e	--	0.01	--	0.01
Average	0.0	0.05	0.0	0.05

Capture velocity = 105 fpm: Stand-off distance = 12 inches

Sample No.	Impinger Concentration (mg/m^3)			$(\Sigma C_i/TLV_i)/\eta_I$
	Cu	Fe	Mn	
SMAW-RH2-a	--	--	0.007	0.005
-b	--	--	0.007	0.005
-c	--	--	0.002	0.001
-d	--	--	0.006	0 004
-e	--	--	0.010	0.007
-f	--	--	--	--
Average	0.0	0.0	0.005	0.004

* Iron concentration converted to iron oxide for summation.

Table D1 (Concluded)

E-7018 Electrodes

Capture velocity = 20 fpm: Stand-off distance = 18 inches

Sample No.	Impinger Concentration (mg/m^3)			$(\Sigma C_i/TLV_i)/\eta_I$
	Cu	Fe	Mn	
SMAW-RH6-a	0.007	0.023	0.001	0.265
-b	0.014	--	0.010	0.490
-c	0.008	0.101	0.032	0.398
-d	0.008	0.073	0.015	0.358
-e	0.003	0.044	0.012	0.155
Average	0.008	0.048	0.014	0.333

Capture velocity = 31 fpm: Stand-off distance = 18 inches

Sample No.	Impinger Concentration (mg/m^3)			$(\Sigma C_i/TLV_i)/\eta_I$
	Cu	Fe	Mn	
SMAW-RH5-a	--	0.25	0.06	0.29
-b	--	0.20	0.04	0.23
-c	--	0.25	0.04	0.27
-d	--	0.19	0.03	0.21
-e	--	0.14	0.03	0.16
-f	--	0.17	0.02	0.18
Average	0.0	0.20	0.04	0.22

Capture velocity = 100 fpm: Stand-off distance = 18 inches

Sample No.	Impinger Concentration (mg/m^3)			$(\Sigma C_i/TLV_i)/\eta_I$
	Cu	Fe	Mn	
SMAW-RH4-a	--	0.06	--	0.06
-b	--	0.04	--	0.04
-c	--	0.06	--	0.06
-d	--	0.06	--	0.06
-e	--	0.04	--	0.04
-f	--	0.04	--	0.04
Average	0.0	0.05	0.0	0.05

Table D2

E-308-15 Electrodes
Stand-off Distance = 18 inches

No ventilation

Sample No.	Impinger Concentration (mg/m^3)					$(\Sigma C_i/TLV_i)/\eta_I$*
	Cu	Fe	Mn	Cr	Ni	
SMAWSS-RH7-a	0.013	0.351	0.320	0.235	--	16.57
-b	0.029	1.024	0.845	0.731	--	50.99
-c	0.024	0.678	0.458	0.407	--	28.76
-d	0.017	0.418	0.347	0.264	--	18.72
-e	0.037	1.287	1.160	0.892	--	62.40
-f	0.036	0.729	0.138	0.245	--	18.28
Average	0.026	0.748	0.545	0.462	0.0	32.60

Capture velocity = 20 fpm

Sample No.	Impinger Concentration (mg/m^3)					$(\Sigma C_i/TLV_i)/\eta_I$
	Cu	Fe	Mn	Cr	Ni	
SMAWSS-RH10-a	0.005	0.025	0.002	--	--	0.198
-b	0.005	0.007	0.005	--	--	0.183
-c	0.002	0.055	0.040	0.016	--	1.210
-d	0.002	0.073	0.039	0.019	--	1.430
-e	0.007	0.016	0.010	--	--	0.264
-f	0.002	0.034	0.037	0.027	--	1.920
Average	0.004	0.035	0.022	0.010	0.0	0.87

Capture velocity = 31 fpm

Sample No.	Impinger Concentration (mg/m^3)					$(\Sigma C_i/TLV_i)/\eta_I$
	Cu	Fe	Mn	Cr	Ni	
SMAWSS-RH9-a	0.014	0.092	--	--	--	0.573
-b	0.008	0.040	--	--	--	0.315
-c	0.005	0.058	--	--	--	0.229
-d	0.003	0.022	--	--	--	0.125
-e	0.017	0.027	--	--	--	0.612
-f	0.005	0.034	-	--	--	0.205
Average	0.009	0.046	0.0	0.0	0.0	0.343

Capture velocity = 100 fpm

Sample No.	Impinger Concentration (mg/m^3)					$(\Sigma C_i/TLV_i)/\eta_I$
	Cu	Fe	Mn	Cr	Ni	
SMAWSS-RH8-a	--	0.063	--	0.006	--	0.459
-b	--	0.045	--	0.006	--	0.442
-c	--	0.045	--	0.006	--	0.442
-d	--	0.153	--	0.012	--	0.945
-e	--	0.071	--	0.019	--	1.330
-f	--	0.069	--	--	--	0.068
Average	0.0	0.074	0.0	0.008	0.0	0.614

* Chrome and iron converted to oxidized form for summation.

☆ U.S. GOVERNMENT PRINTING OFFICE: 1977— 757-057/6741